

NAVAL POSTGRADUATE SCHOOL MONTEREY, CALIFORNIA



THESIS

TOWED ARRAY PERFORMANCE IN THE LITTORAL WATERS OF NORTHERN AUSTRALIA

by

James A. M. Crouch

June, 1997

Thesis Advisors:

Robert H. Bourke
James H. Wilson

Approved for public release; distribution is unlimited.

DTIC QUALITY INSPECTED 4

19980102 096

REPORT DOCUMENTATION PAGE

Form Approved OMB No. 0704-0188

Public reporting burden for this collection of information is estimated to average 1 hour per response, including the time for reviewing instruction, searching existing data sources, gathering and maintaining the data needed, and completing and reviewing the collection of information. Send comments regarding this burden estimate or any other aspect of this collection of information, including suggestions for reducing this burden, to Washington Headquarters Services, Directorate for Information Operations and Reports, 1215 Jefferson Davis Highway, Suite 1204, Arlington, VA 22202-4302, and to the Office of Management and Budget, Paperwork Reduction Project (0704-0188) Washington DC 20503.

1. AGENCY USE ONLY (Leave blank)		2. REPORT DATE June 1997	3. REPORT TYPE AND DATES COVERED Master's Thesis
4. TITLE AND SUBTITLE TOWED ARRAY PERFORMANCE IN THE LITTORAL WATERS OF NORTHERN AUSTRALIA			5. FUNDING NUMBERS
6. AUTHOR(S) Crouch James A. M.			
7. PERFORMING ORGANIZATION NAME(S) AND ADDRESS(ES) Naval Postgraduate School Monterey CA 93943-5000			8. PERFORMING ORGANIZATION REPORT NUMBER
9. SPONSORING/MONITORING AGENCY NAME(S) AND ADDRESS(ES)			10. SPONSORING/MONITORING AGENCY REPORT NUMBER
11. SUPPLEMENTARY NOTES The views expressed in this thesis are those of the author and do not reflect the official policy or position of the Department of Defense or the U.S. Government.			
12a. DISTRIBUTION/AVAILABILITY STATEMENT Approved for public release; distribution is unlimited.			12b. DISTRIBUTION CODE
13. ABSTRACT (maximum 200 words) <p>The goal of this research was to investigate the performance of low frequency passive sonars in the Arafura Sea. Sound speed profiles representative of the wet and dry monsoon seasons and geoacoustic data were inputted into a finite element primitive equation transmission loss model to model the expected propagation at three frequencies, 10, 50 and 300 Hz. Initial detection ranges for several source/receiver depth combinations and geoacoustic areas (deep/shallow water) were compared and evaluated. Results demonstrate that low frequency (~10 Hz) detection ranges suffer due to cutoff frequency problems and to surface-decoupling loss. Propagation in deep water has the added disadvantage of excessive loss of signal power due to spherical spreading considerations. Conversely, higher frequencies (300 Hz) provided extended detection ranges in shallow water due to trapping of energy within the entire 50 m to 100 m water column.</p> <p>Additionally, investigation into advantages to be gained through advanced signal processing techniques shows that improvements of the order of 10 to 15 dB of detection gain are possible through the utilization of inverse beamforming.</p>			
14. SUBJECT TERMS Oceanography, Pasive Sonar, Inital Detection Ranges, Arafura Sea, Beamforming			15. NUMBER OF PAGES 121
			16. PRICE CODE
17. SECURITY CLASSIFICATION OF REPORT Unclassified	18. SECURITY CLASSIFICATION OF THIS PAGE Unclassified	19. SECURITY CLASSIFICATION OF ABSTRACT Unclassified	20. LIMITATION OF ABSTRACT UL

NSN 7540-01-280-5500

Standard Form 298 (Rev. 2-89)
Prescribed by ANSI Std. Z39-18 298-102

Approved for public release; distribution is unlimited.

**TOWED ARRAY PERFORMANCE IN THE LITTORAL WATERS OF
NORTHERN AUSTRALIA**

James A. M. Crouch
Lieutenant, Royal Australian Navy
B.Sc., University College of the University of New South Wales, 1985

Submitted in partial fulfillment
of the requirements for the degree of

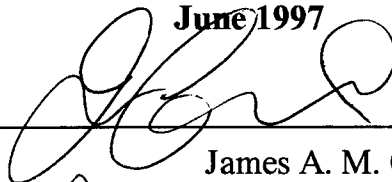
MASTER OF SCIENCE IN PHYSICAL OCEANOGRAPHY

from the

NAVAL POSTGRADUATE SCHOOL

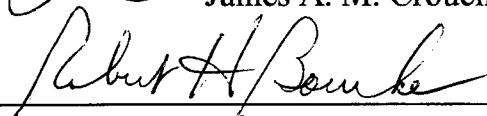
June 1997

Author:

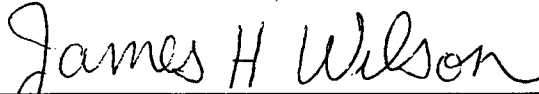


James A. M. Crouch

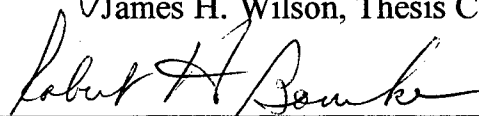
Approved by:



Robert H. Bourke, Thesis Co-Advisor



James H. Wilson, Thesis Co-Advisor



Robert H. Bourke, Chairman, Department of Oceanography

ABSTRACT

The goal of this research was to investigate the performance of low frequency passive sonars in the Arafura Sea. Sound speed profiles representative of the wet and dry monsoon seasons and geoacoustic data were inputted into a finite element primitive equation transmission loss model to model the expected propagation at three frequencies, 10, 50 and 300 Hz. Initial detection ranges for several source/receiver depth combinations and geoacoustic areas (deep/shallow water) were compared and evaluated. Results demonstrate that low frequency (~ 10 Hz) detection ranges suffer due to cutoff frequency problems and to surface-decoupling loss. Propagation in deep water has the added disadvantage of excessive loss of signal power due to spherical spreading considerations. Conversely, higher frequencies provided extended detection ranges in shallow water due to trapping of energy within the entire 50 m to 100 m water column.

Additionally, investigation into advantages to be gained through advanced signal processing techniques shows that improvements of the order of 10 to 15 dB of detection gain are possible through the utilization of inverse beamforming.

TABLE OF CONTENTS

I.	INTRODUCTION	1
A.	BACKGROUND	1
B.	MOTIVATION	1
C.	CLIMATOLOGY	3
1.	Weather	3
2.	Topography	5
3.	Oceanography	6
D.	OBJECTIVES	9
II.	METHOD	11
A.	SCENARIOS	11
1.	Sonar Equation	11
2.	Figure of Merit Values	12
B.	FIGURE OF MERIT	14
C.	OCEAN DATA	15
1.	Water Column	15
a.	Analysis	16
b.	Transects	20
D.	GEOACOUSTIC DATA	20
E.	FINITE ELEMENT PRIMITIVE EQUATION (FEPE) MODEL	22
III.	DETECTION RANGE RESULTS AND TACTICAL CONCEPTS	25
A.	DETECTION RANGES	25
1.	Shallow Southern Waters	25
a.	Dry season	25
b.	Wet season	27
2.	Deep Northern Waters	29
a.	Dry season	29
b.	Wet season	31
B.	DISCUSSION	33
1.	Ducting/Frequency	33
2.	Season	34
3.	Convergence Zone	34
4.	Up-slope/down-slope propagation	35
C.	TACTICAL CONCEPTS	35
IV.	ADVANCED SIGNAL PROCESSING ALGORITHMS	37
A.	CONVENTIONAL BEAMFORMING (CBF)	37
B.	MATCHED-FIELD PROCESSING	39
C.	INVERSE BEAMFORMING	39
D.	PERFORMANCE ADVANTAGE	40

V.	CONCLUSIONS and RECOMMENDATIONS	43
A.	CONCLUSIONS	43
B.	RECOMMENDATIONS	44
	LIST OF REFERENCES	45
APPENDIX A.	10 HZ TRANSMISSION LOSS CURVES	49
APPENDIX B.	50 HZ TRANSMISSION LOSS CURVES	71
APPENDIX C.	300 HZ TRANSMISSION LOSS CURVES	91
	INITIAL DISTRIBUTION LIST	111

I. INTRODUCTION

A. BACKGROUND

As early as 1987, Dibb (1987) identified that, however unlikely it was that a military threat to Australia would develop, it could be expected that the threat axis would more than likely be from the northwest. The Australian Defence Force then began a process of re-deploying forces to the north of the continent in order to take this possibility into account. As a result, Royal Australian Air Force bases along the northern coast were upgraded, and Australian Regular Army units have been shifted north. This re-disposition of forces also produced a new primary area for naval operations, the North Australian Area (NAA), a complex regime encompassing both deep and shallow waters.

Many operational uncertainties arise concerning the prosecution of these potential threats, including the performance of acoustic surveillance and detection arrays, due to the complicated nature of the water column and sub-bottom profiles of the NAA. It is the purpose of this thesis to provide an initial look at sonar performance in these waters based on scenarios and sensors likely to be faced and employed by the Royal Australian Navy (RAN).

B. MOTIVATION

In June 1996, Australia accepted into service Her Majesty's Australian Ship COLLINS (Figure 1), the first of six Type 206 conventional diesel-electric submarines to be commissioned. These submarines are of Swedish design, but being built in Australia. As part of the submarine's suite of acoustic sensors, the acquisition of either a Narama or a Kariwara towed array (TA) is being considered.

The Kariwara thin line reelable array, developed at the Australian Defence Research Centre, has been field tested on the older OBERON class of submarines which are being replaced by the COLLINS class. The overall length of the Kariwara streamer is 450 m minimum, with an acoustic section length of 70 to 2000 m (Net Resources International, 1996).

Thomson Marconi Sonar, who produce both the Kariwara and the Narama arrays, has recently been awarded a contract to supply two Narama arrays for each of the remaining OBERONS (Matzkows, 1997). Narama is a small diameter array incorporating short tactical design lengths, and longer surveillance array lengths. A final decision however has not been made on which array will be fitted in the COLLINS class.

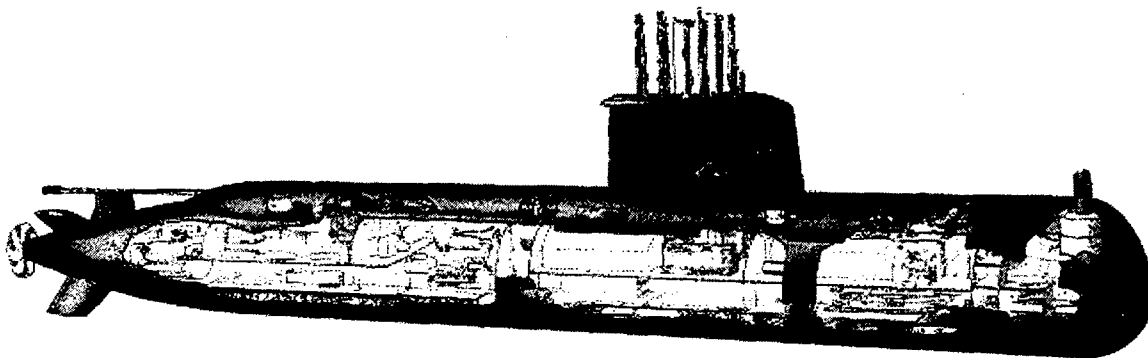


Figure 1. COLLINS class submarine. (Adapted from Australian Submarine Corp photograph)

Although the sophistication of today's towed arrays has increased enormously, engineering limitations force towed arrays to be tuned for peak performance based on conditions that are anticipated to be experienced most often. It is therefore of interest to ascertain how towed arrays designed in this matter perform in specific areas of operation.

The Arafura Sea, shown at Figure 2, is a sub-area of the NAA and has been selected for analysis of towed array performance because it contains oceanographic and environmental variations typical of the entire NAA. This will determine the appropriateness of the use of towed arrays in this area. Additionally, it is conceivable that should a threat from the northwest develop, the Arafura Sea would become a strategically important area of any initial conflict.

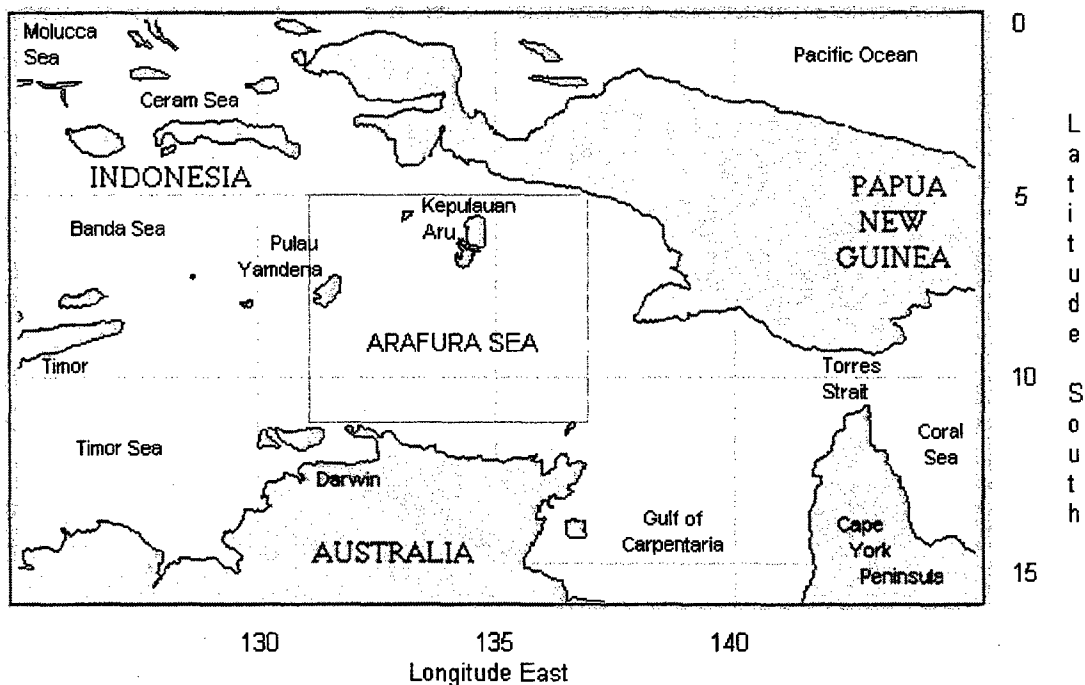


Figure 2. Chart of the Arafura Sea and surrounding waters.
(Adapted from Rand McNally, 1995).

C. CLIMATOLOGY

1. Weather

The NAA lies well to the north of the Tropic of Capricorn, and as such the entire area is predominately tropical. It lies in a traditional monsoon area, typified by a seasonal reversal in wind direction.

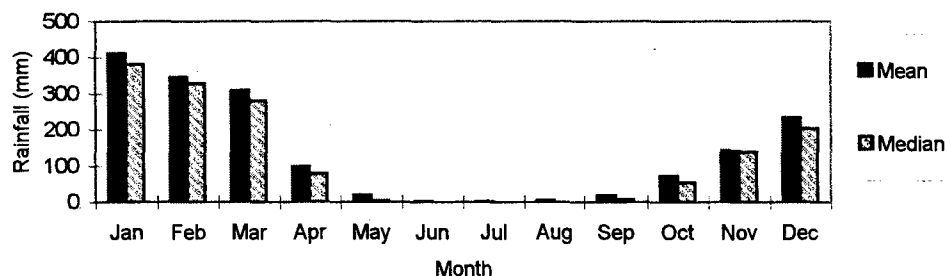


Figure 3. Mean and Median Rainfall for Darwin, Australia.
(Adapted from Bureau of Meteorology Climate Centre, 1995)

The monsoons are divided into two regimes, the wet season and the dry season, as can be seen in the rainfall data of Darwin (Figure 3). During the wet season (November to early April), the monsoon trough lies across northern Australia. The monsoon trough is a trough of low pressure into which the monsoons converge (Neal and Holland, 1977).

A fresh (7 to 9 ms^{-1}) wind (Williams, 1992) usually prevails during the wet season offshore across the Arafura Sea, which is north of the trough. A characteristic of the northwest (wet) monsoon are active periods typified by intense rainfall and convective activity with fresh to strong (9 to 12 ms^{-1}) winds. These periods are known as bursts. An active period occurs in Darwin on average two to three times a year (Williams, 1992). Additionally, on average, eight tropical cyclones develop in the Australian area during each wet season, of which two will have formed in the Arafura Sea (Grey, 1975).

Conversely, the dry monsoon period extends from May to September (there is a brief transition period between monsoon seasons) and is associated with the sub-tropical ridge lying across central and southern Australia. The resultant dry fresh to strong (9 to 11 ms^{-1}) southeasterly trade winds produce generally fine weather, although periods of strong (11 to 13 ms^{-1}) winds occur at times (Williams, 1992). This increase in wind speed in the dry trade winds is reflected in the mean scalar winds for Northern Australia (Figure 4).

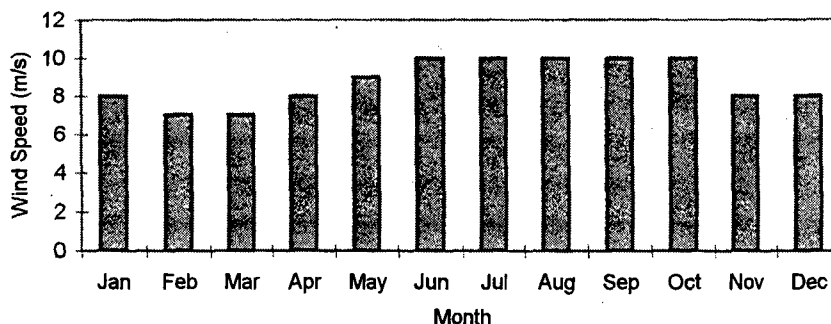


Figure 4. Mean scalar wind speed at 1000 hPa for Northern Australia. (Adapted from Changery et al., 1989)

2. Topography

The bottom topography of the Arafura Sea is mostly a vast expanse of shelf, rising in the north to the Aru Islands, which are located near the shelf break. The shelf serves as a foundation for many coral reefs, before dropping off into the Aru Basin, a small isolated deep basin with maximum depths of around 3650 m (Tomczak and Godfrey, 1994). The Weber Basin is in the northwest corner of the area under consideration and is deeper than 7000 m. In the southeast, the Arafura Shelf is particularly shallow, some parts being less than 50 m in depth, precluding most routine submarine operations. It is an area, however, where submarine operations may have to take place should hostilities develop. A complex series of ridges, and valleys lead towards the Gulf of Carpentaria.

The continental slope also varies greatly. The gradient along the Goodrich and Lynedock Banks in the south is less than 500 m in 40 km whereas along the deep Aru Basin the shelf slopes as steep as 3000 m in 40 km. The topography of the region is depicted in Figure 5.

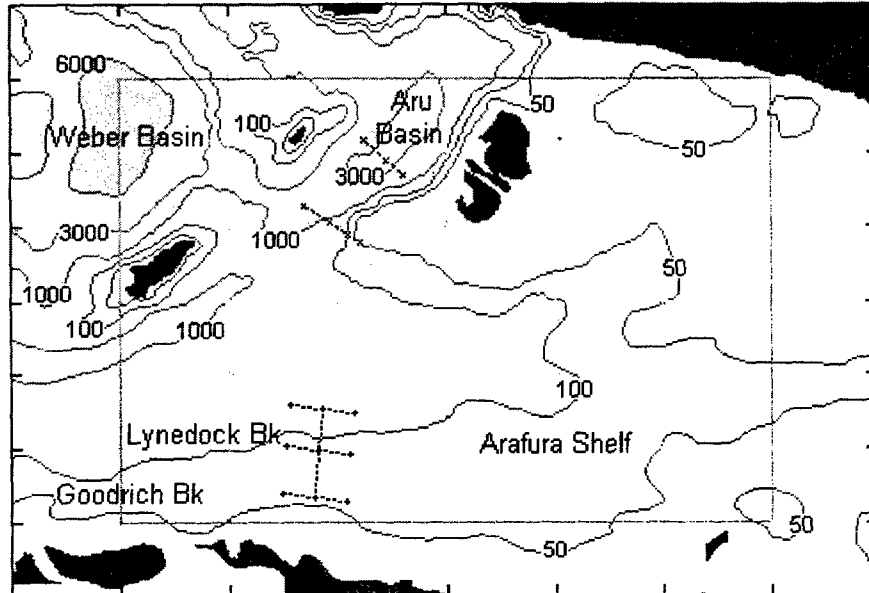


Figure 5. Topography of the Arafura Sea showing location of six transects used to model sonar performance. Depths in meters. (Adapted from National Geophysical Data Center digital relief information, 1988)

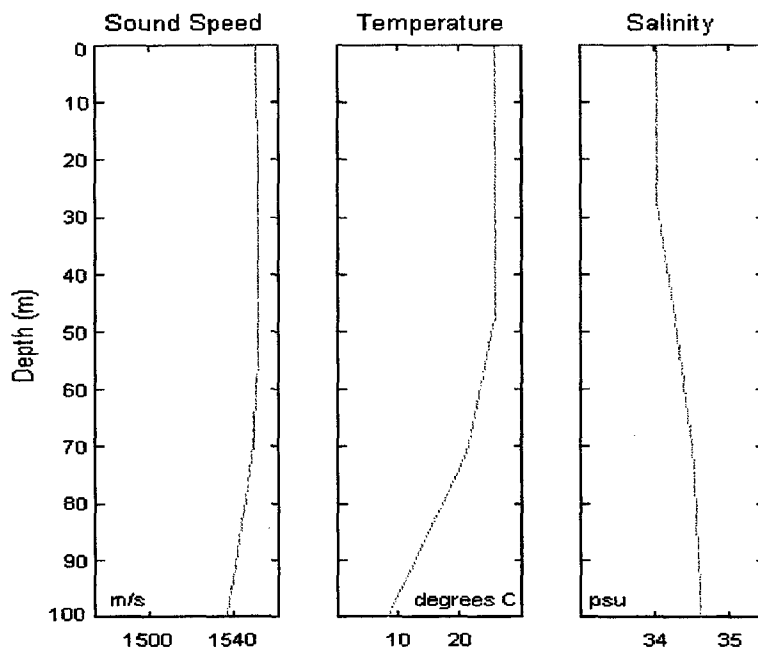
3. Oceanography

The flow of Pacific Ocean water through Torres Strait into the Arafura Sea is weak (Wolanski et al., 1988). Currents in the Arafura Sea are influenced by winds and the flow (Indonesian Throughflow) of Pacific Ocean water through the Australasian Mediterranean (Wyrski, 1987), a name given to the Indonesian Seas. A steady, generally westward, flow is present through the Timor Sea, though farther to the southeast currents are variable due to the variability between monsoon and trade winds (Tomczak and Godfrey, 1994).

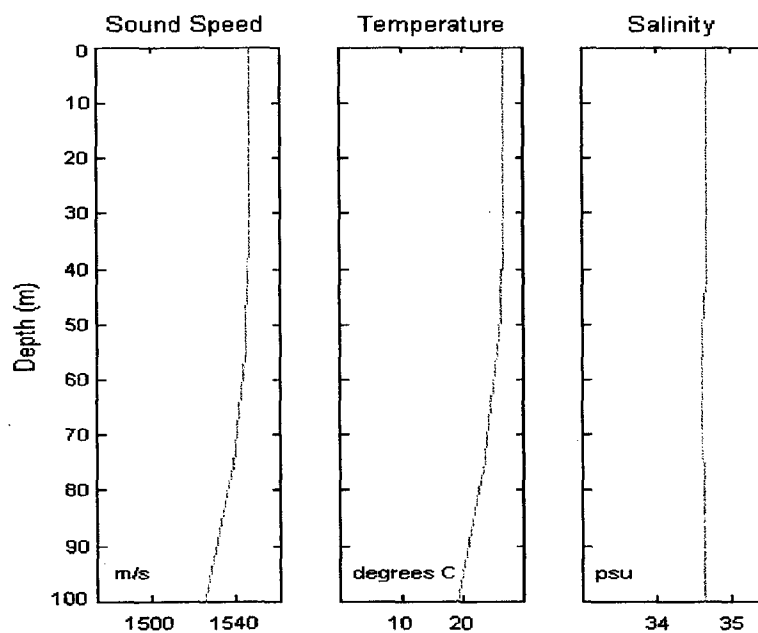
Inspection of profiles of the water column in the southern part of the Arafura Sea (Figure 6) reveals a water column that is generally well mixed almost to the bottom, particularly in the wet season. The surface temperature is warmer by 2-3°C (Thurman, 1997) during the wet season and the mean wind speed is sufficient to mix the increased heat downward heating the entire water column, particularly in more shallow water regions.

Inspection of profiles in deeper waters to the north (an example is at Figure 7), on the other hand, show that they exhibit mixed layer depths of the order 30 to 50 m during the dry season, deepening to 50 to 70 m during the wet season, despite the stronger winds during the dry season. The uniform salinity profile is almost identical to that of Banda Sea water which flows into the Indian Ocean through the Timor/Australia gap. The salt content in the top 200 m is diluted by precipitation and runoff during the wet monsoon season (Schmitz, 1996).

Data on subsurface currents is limited, though Banda Sea waters have been observed to upwell onto the shelf of the eastern Arafura Sea, perhaps part of Schmitz' "meridional cell", formed as Indian Ocean deep water flows through the Indonesian Archipelago and around the Banda Sea to exit through the Timor Sea (Schmitz, 1996). Tides of the Gulf of Carpentaria have been observed which indicate that barotropic diurnal tidal currents dominate the area (Church and Forbes, 1983). Tides range between 3.5 and 4.5 m along the north coast of the Northern Territory (Bird and Schwartz, 1985).

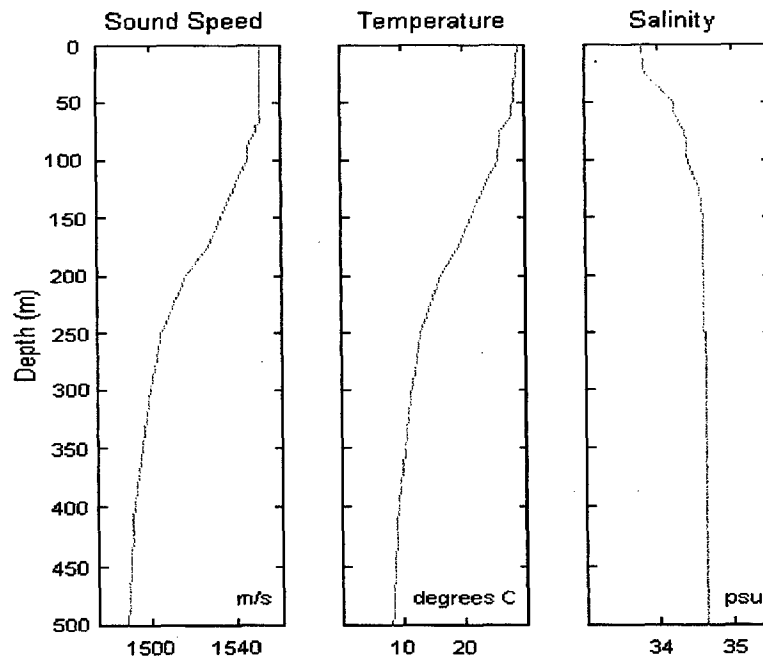


a. Wet Season

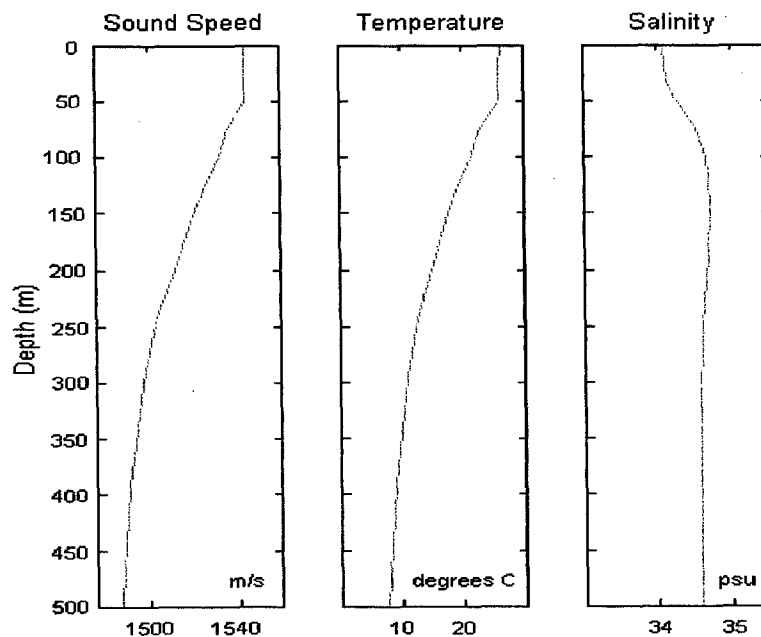


b. Dry Season

Figure 6. Typical shallow water profiles of sound speed, temperature and salinity showing well mixed conditions during (a) the wet season and (b) the dry season.



a. Wet Season



b. Dry Season

Figure 7. Typical deep water profiles of sound speed, temperature and salinity showing a sonic layer of about 70 m in (a) the wet season and about 50 m in (b) the dry season.

D. OBJECTIVES

The objectives of this thesis are to:

- i. Provide an estimation of sonar performance for a towed array operating in the generally shallow waters of the North Australian Area.
- ii. Assess the degradation of a towed array plane wave beamformer when used in shallow waters.

These objectives will be met by first investigating (Chapter II) the passive sonar equation for this area in order to arrive at a Figure of Merit (FOM). The FOM will be modeled as a function of spatially and temporally varying ambient noise levels for three different frequencies, and array gain degradation in shallow water. Also in this chapter will be a discussion of the model used to calculate the transmission loss and the inputs to the model, including a detailed discussion of the water column sound speed profile and the geoacoustic parameters of the sea bed.

A scenario relevant to possible situations encountered by a submarine of the Royal Australian Navy will be modeled and the results analyzed in Chapter III to determine the detection performance of a towed array that could be encountered in the Arafura Sea. These results will then be employed to suggest possible tactics to be considered.

Improvements in technology which can increase the probability of detection is a continuous and major goal of antisubmarine warfare. Improvements to be expected as a result of advanced signal processing techniques will be discussed in Chapter IV.

Throughout this thesis, every attempt will be made to use typical, but non-specific, values of components of the passive sonar equation. This will have the dual affect of making the thesis non-system specific and avoiding security issues. As a result, this thesis will remain unclassified.

II. METHOD

A. SCENARIOS

Because defense of the northern coastline of Australia is a primary concern, shallow water operations are certainly possible. As such, sonar performance will be examined with both source and receiver at periscope depth in shallow water areas. In addition, the effect of the shallow bottom gradients will be modeled, with propagation both up and down slope considered. In the deeper regions to the north, situations will be modeled wherein source and receiver are both within the mixed layer, both below the layer, or on either side of the layer. The effect of the steeper gradients of the continental slope in this region will also be considered.

The target is anticipated to be a diesel electric submarine, either at periscope depth, or operating well below the layer. Hence, source depths will be at either 15 m or 200 m. Three frequencies will be investigated, 10, 50 and 300 Hz, assumed to represent broadband or tonal sources radiated by a diesel electric submarine during snorkeling or high speed operations. The detecting platform will be assumed to be a COLLINS class submarine towing a linear array at either shallow (15 m) or deeper (200 m) depths.

1. Sonar Equation

Our measure of sonar performance will be taken as the maximum range for which a detection can occur with a specified probability of detection. This is the range at which the signal excess (SE) = 0, i.e., the range where the transmission loss (TL) has increased to a value numerically equal to the figure of merit (FOM). The FOM is essentially the difference between the signal and noise levels for a specific sonar setup:

$$TL = SL - AN + AG - DT = FOM$$

where AN is the Ambient Noise
 AG is the Array Gain and
 DT is the Detection Threshold

The FOM is the amount of energy available for detection and by definition the initial detection range (IDR) occurs at that range where the TL has decayed to a value equal to the FOM. The various terms of the sonar equation can be found discussed in length in various references including Urick (1983), Seto (1971) and Kinsler et al. (1982).

2. Figure of Merit Values

A source level of 130 dB will be used for all three frequencies. This generic value is midway between modern, quiet submarines (traveling on batteries) and the older, yet still commonly employed, Russian-made units such as Victor III's or Foxtrots, particularly when snorkeling (Marschall et al., 1995). This value is also slightly less than measurements of post World War II submarine source levels (Urick, 1983). A constant value for each of the frequencies also allows for quantitative comparisons to be made.

Ambient noise values in the NAA have been extensively investigated by Cato (1976, 1997). Ambient noise values in the frequency range of this study (Figure 8) indicate that Arafura Sea ship traffic noise (Cato, 1997) in the south is relatively quiet, increasing slightly towards the deep water in the Aru Basin. In general, ship traffic noise is probably not a significant component of the ambient noise field in this area (Cato, 1976). Attenuation of the low frequency traffic noise in the Arafura region is obvious when compared to that in the Tasman and Coral Seas or to the Indian Ocean. The fact that traffic noise is so low in this area implies that the major component of the ambient noise field will be the wind dependent component (sea surface agitation) and hence exhibit a seasonal variability. This is not an unexpected result as Burgess and Kewley (1983) have reported a significant wind dependence on ambient noise levels in other areas around Australia. During the dry winter season mean wind speeds of $10\text{--}12\text{ ms}^{-1}$ (Williams, 1992) equate to noise levels based on the Cato (1997) curves (Figure 8) of 72-79 dB. Similarly, for the wet summer season, the lower mean $8\text{--}10\text{ ms}^{-1}$ wind speeds result in a 1-2 dB reduction in the noise level to 70-78 dB (Table 1). Other more transient ambient noise sources such as precipitation and bioacoustic noise sources will be ignored in this study, though these intermittent noise sources can raise ambient noise levels by at least 12 dB (Kelly et al., 1985) or as much as 30 dB (Cato, 1997) above background levels.

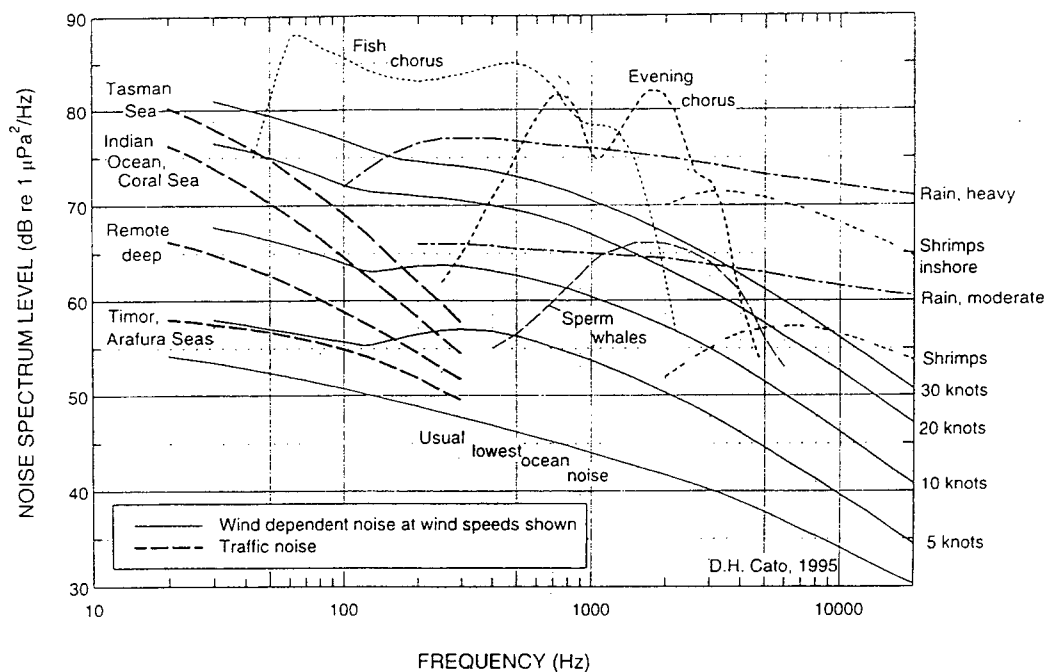


Figure 8. Sea noise prediction curves for Australian waters. (Adapted from Cato, 1995)

Table 1. Selected Ambient Noise Values (dB). (Adapted from Cato, 1995)

Frequency (Hz)	Northern Arafura Sea	Southern Arafura Sea
Dry Season		
10	79	78
50	77	77
300	73	72
Wet Season		
10	78	77
50	76	75
300	70	70

An array gain (AG) of 6 dB will be used assuming that $AG = 10 \log M$ where M is the number of hydrophones in the array. Additionally, for simplicity AG is assumed to be constant over the frequency range being investigated.

The detection threshold is about -8 dB for a standard LOFARGRAM display (Marschall et al., 1995) and this value will be used in this study as representative of typical conditions.

B. FIGURE OF MERIT

The resulting figure of merit, listed for frequency, location (shallow, southern area or deeper, northern area) and season (wet or dry monsoon) is listed below. The FOM varies due only to changes in ambient noise as a function of frequency, season and location (Table 2).

Table 2. Figure of Merit (dB).

Frequency (Hz)	Location	Season	Figure of Merit (dB)
10	South	Dry	66
10	South	Wet	67
10	North	Dry	65
10	North	Wet	66
50	South	Dry	67
50	South	Wet	69
50	North	Dry	67
50	North	Wet	68
300	South	Dry	72
300	South	Wet	74
300	North	Dry	71
300	North	Wet	74

The reasonably arbitrary selection of values for the figure of merit leads to an assumed uncertainty in the initial detection range. This uncertainty can be accounted for in part by assuming one standard deviation of error around the FOM value. A value of ± 6 dB was selected based on the arbitrariness associated with the FOM terms.

C. OCEAN DATA

The bulk of the oceanographic sound speed data was supplied by the Australian Oceanographic Data Centre (AODC).

1. Water Column

The temperature data were primarily acquired by reversing thermometers while salinities were chemically determined from bottle data. Station information not only contained the data of interest (date, position, temperature, salinity and sound-speed), but they also contained extraneous data such as ship details, weather information, phosphate and silicate profiles, to name a few. The sound speeds were calculated from the temperature and salinity profiles using the Chen and Millero relationship (1983).

The data represent values obtained during 17 different years, dating as far back as 1929. Only 127 complete profiles were available for the entire Arafura Sea, an indication of the paucity of data in the area. From Figure 9 it is obvious, however, that very little interannual variation is evident, particularly in the upper levels when the profiles are grouped by season.

Since so little variation was present from year to year, it was possible to select an actual profile to represent the typical water column. Profiles were categorized by season and individual profiles selected to represent each season and location. When selecting profiles, attention was paid to ensure that outlying profiles were not included, ensuring not only that sound-speed profiles were representative, but that temperature and salinity profiles were typical. It is important to note that though profiles within a particular transect may not be synoptic, the lack of interannual variation makes it possible to treat the profiles as such.

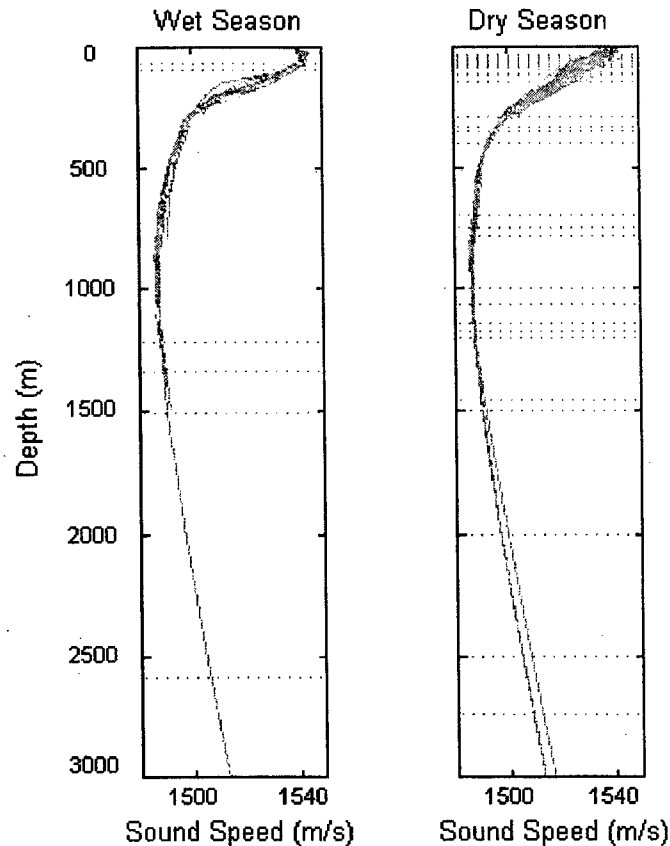


Figure 9. Overlaid SSP's for the wet and dry seasons showing lack of interannual variability. All years available are displayed, the dashed horizontal lines are the sea bottom of a particular profile.

a. Analysis

Examination of the temperature and salinity profiles indicates that the mixed layer depths (MLD) are of the order 30 to 50 m in the dry season, deepening to 50 to 70 m in the wet season. This means that profiles obtained in shallow water (~50 m) are invariably well mixed to the bottom. Often the profiles in areas where the water depth is slightly greater than these MLD (i.e., 100 m) are also well mixed in either season.

At very low frequencies, sound ceases to be efficiently trapped in the mixed layer. This occurs when the frequency approaches the cut off frequency (COF) for the first mode of normal mode theory, i.e., when the wavelength of the sound becomes too large to "fit" into the duct (Urlick, 1983, p 151). The cutoff frequency can be approximated from;

$$\text{COF} = 1500 / (8.5 * 10^{-3} * H^{3/2})$$

where H is the layer depth in meters

It follows then that the cut off frequency in the dry season is approximately 698 Hz (for MLD = 40 m) reducing to 379 Hz (for MLD = 60 m) in the wet season. In instances where the 100m deep water is well mixed to the bottom, the cut off frequency would be 176 Hz (see Table 3). Refraction of acoustic energy in the sea bottom may appreciably extend these cutoff values to lower frequencies.

Of the three frequencies to be modeled (10, 50 and 300 Hz), it is likely that only the highest frequency will experience extended ranges due to trapping in the water column. For shallow water areas the entire water column may act as a wave guide with the sea bed providing a much sharper boundary than the weak thermocline. Hence, one must consider trapping in the mixed layer as well as trapping over the depth of the water column when considering propagation in shallow water. Overall, the propagation of very low frequencies is expected to be poor due to cutoff considerations, despite the fact that the initial spreading loss is much less at short ranges in shallow water than deeper water where spherical spreading prevails (Marschall et al., 1995).

Another factor that will reduce detection ranges, particularly at the lowest frequency, is surface-decoupling (Pederson et al., 1975) as a result of surface interference when the source depth is above the surface-decoupling depth. Energy reflected from the sea-surface reduces the power output of a source due to destructive interference at all three frequencies, though to a lesser extent at the two higher frequencies. Assuming the surface-decoupling depth (Z_{sd}) for 10, 50 and 300 Hz (Pederson et al., Figure 33) are 250, 70 and 20 m, respectively, the following decoupling loss values can be expected (Table 4 and Figure 10).

Table 3. Relevant Cutoff Frequencies.

Depth (m)	Cutoff Frequency (Hz)	For Mixed Layer	For Water Column Depth
40	698	Dry season	-
50	499	-	South
60	379	Wet season	-
100	176	100 m water depth in dry season	South

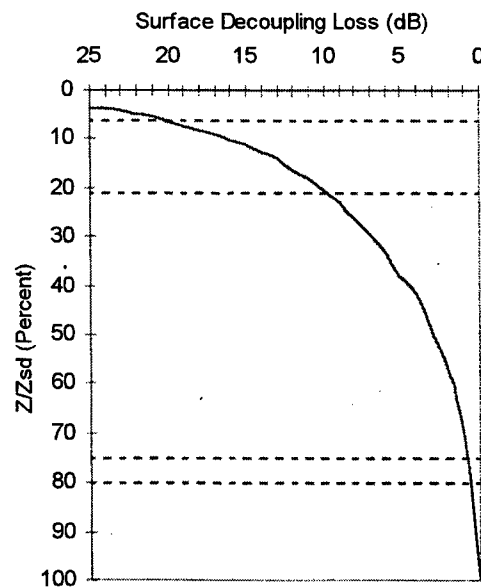


Figure 10. Surface-decoupling loss vs the ratio of source depth (Z) to surface-decoupling depth (Z_{sd}) (linear approximation). (Adapted from Pedersen et al., 1975)

Table 4. Surface-decoupling loss.

Frequency (Hz)	10		50		300	
Z (m)	15	200	15	200	15	200
Z _{sd} (m)	250	250	70	70	20	20
(Z/Z _{sd}) * 100	6	80	21.4	286	75	1000
Loss (dB)	20	1	9	0	1	0

Therefore, it can be expected that the detection range, particularly at 10 Hz, will be adversely effected by surface-decoupling.

An additional factor in the deeper water of the Aru Basin is the presence of a deep sound channel with an axial depth of 800 m and a channel width of the order 1500 m. In this instance (Urick, 1983)

$$\text{COF} = 1500 / (8.5 * 10^{-3} * (W/2)^{3/2})$$

where W is the sound channel width in meters

In this case the cut off frequency is of the order of 8 Hz and as such there should be extended ranges in the deep sound channel at all frequencies. Because the depth of the channel is much deeper than the anticipated source depths and because of the limited extent of the basin, this deep sound channel is not tactically important and its role will not be investigated in this study.

The depth of the Aru Basin, and certainly the Weber Basin, also allows for convergence zone (CZ) formation under ray theory, the critical depth being of the order of 1600 m. CZ's can be anticipated to occur at intervals of 60 km.

b. Transects

The FEPE model (to be described below) calculates transmission loss as a function of depth and range. Therefore it becomes necessary to produce transects or radials along which the water column and bottom parameters may vary. Six transects were considered, based on the ocean bottom profile. Four cases assumed a flat bottom, and as such the water depth was considered to be invariant along the transect. The other two cases (Figure 11) involved sloping bottom profiles. In these cases the water column was allowed to vary with range. The transects modeled are indicated by the darker lines on Figure 5.

D. GEOACOUSTIC DATA

The geoacoustic data were derived from a variety of sources. Twenty-six point samples of seabed bottom type data were supplied by the Australian Oceanographic Data Centre obtained from RAN Hydrographic Office surveys. Additionally, seabed sound-speed profiles as deep as 900 m inferred from refraction profiling were obtained (Hall, 1996) as were values obtained from measurement of sediment cores (Dunlop, 1995). Sediment properties observed during the Arafura Sea bottom backscattering experiment (Briggs et al., 1989) were noted. Australian Bureau of Mineral Resources sediment distribution charts were examined for bottom sediment classification by Marschall et al. (1995). Marschall et al. also accessed well logs, seismic sections from publications of the West Australian Petroleum Pty. Ltd., the Earth Resources Foundation at the University of Sydney data, and journals of the APEA and of the Geological Society of Australia. They concluded that the geoacoustic properties could be represented by a single parameterization for the entire NAA. The Marschall et al. bottom study was therefore the basis of the model used in this study following the approach of Scanlon (1995). The data of Marschall et al. was spatially varied, however, in order to reflect the observations of Hall (1996), Dunlop (1995), Briggs et al. (1989) and the Hydrographic Office.

Bottom sediment type can also be used to provide a geoacoustic model (Hamilton, 1980). The sound speed profile in the sediment for compressional waves is needed. When combined with the sediment density and attenuation as functions of depth, the model provides for both reflection and refraction by the bottom.

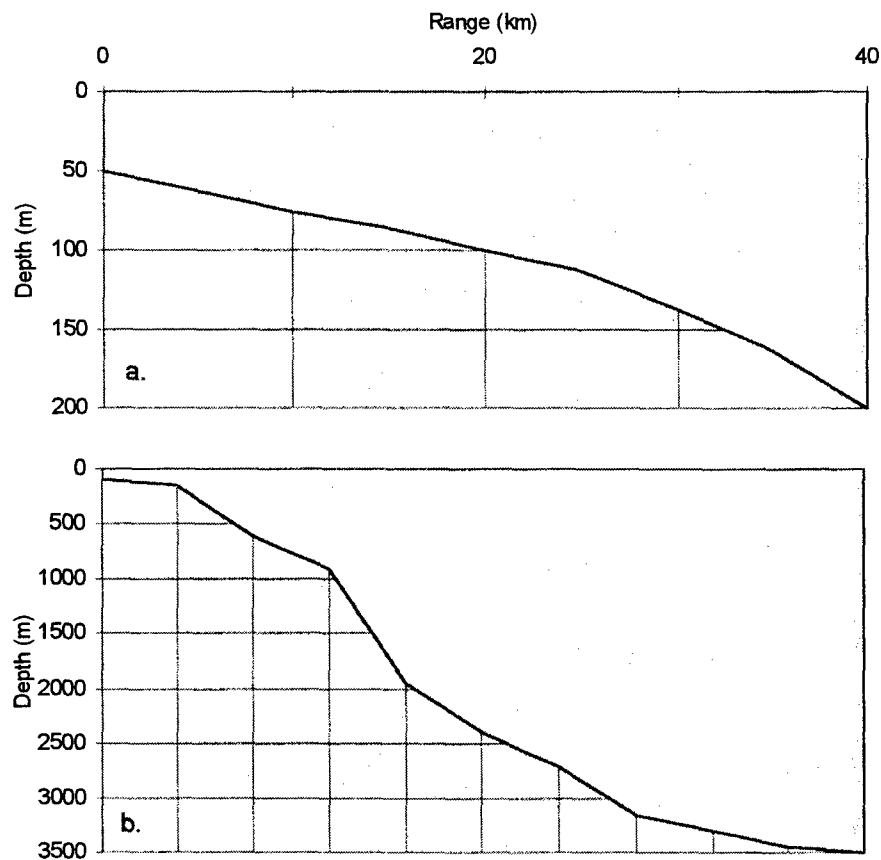


Figure 11. Model bottom profiles for (a) the shallow, gentle sloping shelf in the south and (b) the deeper, steeper shelf in the north.

The combination of the oceanographic sound-speed profiles and the inferred/observed geoacoustic profiles formed the basis of the FEPE input fields. The sediment profiles utilized in the FEPE input files are listed in Table 5.

The spatial distribution of marine sediments for the Arafura Sea is complex. Generally the bottom consists of a thin veneer of calcareous, coarse-grained mixtures of sand, silt and mud, overlying older Plio-Pleistocene sedimentary sequences (Marschall et al., 1995) of mixed terrestrial and marine character (Briggs et al., 1989).

Table 5. Sediment model sound speed, attenuation and density profiles for the Arafura Sea.

Depth Below Bottom (m)	Sound Speed (m s ⁻¹)	Attenuation (dB m ⁻¹ kHz ⁻¹)	Bulk Density (g cm ⁻¹)
Southern Arafura Sea			
0	1710	1.53	0.33
205	4475	2.40	0.18
1150	4800	2.53	0.02
3750	5700	2.62	0.02
5500	6400	2.70	0.02
Northern Arafura Sea			
0	1507.0	1.53	0.33
20	1541.0	1.58	0.28
160	1560.0	2.15	0.25
300	2500.0	2.50	0.02
936	2800.0	2.50	0.02
1150	4800.0	2.52	0.02
3750	5700.0	2.62	0.02
5500	6400.0	2.70	0.02

The bottom, being a sand/silt/clay mix (Briggs et al., 1989), is therefore neither reflective, nor absorptive, lying somewhere in between. It therefore can be anticipated that both reflection and absorption of energy by the bottom will affect predicted transmission loss and sonar performance.

E. FINITE ELEMENT PRIMITIVE EQUATION (FEPE) MODEL

FEPE is a highly developed acoustic Primitive Equation code for time harmonic sound propagation in an ocean overlying a sediment that supports only the propagation of compressional waves (Collins, 1988). The model contains the

latest improvements in PE modelling, including high accuracy for wide propagation angles and large depth variations in the acoustic parameters, high accuracy for problems involving range dependence (including steep bottom slopes), a highly-accurate self starter, and an algorithm for solving tridiagonal systems that is efficient for problems involving variable ocean depth.

FEPE solves for time harmonic sound propagation in marine and land seismic environments where the sediments and the geology support both compressional and shear waves. This means that all elastic wave types are considered including interface waves. FEPE is powerful due to its ability to deal with nearly all practical two-dimensional problems where the geology and the water column are functions of both depth and range. The sound field transmission is modeled as three-dimensional. Other input parameters required for FEPE are listed in Table 6.

Table 6. Other FEPE input values.

Frequency (Hz)	10	50	300
Maximum Range (m)	200000	200000	200000
Minimum Range (m)	0	0	0
Range Step (m)	37.5	7.5	1.25
Skip Factor	2000	50	16
Depth Max (m)	60000	12050	7500
Depth Step (m)	18	3.75	0.625
Depth Skip Factor	5	5	5
Output Depth Max (m)	3000	3000	3000
Number of Pade Terms - N	2	2	2
Number of Pade Terms - M	1	1	1
Indicator For Starter	Gaussian	Gaussian	Gaussian
Initial PE Angle	89	89	89

III. DETECTION RANGE RESULTS AND TACTICAL CONCEPTS

A. DETECTION RANGES

Sonar performance will be analyzed based upon a comparison of the initial detection ranges. The initial detection range (IDR) is defined as the range at which the signal excess is zero for a selected probability of detection, 50%, as prescribed in defining the figure of merit. Uncertainty due to temporal and spatial variations and inaccuracies in specifying the values of each term of the FOM will be overcome by defining one standard deviation as the range over which the IDR may vary. This 1-sigma range bin has been selected to vary 6 dB either side of the FOM. The transmission loss curves can be found at Annexes A, B and C for 10, 50 and 300 Hz, respectively. The reference curve is an arbitrary TL curve where $TL = 66 + 10 \log r$, i.e., spherical spreading.

The generic system approach used in this study eliminates variables such as advanced signal processing, display equipment and operator competence. This still leaves many factors to contrast. The obvious factors are season, location and frequency.

1. Shallow Southern Waters

It should be remembered that the shallow region suffers in sonar performance due to the relatively high ambient noise levels encountered. A total of 29 scenarios were modeled for the shallow region, with the target and receiver depths at 15 m throughout. The IDR and the 1- σ range bins are listed for various frequencies and bottom depths/slopes in Tables 7 and 8.

a. Dry season

In the dry season, the initial detection range increases with increasing frequency. This is due to the cutoff frequency being well above the lower frequencies. The average IDR at 10 Hz is 1.2 km, 28.8 km at 50 Hz and 87 km at 300 Hz.

At 10 Hz, the IDR suffers dramatically as a result of surface-decoupling, with short ranges (< 2 km) that decrease with increasing water depth. The range is greater for a water depth of 50 m than for one of 200 m because energy is trapped in the 50 m water column (isothermal profile) and reflects/refracts from the bottom. In 200 m deep water, energy leaks out of the 40 m surface duct and refracts downwards to the bottom. Only limited trapping occurs and much energy is lost in bottom interactions. Propagation of energy down the slope produces IDR's five times greater than that up-slope because of the initial trapping of energy in the shallow water wave guide. For up slope propagation, the source is in deep water where spherical spreading vice cylindrical spreading initially occurs. This combines with leakage in the deeper water to produce shorter up-slope IDR's.

At 50 Hz, ranges are much greater, on average 24 times greater than at 10 Hz due to less propagation loss through surface-decoupling. Maximum IDR is achieved for water depths of 100 m for which the entire water column behaves as a wave guide. Detection ranges are not optimal at this frequency because 50 Hz is still well below the 176 Hz cutoff frequency for a 100 m water column. The IDR for the deeper 200 m is similar to that at 50 m because the mixed layer is 40 m and leakage out of the surface duct is appreciable resulting in reduced IDR's. Propagation is slightly greater than for a 50 m deep water column due to the increased bottom interactions in this shallow wave guide. At 50 Hz the up-slope propagation is slightly better than down-slope propagation perhaps due to an optimal combination of lower initial bottom loss (while in deep water) due to initially fewer bottom interactions compared to propagation starting in the shallow water.

The trend of decreasing detection range with increasing water depth observed at 10 Hz is again observed at 300 Hz. Ranges are three times greater than at 50 Hz as the frequency increases to near (water depth = 50 m) or past (water depth = 100 m) cutoff. Therefore, true ducting within the water column can occur and, as a result, vastly improved detection ranges are experienced. The maximum possible range, indicated by the standard deviation error bin, is substantial, in excess of 200 km. As a general trend, increased IDR means an increase in the width of the ± 6 dB bin as the general gradient of the TL is initially steep and decreases with distance. Up-slope and down-slope

propagation ranges are almost identical, with up-slope propagation slightly greater.

Table 7. Initial Detection Ranges, Bottom Depth, Mixed Layer Depth and 1 Standard Deviation Range Bins in Shallow Southern Arafura Sea Waters for the Dry Season. Source and receiver at 15 m. Arrows indicate variation along transect.

Freq (Hz)	Bottom Depth (m)	MLD (m)	IDR (km)	1 σ Band (km)	Band Width (km)
10	50	50	2.1	0.6-5.2	4.6
10	100	100	0.7	0.2-3.3	3.1
10	200	40	0.5	0.1-1.6	1.5
10	50→200	50→100→40	2.1	0.7-6.8	6.1
10	200→50	40→100→50	0.4	0.2-2.9	2.7
50	50	50	27.0	15.0-57.0	42.0
50	100	100	42.0	15.0-88.0	73
50	200	60	29.0	11.0-89.0	78.0
50	50→200	50→100→40	20.0	12.0-30.0	18.0
50	200→50	40→100→50	26.0	12.0-36.0	24.0
300	50	50	128.0	54.0-193.0	139.0
300	100	100	98.0	35.0-200+	165.0
300	200	40	93.0	27.0-200+	173.0
300	200→50	40→100→50	29.0	12.0-39.0	27.0

b. Wet season

In the wet season the initial detection range increases with increasing frequency. Environmentally, the primary difference between the two seasons is not related to seasonal SSP changes but rather to ambient noise being less due to generally lighter winds during the wet season. The average IDR for the wet season at 10 Hz is 1.4 km, 37.8 km

at 50 Hz and 111 km at 300 Hz. In general, the IDR is greater during the wet season for most of the TL runs due to the decreased FOM inherent to the wet season.

Table 8. Initial Detection Ranges, Bottom Depth, Mixed Layer Depth and 1 Standard Deviation Range Bins in Shallow Southern Arafura Sea Waters for the Wet Season. Source and receiver at 15 m. Arrows indicate variation along transect.

Freq (Hz)	Bottom Depth (m)	MLD (m)	IDR (km)	1 σ Band (km)	Band Width (km)
10	50	50	2.5	0.7-5.9	5.2
10	100	100	0.9	0.2-4.2	4.0
10	200	60	0.6	0.2-2.0	1.8
10	50→200	50→100→60	2.3	0.7-6.5	5.8
10	200→50	60→100→50	0.5	0.2-4.2	4.0
50	50	50	31.0	18.0-73.0	55.0
50	100	100	58.0	22.0-120.0	98.0
50	200	60	50.0	17.0-130.0	113.0
50	50→200	50→100→60	22.0	14.0-31.0	17.0
50	200→50	60→100→50	28.0	19.0-47.0	22.0
300	50	50	173.0	62.0-200+	138.0
300	100	100	162.0	67.0-200+	133.0
300	200	60	144.0	42.0-200+	158.0
300	50→200	50→100→60	29.0	25.0-114.0	89.0
300	200→50	60→100→50	46.0	22.0-62.0	40.0

As was evident during the dry season, at 10 Hz, the initial detection ranges decrease with increasing water depth. Ranges in the wet season at 10 Hz are on average 17% better than in the dry season as a result of the decreased ambient noise, though overall ranges are still significantly reduced as a result of surface-decoupling. Again, the up-slope propagation is poorer than the down-slope, this time by a factor of 4.6.

As was seen in the dry season at 50 Hz, the well mixed 100 m deep transect offers the greatest detection range at this frequency. Ranges are almost 27 times greater than at 10 Hz and 31% greater than the dry season at the same frequency. The transmission loss curves are nearly the same in each season; this increase in IDR is due primarily to the gain of 2 dB in the figure of merit. Up-slope propagation is better than down-slope, as expected, by a factor of almost 1.3.

The pattern for the dry season at 300 Hz is repeated in the wet season. Detection ranges decrease with increasing water depth, are 27% greater than was the case in the dry season, and are 2.9 times farther than those at 50 Hz. The substantial increase in IDR results from the initial low rate of TL in shallow water. Ranges in shallow water, during the wet season, are the greatest to be expected at any time over the entire Arafura Sea. The phenomenal ranges predicted are a pleasing result.

2. Deep Northern Waters

In the deep water regions to the north, both source and receiver were varied in depth to simulate different strategies. Both were placed at 15 m depth to represent operations at periscope depth. For situations where the mixed layer depth is of the order of 50 m, two submarines (source and receiver) both below the layer are modeled using a depth of 200 m. The source and receiver at 15 m and 200 m, respectively, models the cross layer situation of shallow source/deep receiver. A total of 37 different scenarios were run for the northern, deeper part of the Arafura Sea. The initial detection ranges for the northern waters are listed in Tables 9 and 10 for the dry and wet seasons, respectively.

a. Dry season

The northern, deeper reaches of the Arafura Sea suffer increased ambient noise during the dry season as has previously been discussed. In the dry season, initial detection range in the north of the Arafura Sea increases with increasing frequency but not nearly as dramatically as in shallow water. Average IDR at 10 Hz is 0.9 km, 2.1 km at 50 Hz and 4.1 km at 300 Hz. In addition to duct leakage, a consequence of low frequency cutoff considerations, and surface-decoupling loss (especially and 10 Hz), propagation

in deep water is significantly shorter than in shallow water due to the near spherical initial rate of TL inherent to deep water propagation. The low FOM exacerbates the problem resulting in IDR's of 5 km or less in most situations. This difference in detection capability between shallow and deep water is especially noted at 50 and 300 Hz.

Table 9. Initial Detection Ranges, 1 Standard Deviation Range Bins and 1st Convergence Zone for Deeper Northern Arafura Sea Waters in the Dry Season. MLD is 40 m with a cutoff frequency of 698 Hz. Arrows indicate variation along a transect.

Freq (Hz)	Source Depth (m)	Receiver Depth (m)	Bottom Depth (m)	IDR (km)	1 σ Band (km)	Band Width (km)	CZ (km)
10	15	15	3500	0.1	0.0-0.2	0.2	-
10	15	200	3500	0.4	0.3-0.6	0.6	-
10	200	200	3500	1.6	1.1-2.1	1.0	-
10	15	15	100-3500	0.2	0.0-0.9	0.9	-
10	15	200	100-3500	1.9	0.6-4.6	4.0	-
10	15	15	3500-100	0.2	0.1-0.3	0.2	-
50	15	15	3500	0.5	0.4-0.6	0.2	-
50	15	200	3500	1.4	1.1-1.7	0.6	-
50	200	200	3500	1.9	1.1-3.6	2.5	-
50	15	15	100-3500	3.5	1.5-4.9	3.4	-
50	15	200	100-3500	2.7	1.5-11.2	9.7	-
300	15	15	3500	0.5	0.2-0.6	0.4	59
300	15	200	3500	2.0	1.8-4.0	2.2	62
300	200	200	3500	2.5	2.0-4.5	2.5	48
300	15	15	100-3500	4.0	3.0-4.6	1.6	-
300	15	200	100-3500	6.5	4.0-12.0	8.0	-

At 10 Hz, with propagation in the surface duct affected by low frequency cutoff considerations and high loss to surface-decoupling, it is not surprising that the greatest ranges occur when source and receiver are both below the layer. A slight advantage occurs when the receiver is below the layer if the target is in the layer. The deep sound channel, as has been discussed, has reasonable detection ranges, but is tactically not useful. The propagation of energy up or down the slope at 10 Hz is identical unless the receiver has the advantage of being down the slope, below the source.

At 50 Hz the trend of greatest range for source and receiver both below the layer continues. Average ranges at 50 Hz are 2.3 times greater than those at 10 Hz. The down-slope propagation at this frequency, however, is the reverse of that at 10 Hz, with somewhat greater ranges expected if both source and receiver are in the layer, the result of more efficient trapping of energy at 50 Hz.

As frequency increases, propagation in the surface duct is less affected by cutoff problems and the initial detection range increases. The ranges predicted for 300 Hz are another two times greater than those at 50 Hz. Ranges are greatest for source and receiver below the layer. Convergence zone propagation is viable at 300 Hz, with greatest range achieved for a shallow source in the layer. Down-slope detection of shallow depth targets is optimized when the receiver is placed at depths below the layer

b. Wet season

With transmission loss curves being so similar in each season, the main factor in initial detection range becomes the reduction in ambient noise. The resultant lower figure of merit produces only somewhat greater ranges in the wet season than in the dry season (< 1 km difference at each frequency). Average initial detection range at 10 Hz is 1.0 km, at 50 Hz is 2.9 km and at 300 Hz is 5.8 km.

Propagation at 10 Hz shows no substantial improvement in propagation loss due to surface-decoupling and low frequency cutoff effects. Ranges slightly improve for source or receiver below the layer. Ranges are 11% greater than those for the same frequency and area during the dry season due only to reduced ambient noise. Down-slope propagation is marginally better than up-slope propagation, a balance between energy lost into the sediment

layer and spherical spreading associated with propagation commencing in deep water.

50 Hz ranges are 2.9 times greater than those for 10 Hz. Ranges again increase with depth of the receiver. Cross-layer ranges exceed those for source and receiver both within the layer due to leakage of sound from the surface mixed layer.

Finally, 300 Hz average ranges during the wet season exceed those at 50 and 10 Hz in the deeper northern waters, two times greater than those at 50 Hz, and almost 42% farther than during the dry season. Again it is

Table 10. Initial Detection Ranges, 1 Standard Deviation Range Bins and 1st Convergence Zone for Deeper Northern Arafura Sea Waters in the Wet Season. MLD is 60 m with a cutoff frequency of 379 Hz.

Freq (Hz)	Source Depth (m)	Receiver Depth (m)	Bottom Depth (m)	IDR (km)	1 σ Band (km)	Band Width (km)	CZ (km)
10	15	15	3500	0.2	0.1-0.3	0.2	-
10	15	200	3500	0.5	0.3-0.7	0.4	-
10	200	200	3500	1.6	1.1-2.1	1.0	-
10	15	15	100-3500	0.3	0.0-0.9	0.9	-
10	15	200	100-3500	2.1	0.8-4.8	4.0	-
10	15	15	3500-100	0.2	0.1-0.3	0.2	-
50	15	15	3500	0.5	0.3-0.7	0.4	-
50	15	200	3500	1.4	1.0-1.6	0.6	-
50	200	200	3500	2.5	1.3-3.8	2.5	-
50	15	15	100-3500	4.0	1.5-6.0	4.5	-
50	15	200	100-3500	5.0	2.0-10.5	8.5	-
300	15	15	3500	1.5	0.5-2.1	1.6	61
300	15	200	3500	2.8	1.0-3.2	2.2	-
300	200	200	3500	4.0	3.0-5.0	1.7	48
300	15	15	100-3500	5.0	4.0-6.0	2.0	-
300	15	200	100-3500	8.5	6.5-10.9	4.4	-

advantageous for a receiver to be down the slope below a target. As has been the trend, ranges are greatest below the layer due to in-layer cutoff problems, however the convergence zone is particularly marked for a shallow in-layer source, peaking some 10 dB above the figure of merit, as opposed to 6 dB for the wet season. Convergence zone propagation is possible for all the deep water profiles except when source and receiver are on opposite sides of the thermocline, and as would be expected, does not occur where the bottom shoals to depths shallower than the critical or conjugate depth (Urlick, 1983). The deep sound channel continues to have extended ranges, as would be expected.

B. DISCUSSION

1. Ducting/Frequency

It is not surprising that with the layer depth required to trap a 300 Hz signal being 70 m, the model run at 300 Hz in 50 m water depth (in the wet or quieter season) demonstrates the greatest predicted range. This is the classic ducting situation, producing extended ranges and occurs to some extent at 50 Hz also. In general, the one standard deviation range bin width increases with increased IDR, due to the shape of the transmission loss curves.

10 Hz propagation in both deep and shallow water produces similar initial detection ranges with both areas suffering strong duct leakage and surface-decoupling losses (and to varying degrees bottom interaction losses), severely reducing the predicted initial detection ranges, i.e., values of 2 km or less.

In the deeper water, with layer depths of the order of 40 to 60 m, it follows that 300 Hz propagates farther for in-layer sources and receivers. However, due to the rapid, near-spherical rate of TL in deep water, ranges are generally short and similar regardless of source or receiver depth, season or frequency. Both cross layer ranges and below layer ranges increase with increasing frequency due to better trapping of energy in the mixed layer and within the water column, respectively, with shorter acoustic wavelengths.

2. Season

The absolute value of the sound speed varies slightly with season but the profile shape remains relatively invariant between seasons. The greatest effect of the wet and dry seasons on predicted detection ranges is therefore due to the seasonal change in ambient noise. Winds are generally stronger in the dry season, effectively decreasing the figure of merit by 1-2 dB. Of the 34 cases run, only four demonstrate lower IDR's in the wet season than the dry season, and these only occurred when the initial detection ranges were short. Figure 12 shows the trend towards longer ranges in the wet season than in the dry season.

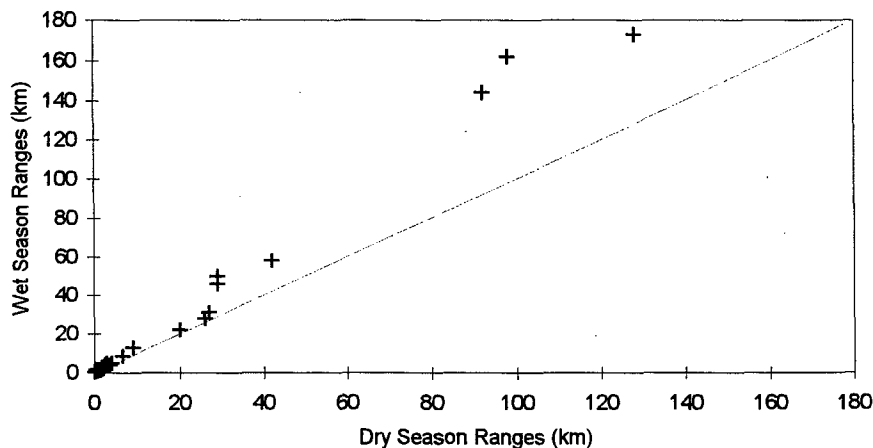


Figure 12. Bias of initial detection ranges in favor of the wet season, for both deep and shallow waters.

3. Convergence Zone

Convergence zone propagation is possible in the far north utilizing the Aru and Weber Basins but only at 300 Hz. Duct leakage and bottom refraction losses combine to inhibit CZ propagation at 10 Hz and 50 Hz.

4. Up-slope/down-slope propagation

Propagation of energy down the slope yields generally better ranges than that up the slope. This is related to the initial trapping of acoustic energy in a shallow depth wave guide in contrast to propagation initially occurring in deep water where the trapping of the radiated energy from the source is not nearly as efficient. Advantage can be taken of the leakage of energy from the surface mixed layer by placing the receiver below the layer.

C. TACTICAL CONCEPTS

As a result of these findings, there are a number of ways that a submarine commander could take advantage of conditions within the Arafura Sea.

1. It will be unlikely that should a conflict develop, the submarine commander can choose the season. However, he should remember that ranges are generally somewhat better in the wet season due to reduced ambient noise levels in response to the lower wind speeds of this season.

2. It is generally better to listen at 300 Hz because of the greater ranges predicted and the effects of surface-decoupling at lower frequencies. This has the disadvantage in that modern submarine construction will likely continue to reduce tonal sources at this and similar frequencies, and it will become necessary to exploit tonals at lower frequencies which are more difficult to damp. If advantage is to be taken of convergence zone propagation, 300 Hz is the only option.

3. When conducting operations over a sloping sea floor, generally greatest advantage can be achieved by listening in deeper water, below the layer, for targets in shallow water.

4. On the shelf, extended ranges can be expected, with greatest ranges in shallower water.

5. Of primary significance, when both source and receiver are to the north in deep water (a possible tactic to gain early detection) the chance of acoustic detection is very low. This means that for early detection of targets

approaching from north, some other form of detection may be required such as active sonar. Conversely, should the target reach the shallow shelf waters, detection chances improve dramatically, particularly at the higher frequency, and as such moored arrays could be deployed as an early warning system.

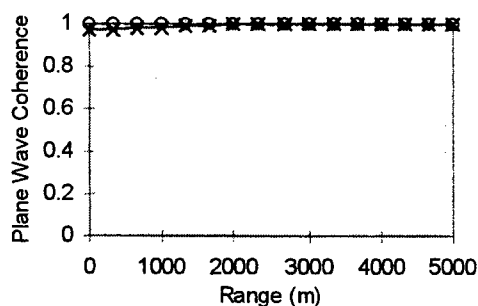
IV. ADVANCED SIGNAL PROCESSING ALGORITHMS

The purpose of this chapter is to provide an overview of current advanced signal processing algorithms that could be employed by the RAN to overcome performance degradation of plane wave-beamformers in shallow water. Much of the information of this chapter can be found in Nuttall and Wilson (1991), Wilson (1995), Fabre and Wilson (1995) and Wilson and Veenhuis (1997).

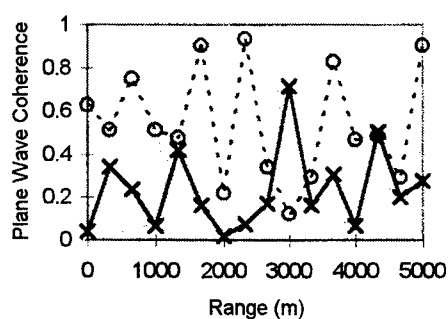
A. CONVENTIONAL BEAMFORMING (CBF)

Plane-wave beamformers suffer significant, fundamental performance degradation in shallow water for horizontal arrays (Wilson and Veenhuis, 1997) due to decreased horizontal (plane wave) signal coherence inherent in shallow water. Normal modes, not plane waves, dominate propagation in shallow water acoustic propagation. Propagating normal modes, leaky modes interacting with the bottom sediment, and continuous modes define a complex propagation pattern in shallow water that results in a wave front that is not plane. Linear arrays have many hydrophones that are time or phase delayed generally based upon the plane wave assumption. Beamformed energy levels are obtained by adding the time or phase delayed components of the energy received by each hydrophone of the array. When the incoming energy is not a plane wave, the signal energy of each hydrophone is not added coherently in the beamforming process. From a passive sonar equation viewpoint, this incoherent summation causes the array signal gain (ASG) to be degraded from the theoretical value of $20 \log M$, where M is the number of hydrophones in the array. The ASG degradation is most severe for frequencies near the array design frequency, or when the signal arrival angle occurs at bearings other than broadside.

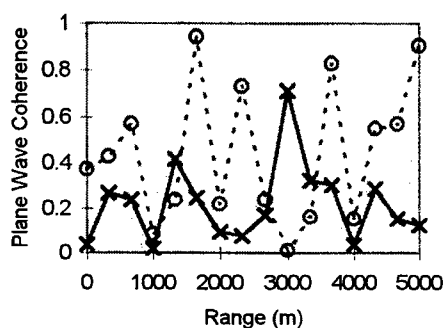
This is illustrated in Figure 13 where the coherence between the signal and the plane wave model decreases significantly, as the relative bearings of the target from the array vary from 90° (broadside) to 0° (endfire) (Wilson and Veenhuis, 1997). Figure 13 shows the plane wave spatial coherence response of a 48-element towed array to a simulated signal in shallow water for ranges of 0 to 5 km.



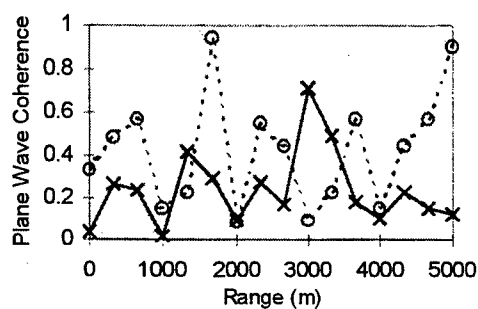
a. 90° - (Broadside)



b. 60°



c. 30°



d. 0° - (Endfire)

Figure 13. Normalized plane-wave beamformer output as a function of the angle of arrival of acoustic energy to a linear array. $\times \Rightarrow$ design frequency, $o \Rightarrow$ 21% of design frequency. (Adapted from Wilson and Veenhuis, 1997)

This decreased plane wave signal coherence is caused by the time/phase delays from the propagation of normal modes being significantly different from the time/phase delays of a plane wave. When the range from each hydrophone to the source varies across the array (i.e., for off broadside beams), the difference in time/phase delays between normal modes and plane waves is significant, especially near design frequency.

Unfortunately, current operational and developmental line arrays of Australia and all other navies utilize conventional beamforming theory. As emphasis is switched to littoral warfare in shallow water, this significant degradation in ASG needs to be addressed.

B. MATCHED-FIELD PROCESSING

Matched-field processing (MFP) is a beamforming technique which allows for the detection and localization of an acoustic source in range and depth using passive sonar arrays (Wilson and Veenhuis, 1997). MFP enhances, or augments, the performance of plane wave beamforming in situations where the acoustic arrival is not approximated well by a single plane wave (e.g., in shallow water). Such situations occur when vertical arrays are used in deep water or when horizontal or vertical arrays are utilized in shallow water where multipath arrivals or normal modes dominate the arrival structure.

MFP supplements the plane-wave beamformer detection and tracking capability by not requiring a change of course or speed to arrive at a tracking solution for a horizontal line array. Matched-field processing utilizes the multiple acoustic arrival paths in the shallow water environment to estimate target bearing, range and depth. It utilizes steering vectors which are generated from a propagation model with the source located at a specified range and depth, instead of at infinite range as is the case in plane-wave beamforming. The fact that MFP requires no course changes to estimate the target bearing, range and depth makes it a promising solution to the problem.

Recent improvements in computer hard- and soft-ware have made this computationally intensive method a viable supplement to conventional ranging methods such as the Spiess Plot (1958) and Ekelund ranging (1958).

C. INVERSE BEAMFORMING

The plane wave beamformer, we have seen, needs to be augmented by IBF to optimize performance in shallow water. Inverse beamforming (IBF) provides a spikier beam algorithm for MFP and a sophisticated, robust M of N tracker to track MFP correlation peaks in range/depth space (Wilson, 1995). IBF was derived from considerations of the environmental

acoustic properties of the measured ambient noise field as opposed to the simplified ideal signal and noise conditions normally assumed in classical detection theory.

IBF is comprised of three algorithms, the Fourier integral method (FIM) beamformer, a data threshold technique called the eight nearest neighbor peak picker (ENNPP) and a sophisticated three-dimensional M of N tracker (Wilson, 1995). The Fourier integral method contains 3 dB less area within its beam pattern than conventional beamforming and thus provides 3 dB more array gain than conventional beamforming for a line array. The ENNPP identifies relative peaks in the MFP correlation surface as correlation coefficients are generated. A peak is defined as a correlation coefficient greater than that of all eight cells around a particular range/depth cell. The M of N tracker is a three-dimensional tracker which operates in conjunction with ENNPP to track persistent peaks on the frequency/azimuth (FRAZ) surface for plane wave beamforming or on the range/depth surface for MFP. The M of N tracker reduces false target detections that do not satisfy the M of N criteria. Combined, the ENNPP and the M of N tracker provide enhanced performance when used in frequency/azimuth space as a plane wave post processing algorithm or in range/depth space for MFP.

D. PERFORMANCE ADVANTAGE

MFP performance is significantly better than plane-wave beamforming in shallow water for higher frequencies, for more reflective bottom types in shallow water, and for relative target bearings away from the broadside beams (Wilson and Veenhuis, 1997). The MFP algorithm, in conjunction with ENNPP and the M of N tracker, performs well in shallow water or in a deep water environment where many multipaths dominate the environment. IBF as a plane-wave beamformer, performs well at very low frequencies (VLF), in mud/silt-clay bottoms, and at beams near broadside. Performance of any plane-wave beamformer, including IBF, is severely degraded in shallow water for relative bearings away from the broadside beams, particularly at higher frequencies (Willson and Veenhuis, 1997).

IBF has been shown (Wilson, 1995) to produce a 3 dB array noise gain (ANG) advantage over conventional beamforming under ideal conditions. Inverse beamforming results in a narrower beamwidth and the 3 dB ANG relates to

less area under the beam pattern curve when compared to conventional beamforming. This means that there is less noise in the signal to noise ratio. The 3 db ANG advantage leads to significant (> 10 dB) minimum detectable level (MDL) performance gains using IBF (Fabre and Wilson, 1995).

Conventional beamforming is the optimum detector for ideal acoustic field conditions. Unfortunately, in the real world these conditions rarely exist. IBF has been successful in detecting signals of very low levels in measured ocean data and during real-time, at-sea, submarine experiments (Wilson and Veenhuis, 1997). The passive IBF algorithms resulted in 10 to 15 dB of detection gain over the performance of the submarine array sonar system. Additionally, IBF provided high bearing resolution tracking solutions at very low frequencies where the towed array aperture was of the order of one wavelength. Therefore, the IBF approach to MFP is expected to greatly outperform the well known conventional, or Bartlett, MFP algorithm.

Three potential solutions to the problem of plane-wave degradation in shallow water are possible: make the array aperture shorter, keep the array oriented so that broadside bearings point toward the threat axis, or use inverse beamforming with MFP. The first two options suffer from poorer performance or operational constraints. Short arrays are operationally undesirable. Tactically, one can not count on targets approaching from broadside. Therefore, the use of inverse beamforming (IBF) with MFP becomes necessary due to its' proven advantage over conventional beamforming. The advantage of 10 to 15 dB of detection gain is an important consideration, particularly as the design of modern submarines improve.

V. CONCLUSIONS AND RECOMMENDATIONS

A. CONCLUSIONS

The goal of this thesis was to investigate the performance of a towed, low frequency, passive sonar array operating in the generally shallow waters of the North Australian Area in line with the recent switch in emphasis to littoral warfare. This was achieved by combining actual sound speed profiles of the Arafura Sea with geoacoustic profiles of sediments of the area. A finite element primitive equation model produced transmission loss curves of sound energy at three frequencies, 10, 50 and 300 Hz, propagating through the area represented by the resultant composite profiles. The data were separated into the two dominant climatic regimes, the wet and dry monsoon seasons, and typical ambient noise conditions provided expected initial detection ranges for each. Various scenarios were considered that could be encountered by a COLLINS class submarine of the Royal Australian Navy. Source and receiver depths were varied between 15 and 200 m to model in-, cross- and below-layer situations. Transects were constructed perpendicular to the bottom contours and up- and down-slope scenarios were modeled.

Very low frequencies (less than or equal to 10 Hz) produce poor initial detection ranges, in both the deep and the shallow waters of the Arafura Sea, due to a combination of surface-decoupling, leakage from the surface duct and bottom interactions. In deep water, IDR's increase with increasing frequency. However, the dominance of spherical spreading produces generally short ranges (less than 6 km on average). The seasonal dependence on initial detection range is primarily a factor of ambient noise, with greater ranges possible in the wet season when wind speeds are lower producing lower ambient noise levels. However, the seasonal ambient noise difference is small (~1-2 dB) causing the IDR to vary slightly (less than 1 km in deep water) from one season to the other.

Propagation is much better on the shallow shelf compared to deep areas because the initial reduction in energy level approaches cylindrical spreading in shallow water vice spherical spreading in deep water. Initial detection ranges improve with increasing frequency, particularly in shallow waters where the sound energy is

partially or completely trapped within the water column. This is true at 50 and 300 Hz but not at 10 Hz where IDR's are nearly similar. Here TL is controlled by surface-decoupling and bottom interaction (refraction in sediment layers) factors.

An additional goal of this study was to investigate possible improvements in detection gain through modern advanced signal processing techniques. As submarine design improves, tonals at higher frequencies are likely to be eliminated producing the requirement to improve detection at lower frequencies. The breakdown of the plane-wave assumption in shallow water causes degradation of a conventional towed array plane wave beamformer.

The combination of Matched Field Processing with Inverse Beamforming has been demonstrated to provide an improvement in array noise gain of between 10 and 15 dB. IBF is the combination of three algorithms, the Fourier integral method beamformer, the eight nearest neighbor peak picker data threshold technique and a three-dimensional M of N tracker.

B. RECOMMENDATIONS

Advantage could be taken of the propagation distances predicted in the shallow waters of the Arafura Shelf. Moored arrays strategically positioned could provide an indication of incursions into Australian coastal waters.

The acquisition of towed arrays for submarines (or indeed surface units) of any country considering shallow water littoral operations should include investigation into the acquisition of modern signal processing equipment and software.

Additionally, in order to gain full knowledge of the NAA environment, the transmission of active sonar in the Arafura Sea should also be investigated.

REFERENCES

Bird, E.C.F. and M.L. Schwartz, "The World's Coastline", Van Nostrand Reinhold Company, New York, 1950, 1985.

Bureau of Meteorology Climate Centre, "Climatic Averages of Australia", Australian Government Publishing Service, Canberra, 1995.

Briggs, K.B., P. Fleischer, W.H. Jahn, R.I. Ray, W.B. Sawyer and M.D. Richardson, "Investigation of High-Frequency Acoustic Backscattering Model Parameters: Environmental Data from the Arafura Sea", NORDA Report 197, Stennis Space Center, MS, 1989.

Burgess, A.S. and D.J. Kewley, "Wind-generated Surface Noise Levels in Deep Water East of Australia", *J. Acoust. Soc. Am.*, 73(1), 201-210, 1983.

Cato, D.H., "Ambient Sea Noise in Waters Near Australia", *J. Acoust. Soc. Am.*, 60, 320-328, 1976.

Cato, D.H., "Cato Curves", unpublished, 1995.

Cato, D.H., "Features of Ambient Noise in Shallow Water", Proceeding of the International Conference on Shallow Water Acoustics, Beijing, April, 1997.

Changery, M.J., C.N. Williams, M.L. Dickenson and B.L. Wallace, "Joint USN/USAF Climatic Study of the Upper Atmosphere", National Climatic Data Center Global Analysis Branch, Asheville, 1989.

Chen, C.T. and Millero F.J., "Algorithms for Computation of Fundamental Properties of Seawater", NODC UNESCO Technical Papers, UNESCO, Section 9, 46, 1983.

Church, J.A. and A.M.G. Forbes, "Circulation of the Gulf of Carpentaria, I", *Aust. J. Mar. Freshw. Res.*, 34, 1-10, 1983.

Collins, M.D., "FEPE User's Guide", NORDA Technical Note TN-365, Naval Ocean Research and Development Activity, Stennis Space Center, 1988.

Dibb, P., Defence White Paper, "The Dibb Report - Defending Australia", Commonwealth of Australia, Canberra, 1987.

Dunlop, J.I., "Measured Acoustic Properties of Sediment Cores from Sites 1817 and 9003", MRL-DSTO, Commonwealth of Australia, Pyrmont, 1995.

Ekelund, J.J., "A Means of Passive Range Detection", Commander Submarine Forces, Atlantic Fleet, Quarterly Information Bulletin, Summer 1958.

Fabre, J.P. and J.H. Wilson, "Minimum Detectable Level Evaluation of Inverse Beamforming using Outpost SUNRISE Data", *J. Acoust. Soc. Am.*, 98, 3262-3278, 1995.

Grey, W.M., "Tropical Cyclone Genesis", *Atmos. Sci. Paper* 234, Colorado State University, Fort Collins, Colorado, 121, 1975.

Hall, M.V., "Measurement of Seabed Sound Speeds from Head Waves in Shallow Water", *IEEE Ocean Eng*, 21 (4), 413-422, 1996.

Hamilton, E.L., "Geoacoustic Modeling of the Sea Floor", *J. Acoust. Soc. Am.*, 68(5), 1313-1340, 1980.

Kelly, L.J., D.J. Kewley and A.S. Burgess, "A Biological Chorus in Deep Water Northwest of Australia", *J. Acoust. Soc. Am.*, 77(2), 508-511, 1985.

Kinsler, L.E., A.R. Frey, A.B. Coppins and J.V. Sanders, "Fundamentals of Acoustics", John Wiley and Sons, New York, 1982.

Marschall, D.L., J.M. Fabre, R.A. Marschall, J.H. Wilson, J.E. Paquin, N.H. Gholson, A.R. Collins, J. Uusioja and D.C. Herringshaw, "Remote Acoustic Surveillance System Feasibility Study", 1995.

Matzkows, A., "Narama for OBERON Class Submarines", *Royal Australian Navy News*, 4 (8), 13, May 1997.

Mitchell, S.K. and K.C. Focke, "The Roll of the Seabottom Attenuation Profile in Shallow Water Acoustic Propagation", *J. Acoust. Soc. Am.*, 73(2), 465-473, 1983.

Neal, A.B. and G.J. Holland, "Australian Tropical Cyclone Forecasting Manual", Bureau of Meteorology, Melbourne, October 1977.

National Geophysical Data Center, "Digital Relief of the Surface of the Earth", Data Announcement 88-MGG-02, NOAA, Boulder, Colorado, 1988.

Net Resources International, Naval Technology Defence Industries Home Page, London, 1996.

Nuttall, A.H. and J.H. Wilson, "Estimation of the Acoustic Field Directionality by use of Planer and Volumetric Arrays via the Fourier Series Method and the Fourier Integral Method", *J. Acoust. Soc. Am.*, 90, 2004-2019, 1991.

Pederson, M.A., D.F. Gordon and D. White, "Low-frequency Propagation Effects for Sources or Receivers Near the Ocean Surface", Naval Undersea Center, San Diego, 1975.

Rand McNally and Company, "Quick Reference World Atlas", Rand McNally, New York, 1995.

Scanlon, G.A., "Estimation of Bottom Scattering Strength from Measured and Modeled AN/SQS-53C Reverberation Levels", Master's Thesis, Naval Postgraduate School, Monterey, 1995.

Schmitz, W.J. Jr., "On the World Ocean Circulation: Volume II - The Pacific and Indian Oceans / A Global Update", Woods Hole Oceanographic Institution Technical Report WHOI-96-08, 1996.

Seto, W.W., "Theory and Problems of Acoustics", McGraw-Hill, New York, 1971.

Spiess, F.N., "Determination of Target Location and Motion from Bearings Only", *Underwater Acoustics*, 8 (2), 237-243, 1958.

Thurman, H.V., "Introductory Oceanography", 8th Edition, Prentice-Hall, New Jersey, 208-209, 1997.

Tomczak, M. and J.S. Godfey, "Regional Oceanography: an Introduction", Pergamon, London, 190-191, 1994.

Urlick, R.J., "Principles of Underwater Sound", 3rd Edition, McGraw-Hill, New York, 1983.

Williams, M., "Regional Forecasting", Bureau of Meteorology Training Centre Course Notes, Melbourne, 57-62, 1992.

Wilson, J.H., "Applications of Inverse Beamforming Theory", *J. Acoust. Soc. Am.*, 98, 3250-3261, 1995.

Wilson, J.H. and R.S. Veenhuis, "Shallow Water Beamforming with Small Aperture, Horizontal, Towed Arrays", *J. Acoust. Soc. Am.*, 101, 384-394, 1997.

Wolanski, E., P. Ridd and Inoue M., "Currents Through Torres Strait", *J. Phys. Oceanogr.*, 18, 1535-1545, 1988.

Wyrtki, K, "Indonesian Through Flow and the Associated Pressure Gradient", *J. Geophys. Res.*, 92, 12941-12946, 1987.

APPENDIX A - 10 HZ TRANSMISSION LOSS CURVES

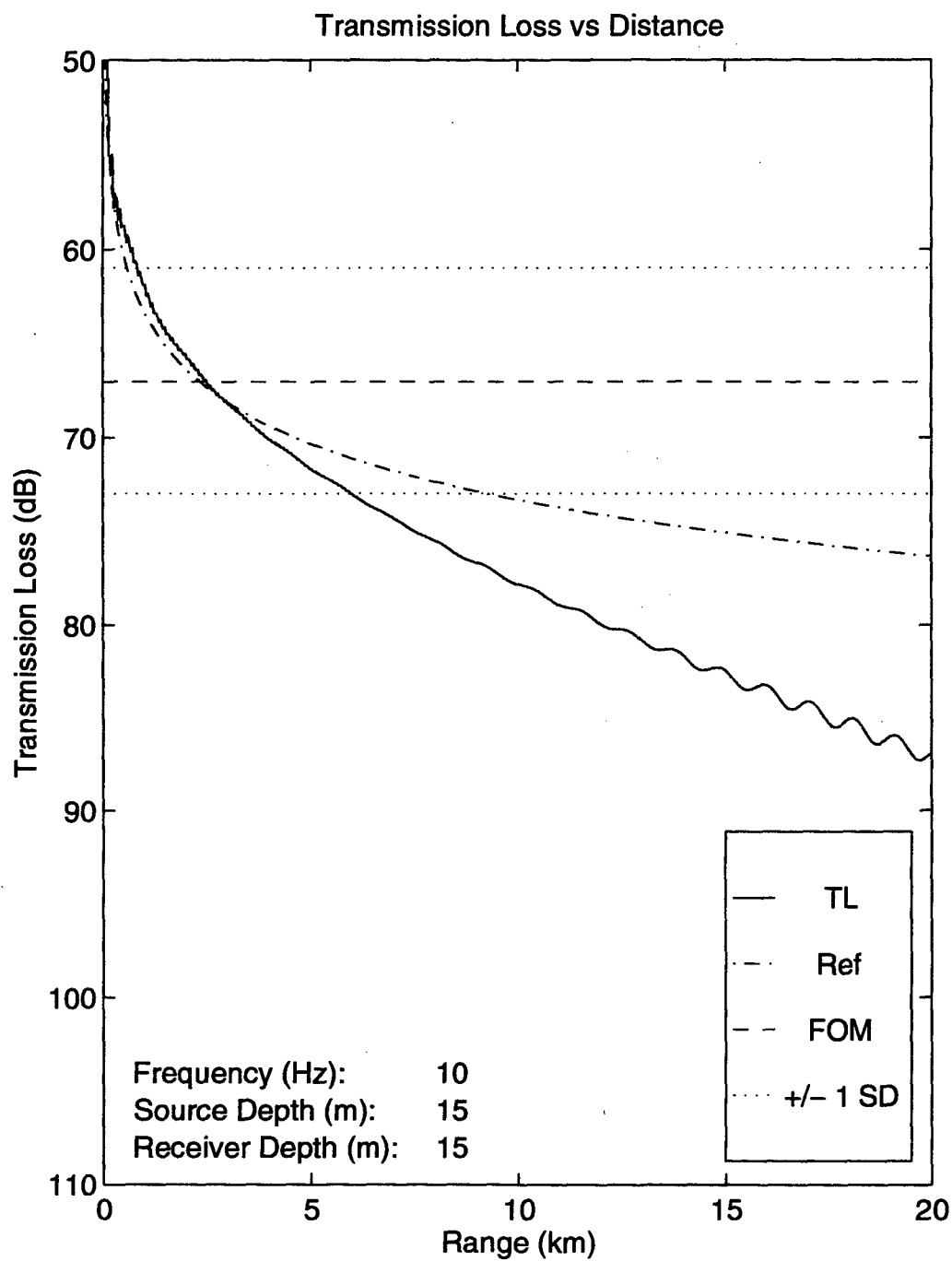


Figure 14. Transmission loss versus distance at 10 Hz for 50 m water depth in the wet season. Source and receiver at 15 m.

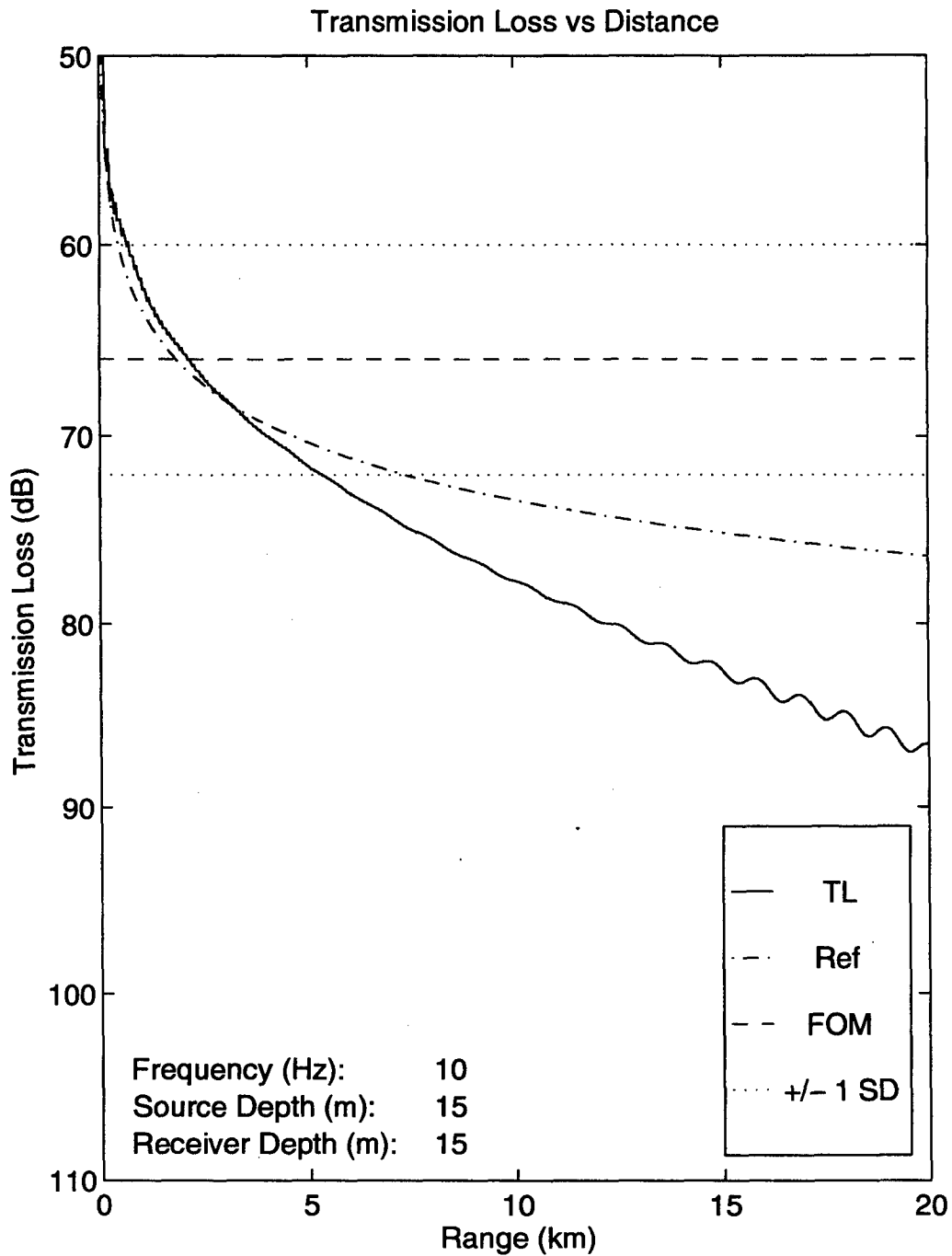


Figure 15. Transmission loss versus distance at 10 Hz for 50 m water depth in the dry season. Source and receiver at 15 m.

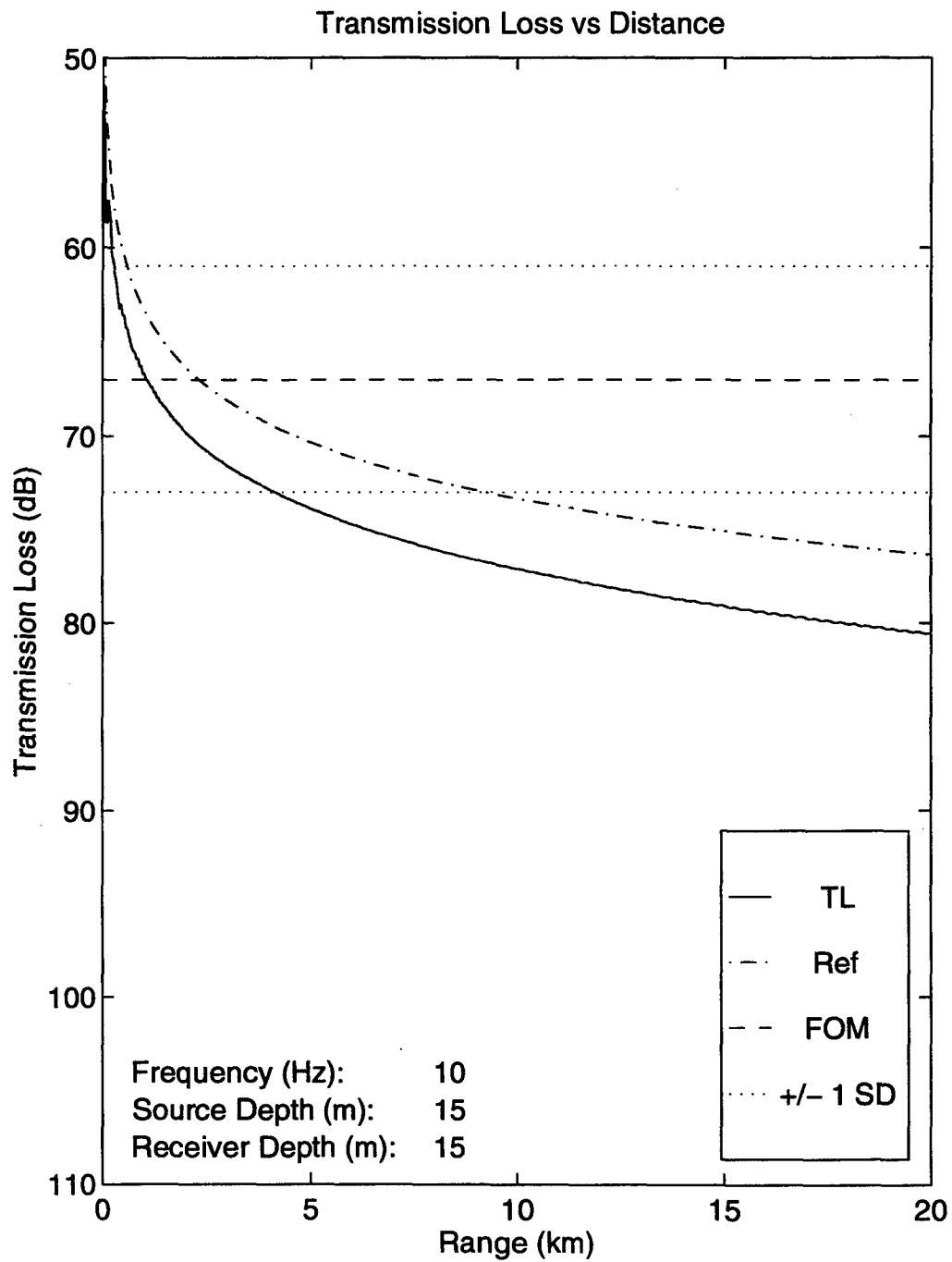


Figure 16. Transmission loss versus distance at 10 Hz for 100 m water depth in the wet season. Source and receiver at 15 m.

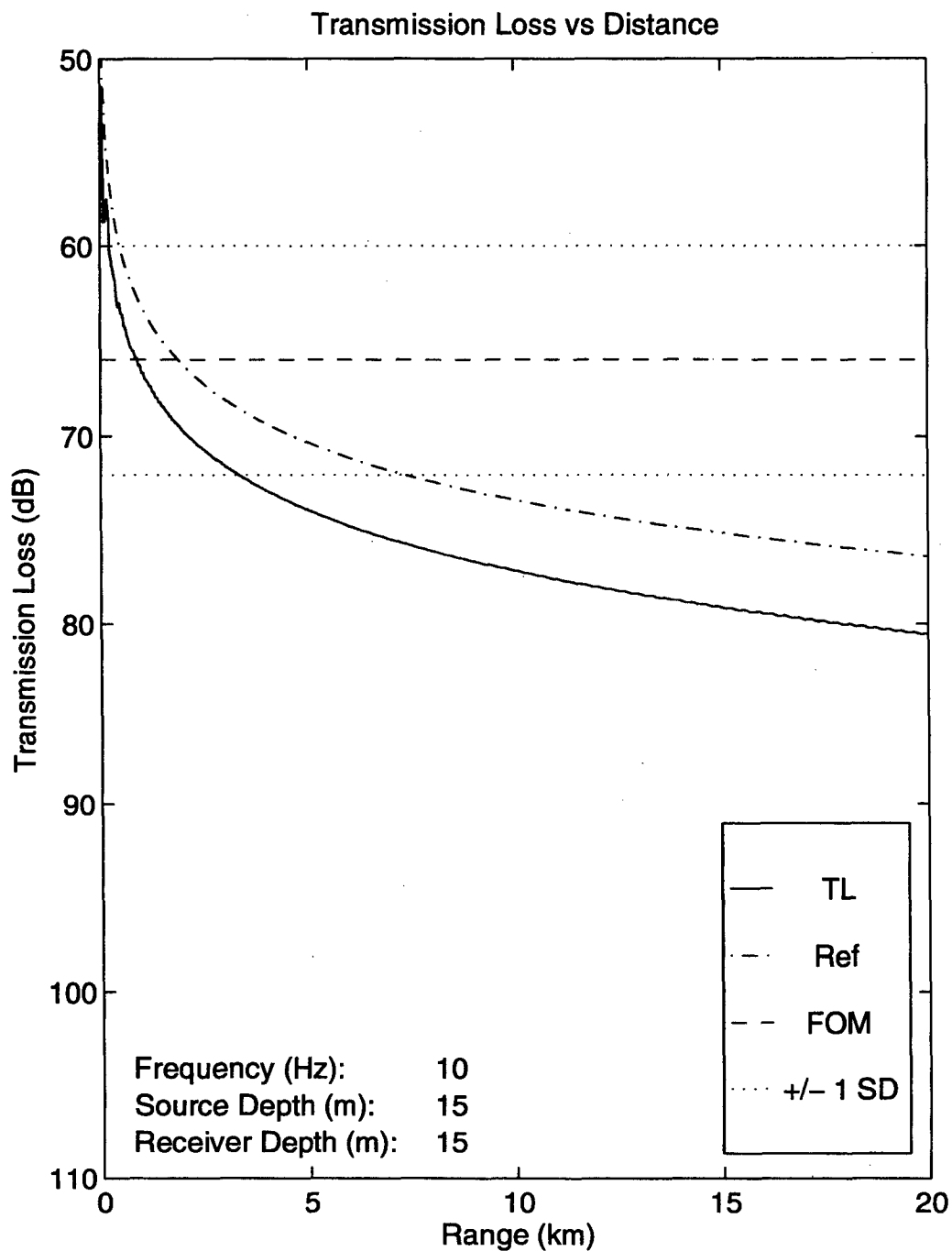


Figure 17. Transmission loss versus distance at 10 Hz for 100 m water depth in the dry season. Source and receiver at 15 m.

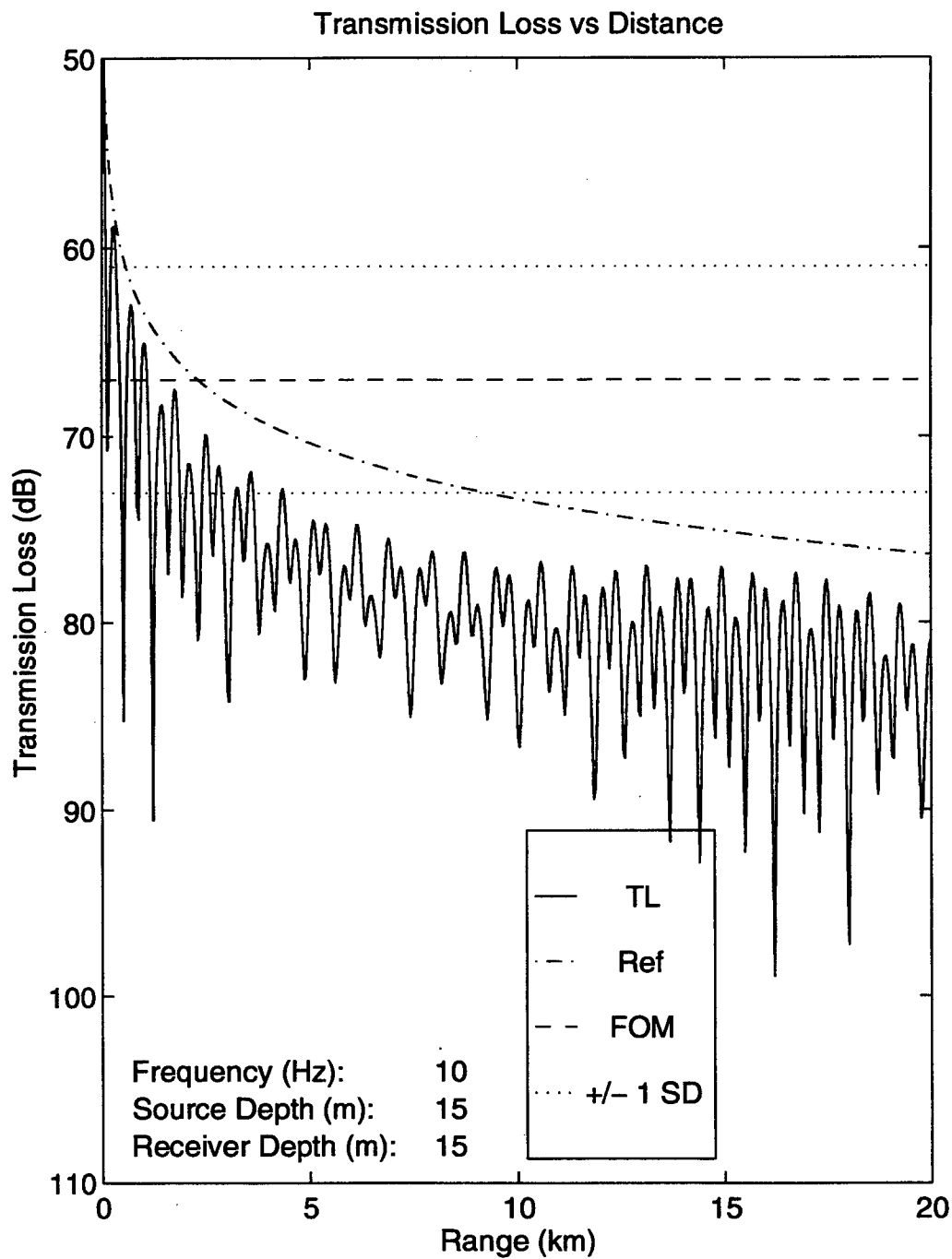


Figure 18. Transmission loss versus distance at 10 Hz for 200 m water depth in the wet season. Source and receiver at 15 m.

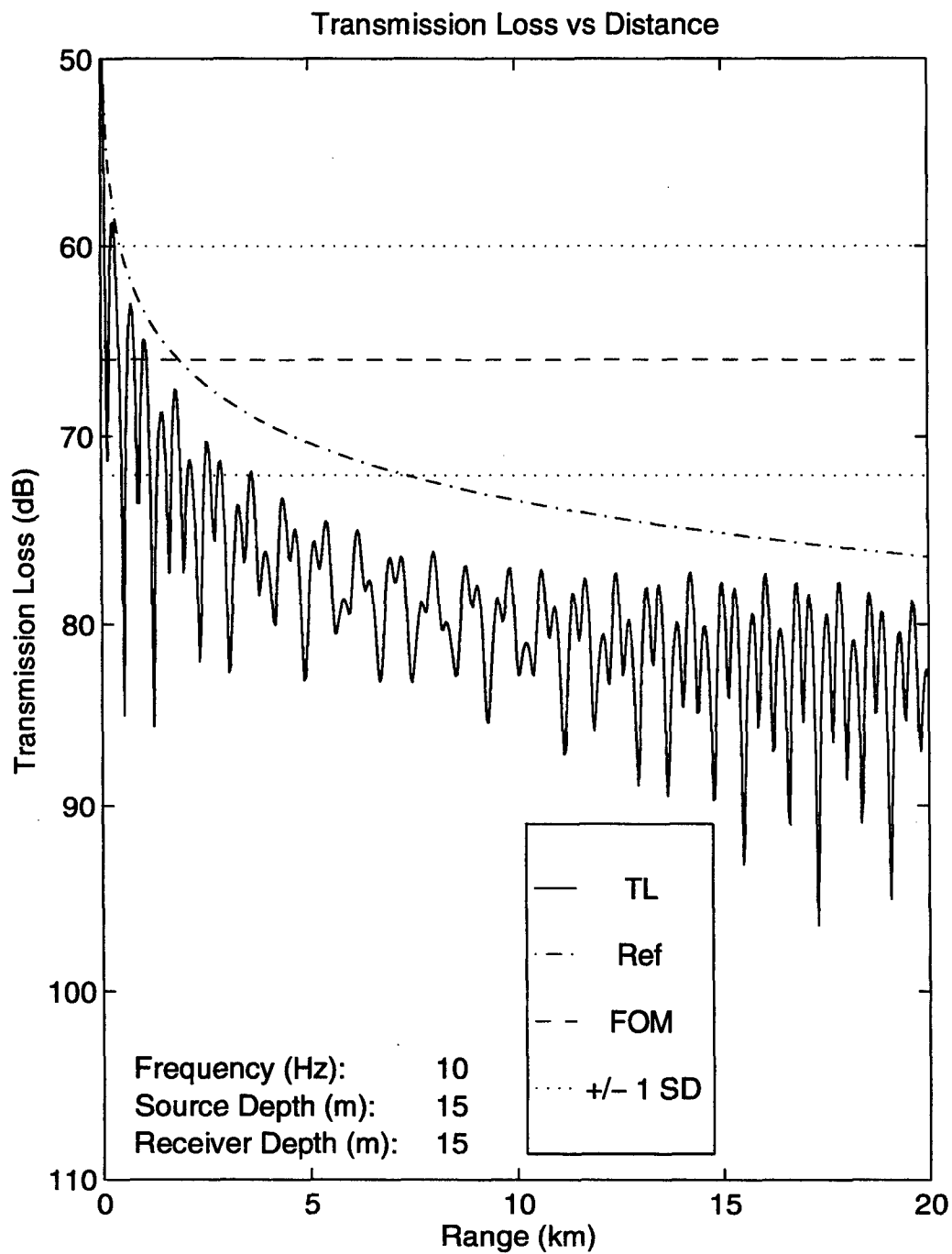


Figure 19. Transmission loss versus distance at 10 Hz for 200 m water depth in the dry season. Source and receiver at 15 m.

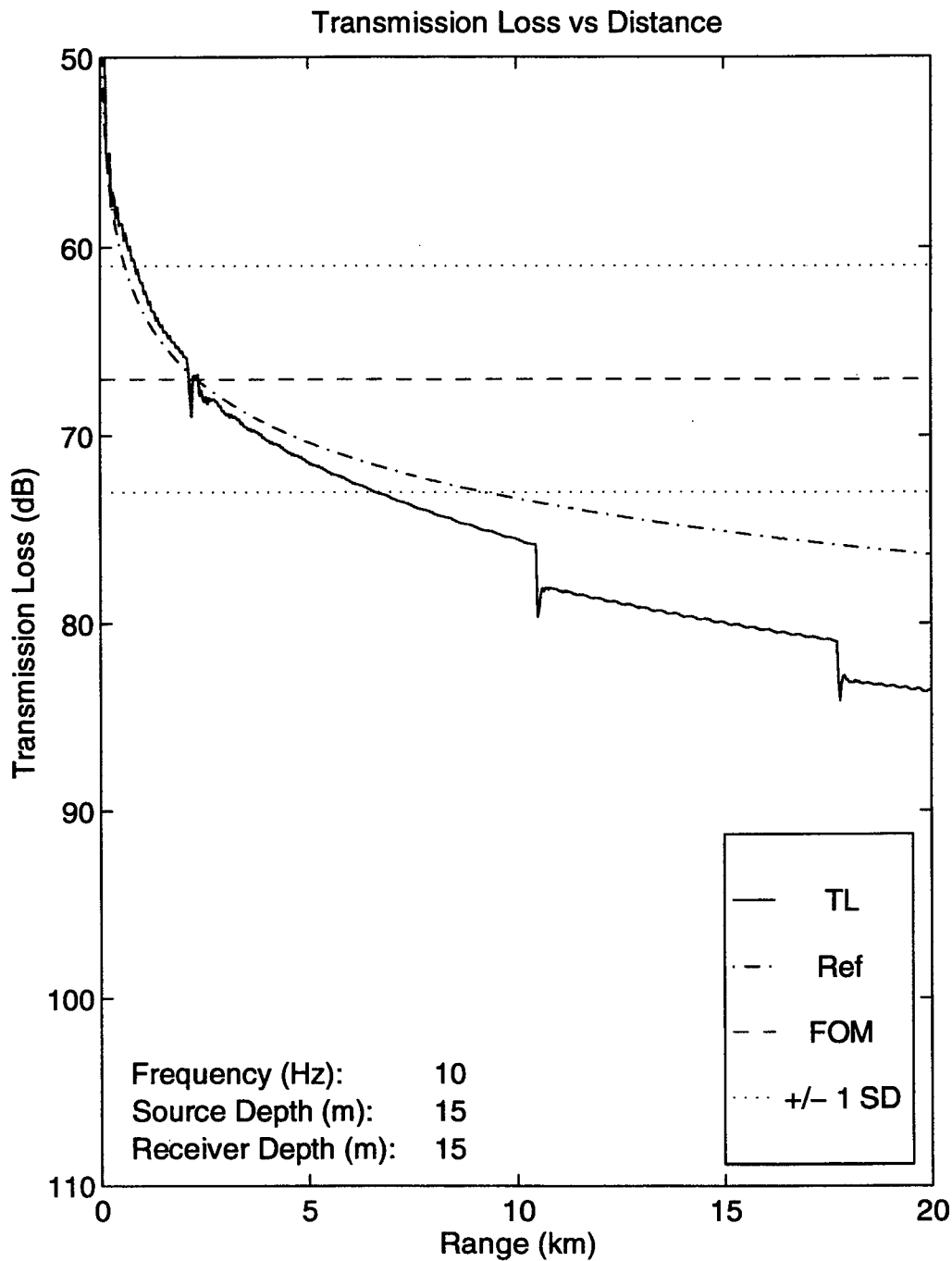


Figure 20. Transmission loss versus distance at 10 Hz for down-slope propagation in shallow water in the wet season. Source and receiver at 15 m.

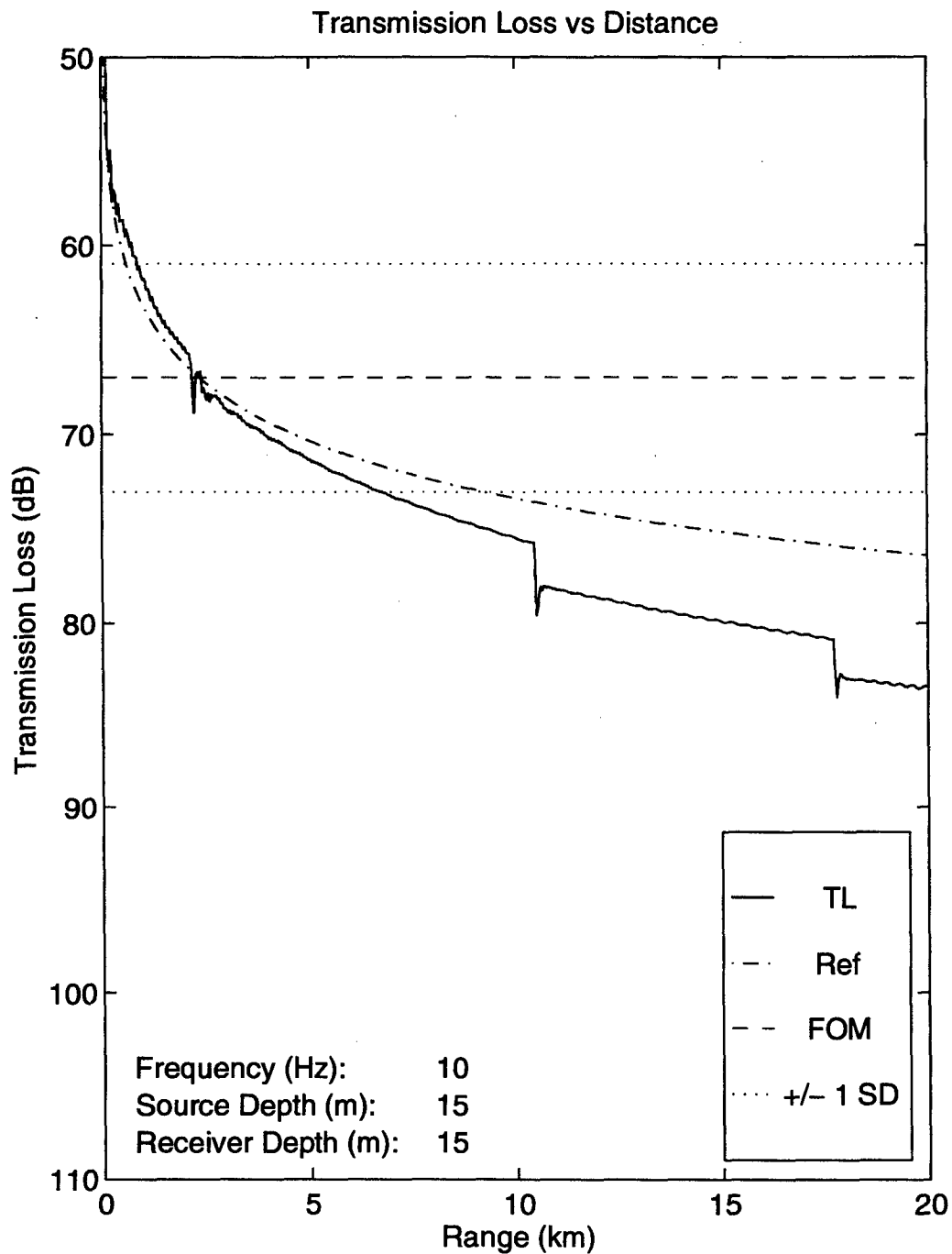


Figure 21. Transmission loss versus distance at 10 Hz for down-slope propagation in shallow water in the dry season. Source and receiver at 15 m.

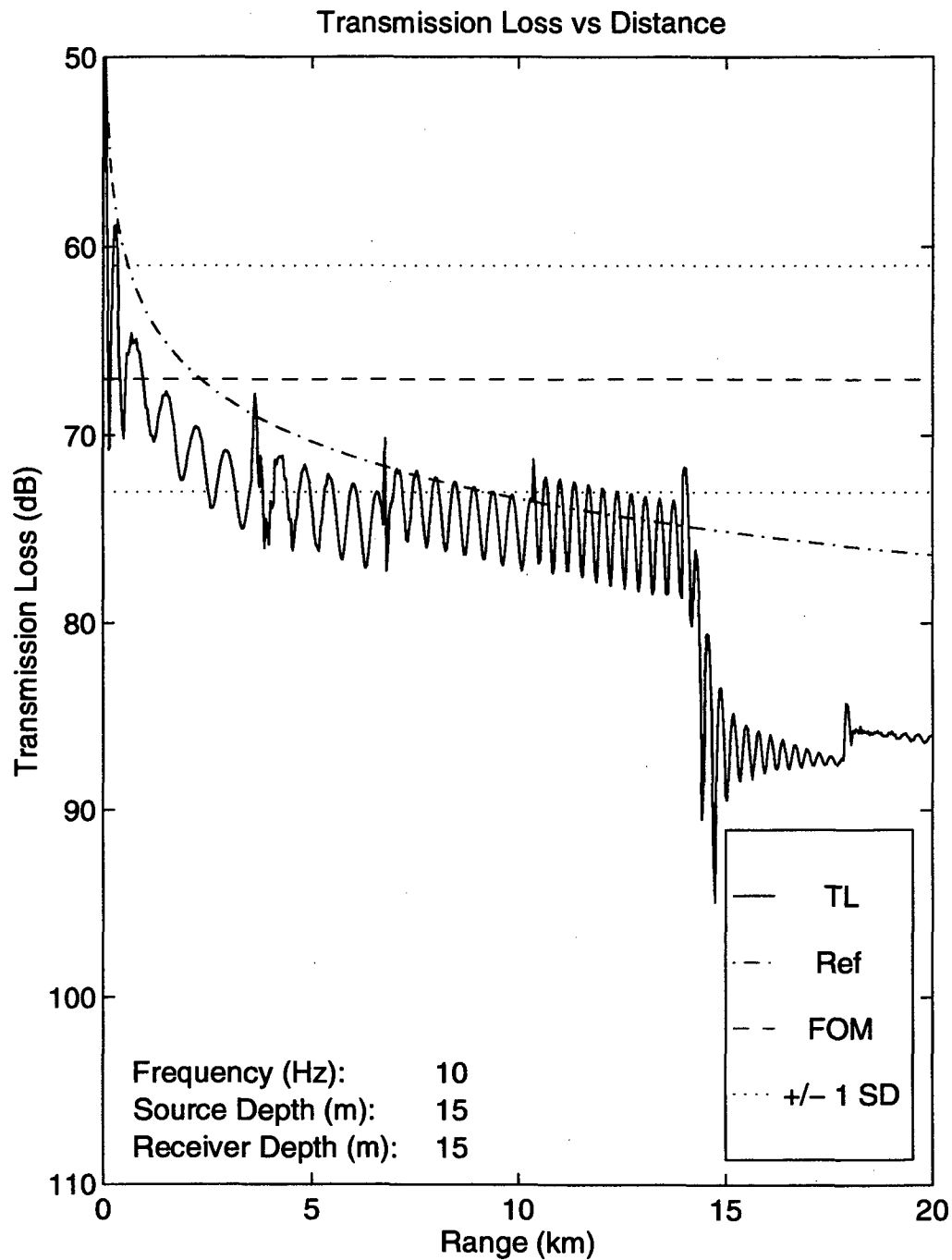


Figure 22. Transmission loss versus distance at 10 Hz for up-slope propagation in shallow water in the wet season. Source and receiver at 15 m.

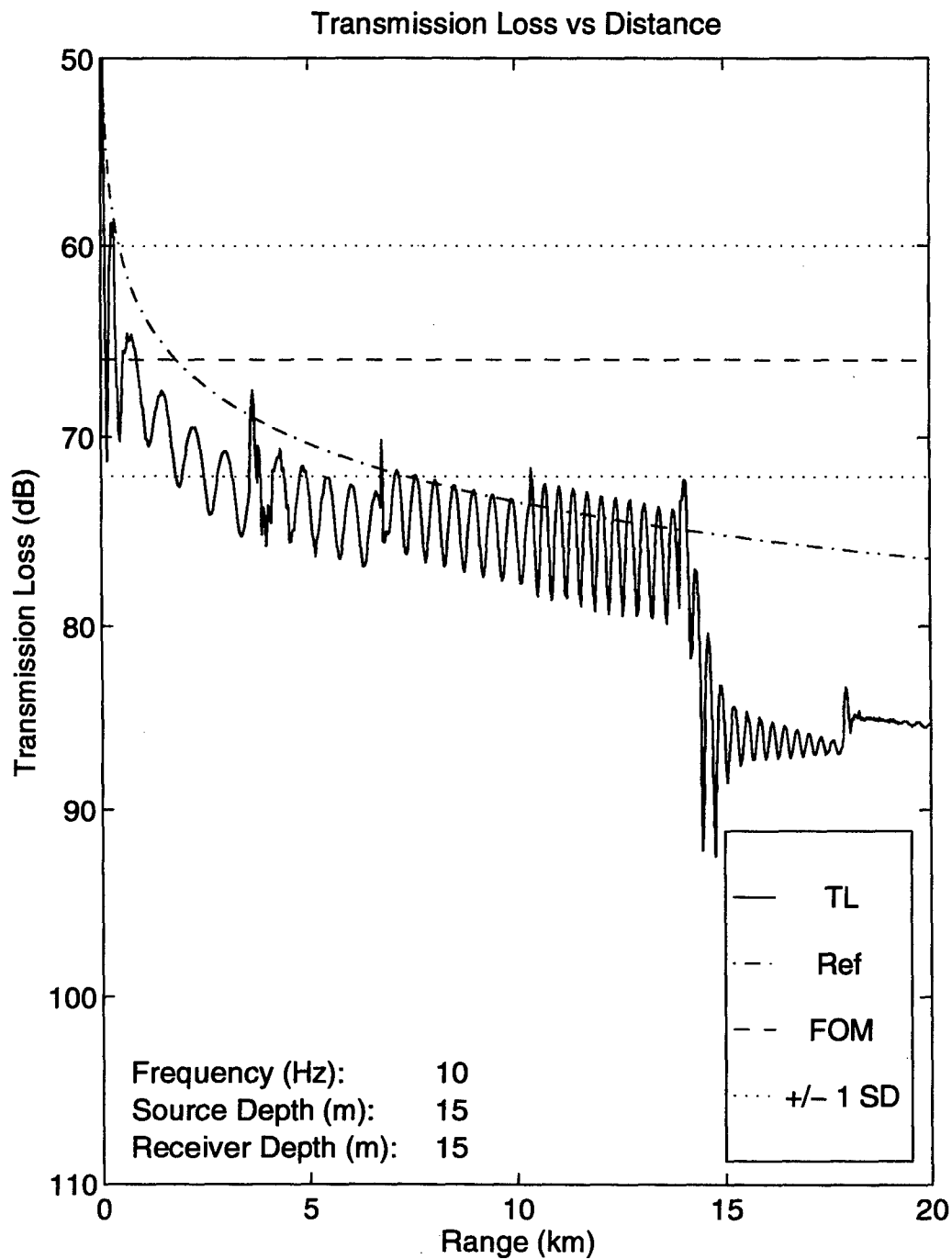


Figure 23. Transmission loss versus distance at 10 Hz for up-slope propagation in shallow water in the dry season. Source and receiver at 15 m.

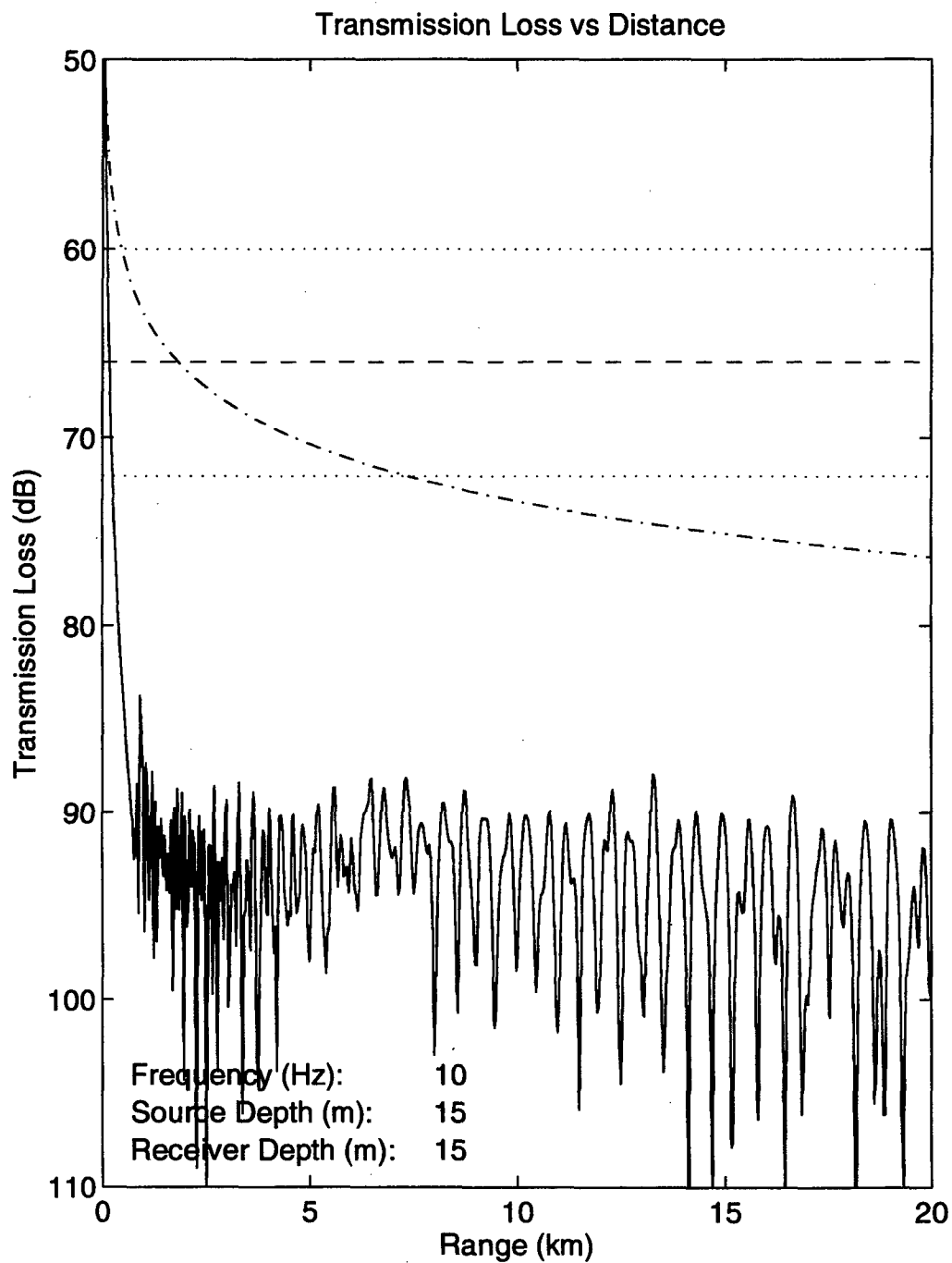


Figure 24. Transmission loss versus distance at 10 Hz for deep water in the wet season. Source and receiver at 15 m.

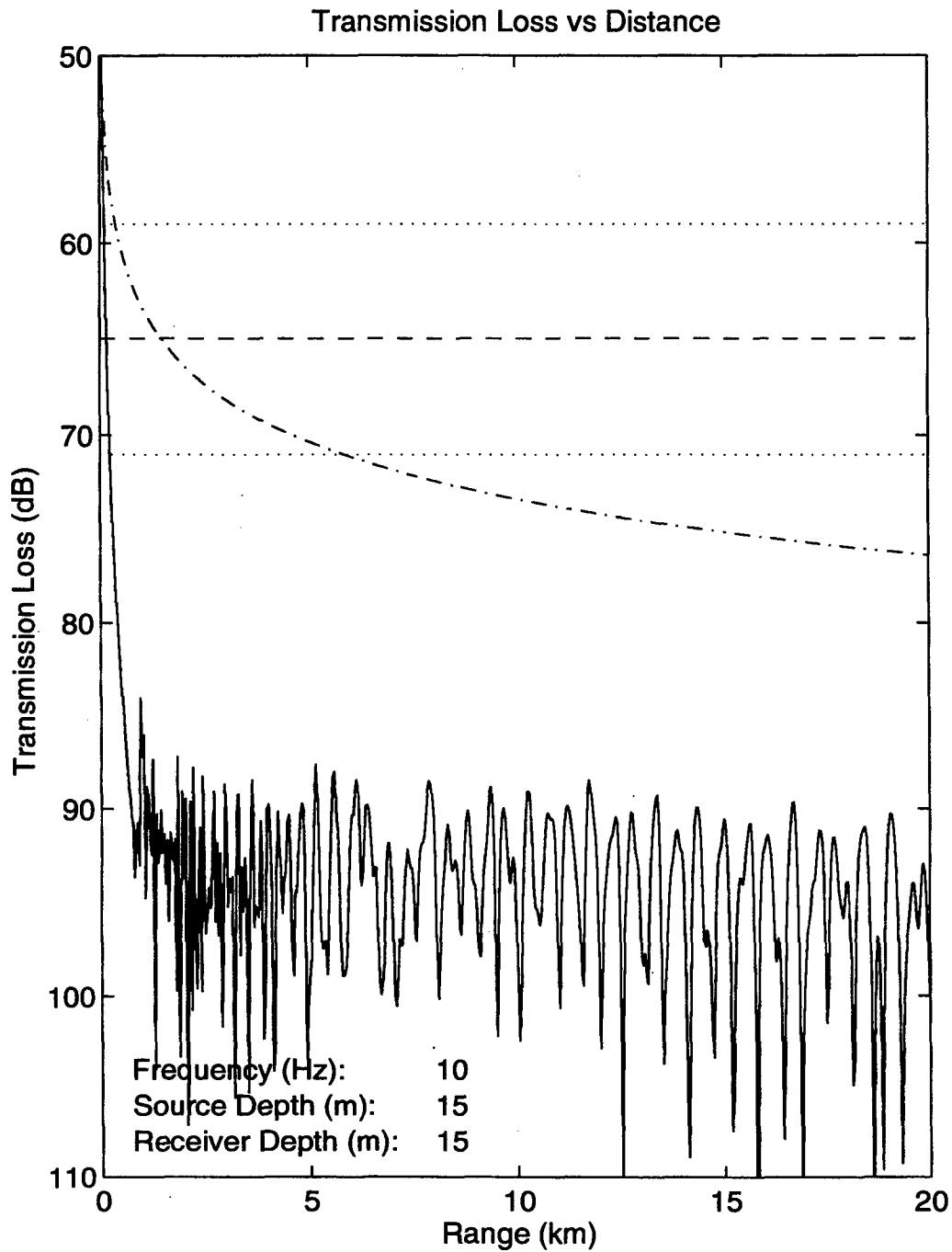


Figure 25. Transmission loss versus distance at 10 Hz for deep water in the dry season. Source and receiver at 15 m.

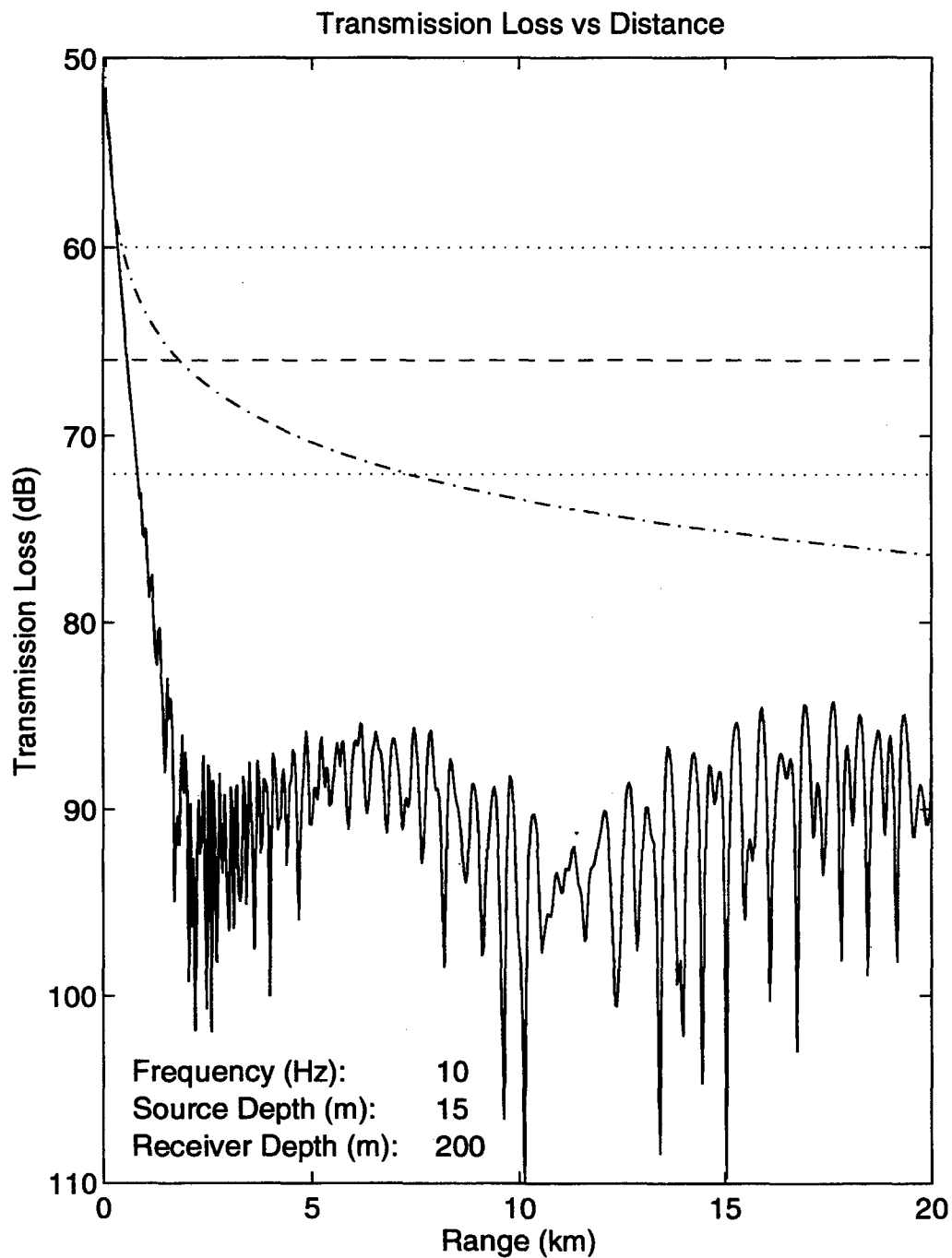


Figure 26. Transmission loss versus distance at 10 Hz for deep water in the wet season. Source at 15 m and receiver at 200 m.

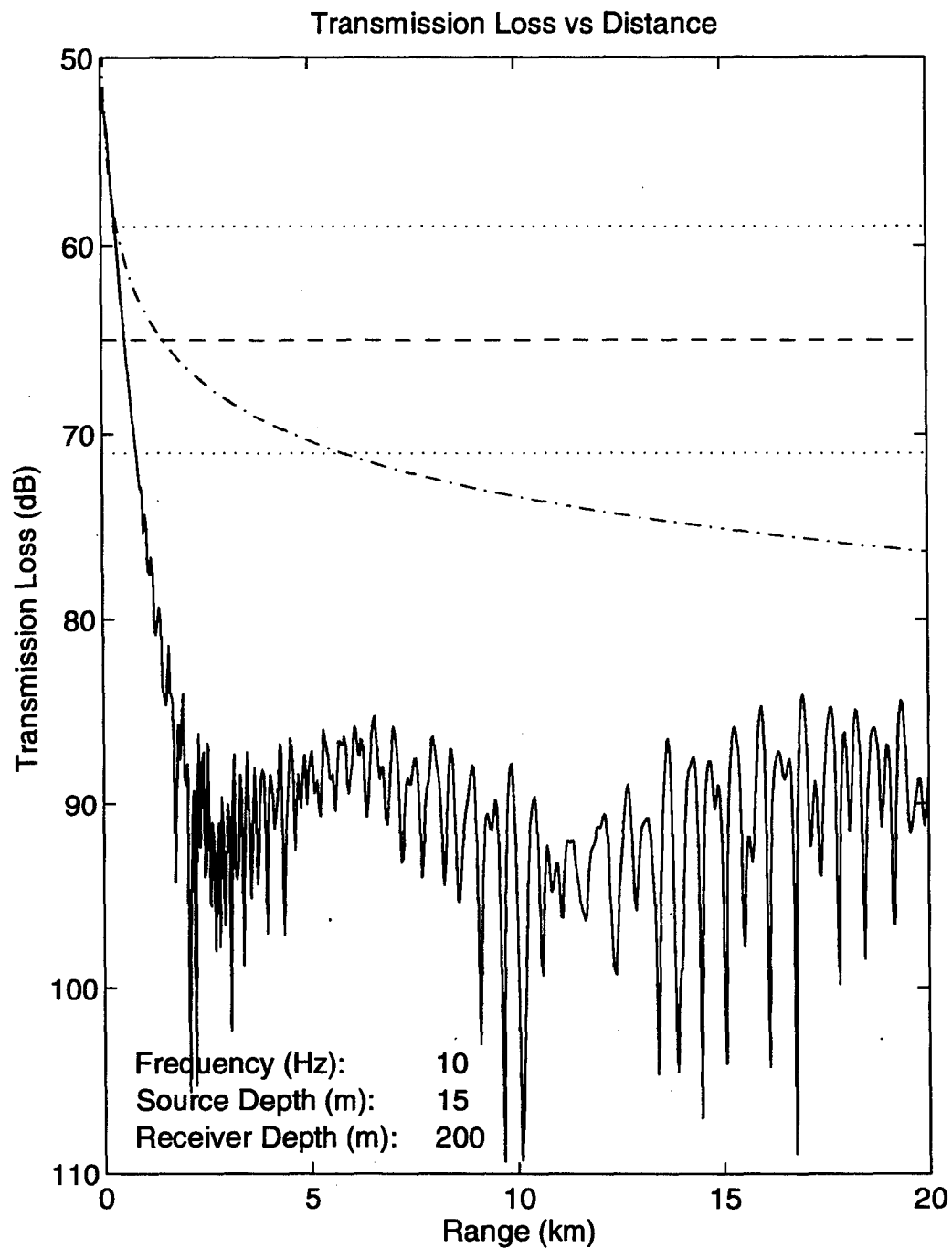


Figure 27. Transmission loss versus distance at 10 Hz for deep water in the dry season. Source at 15 m and receiver at 200 m.

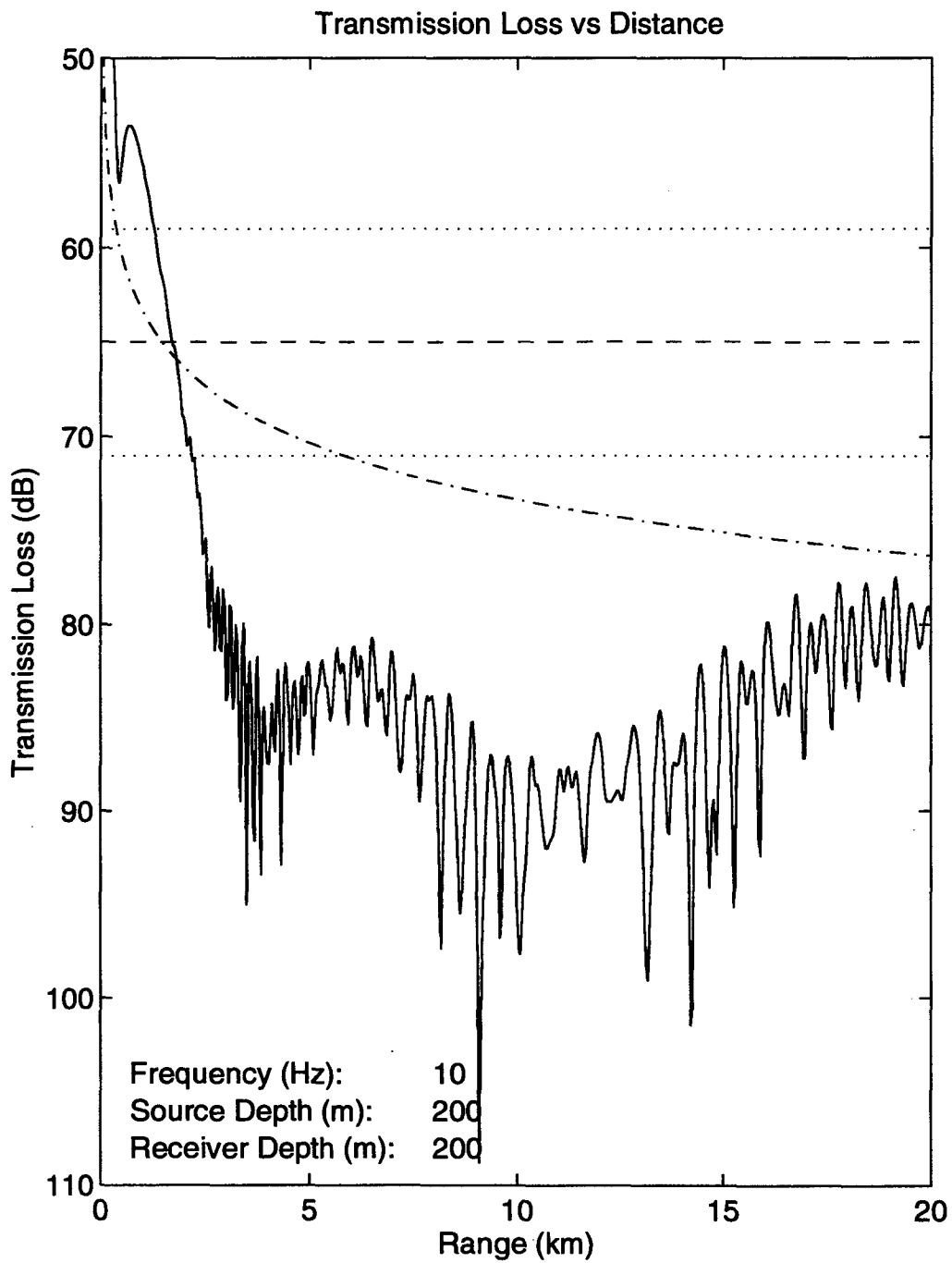


Figure 28. Transmission loss versus distance at 10 Hz for deep water in the wet season. Source and receiver at 200 m.

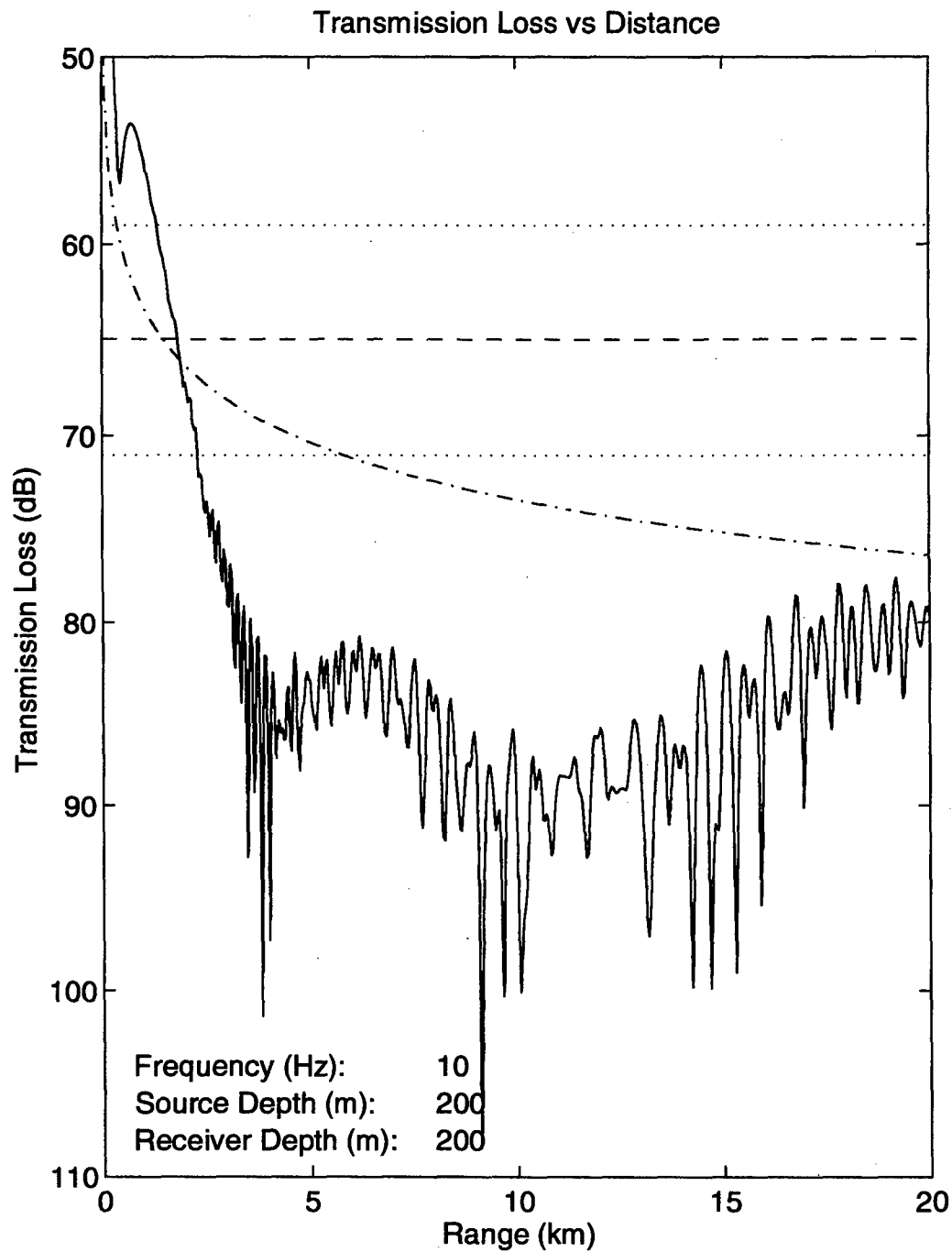


Figure 29. Transmission loss versus distance at 10 Hz for deep water in the dry season. Source and receiver at 200 m.

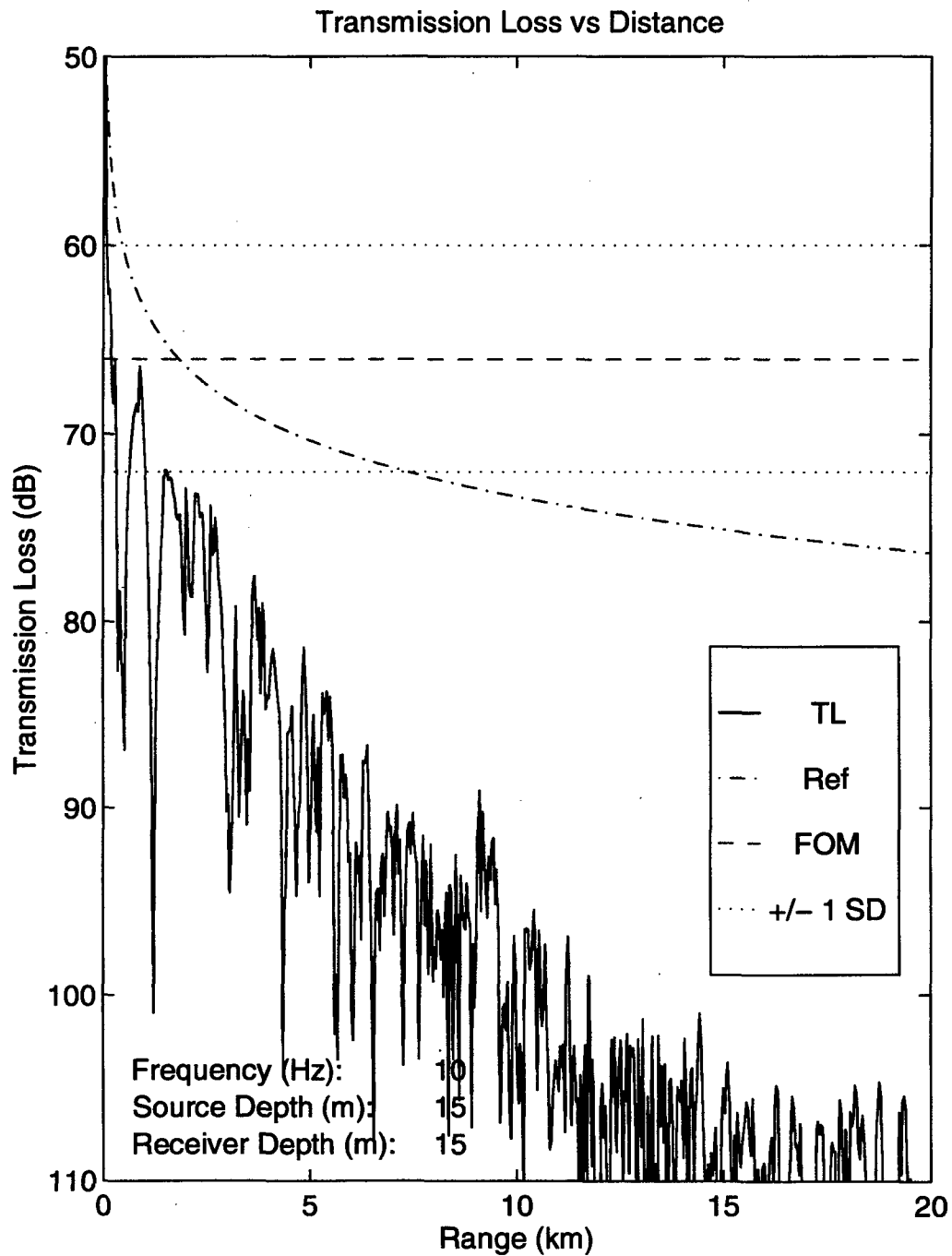


Figure 30. Transmission loss versus distance at 10 Hz for down-slope propagation in deep water in the wet season. Source and receiver at 15 m.

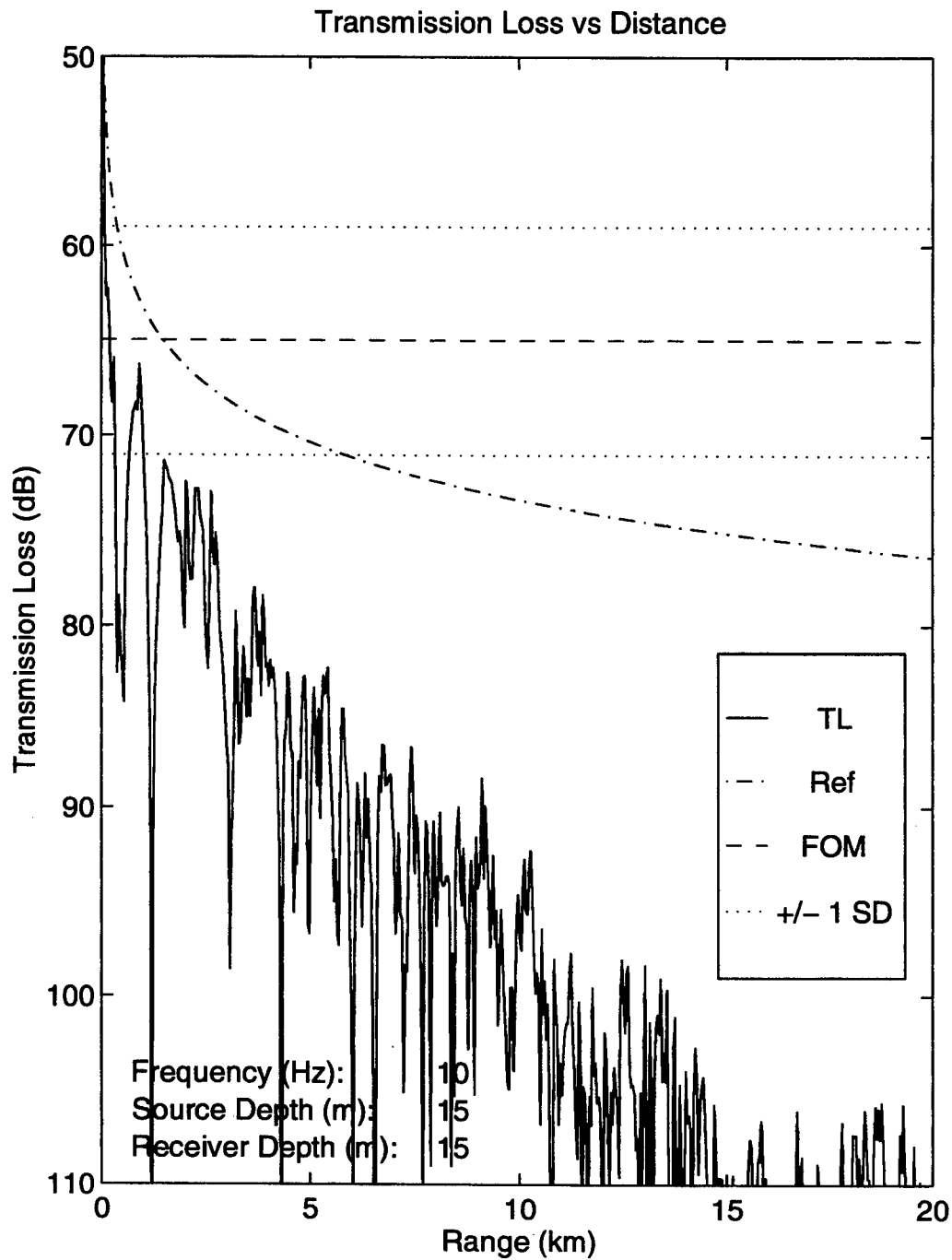


Figure 31. Transmission loss versus distance at 10 Hz for down-slope propagation in deep water in the dry season. Source and receiver at 15 m.

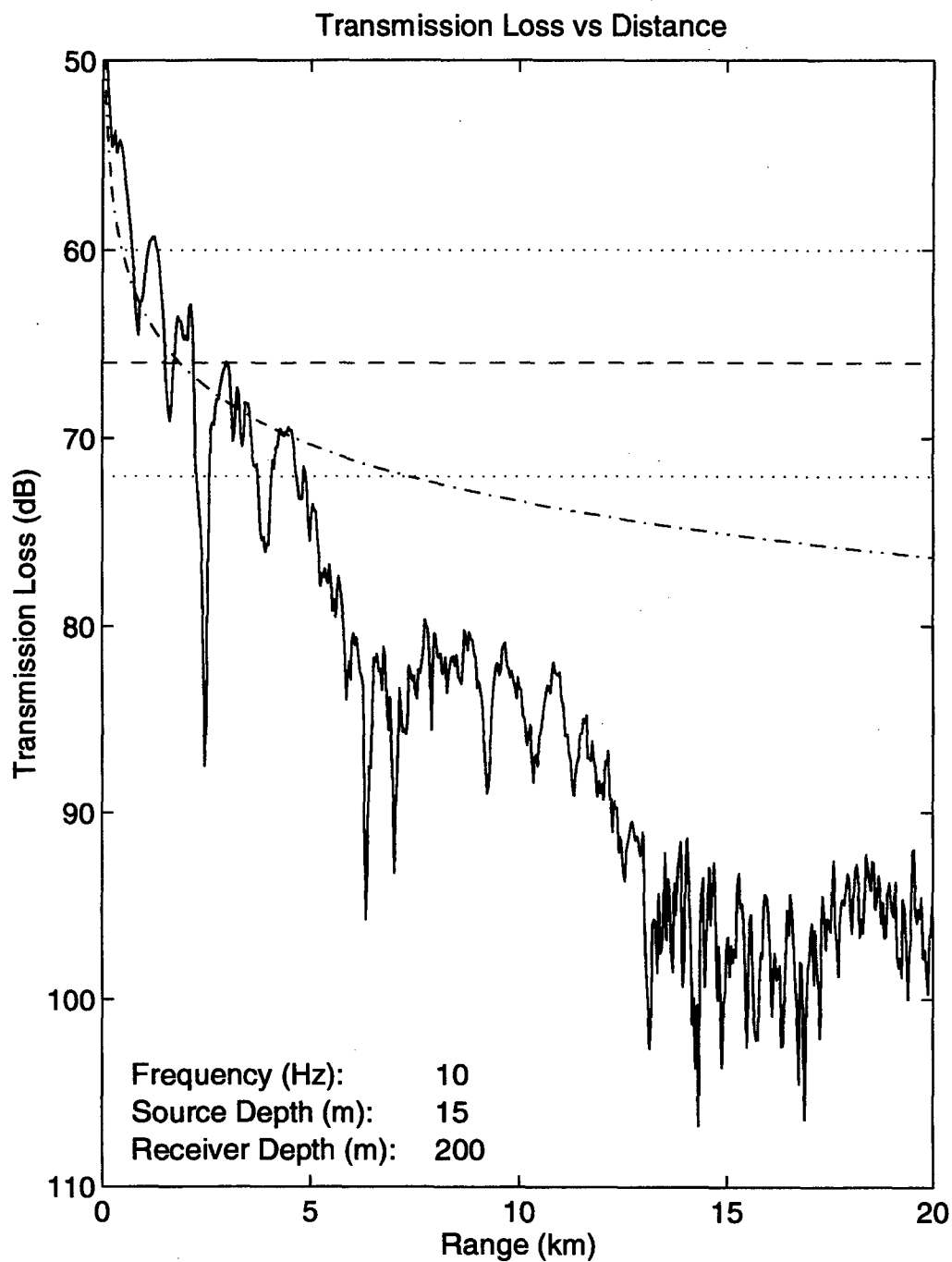


Figure 32. Transmission loss versus distance at 10 Hz for down-slope propagation in deep water in the wet season. Source at 15 m and receiver at 200 m.

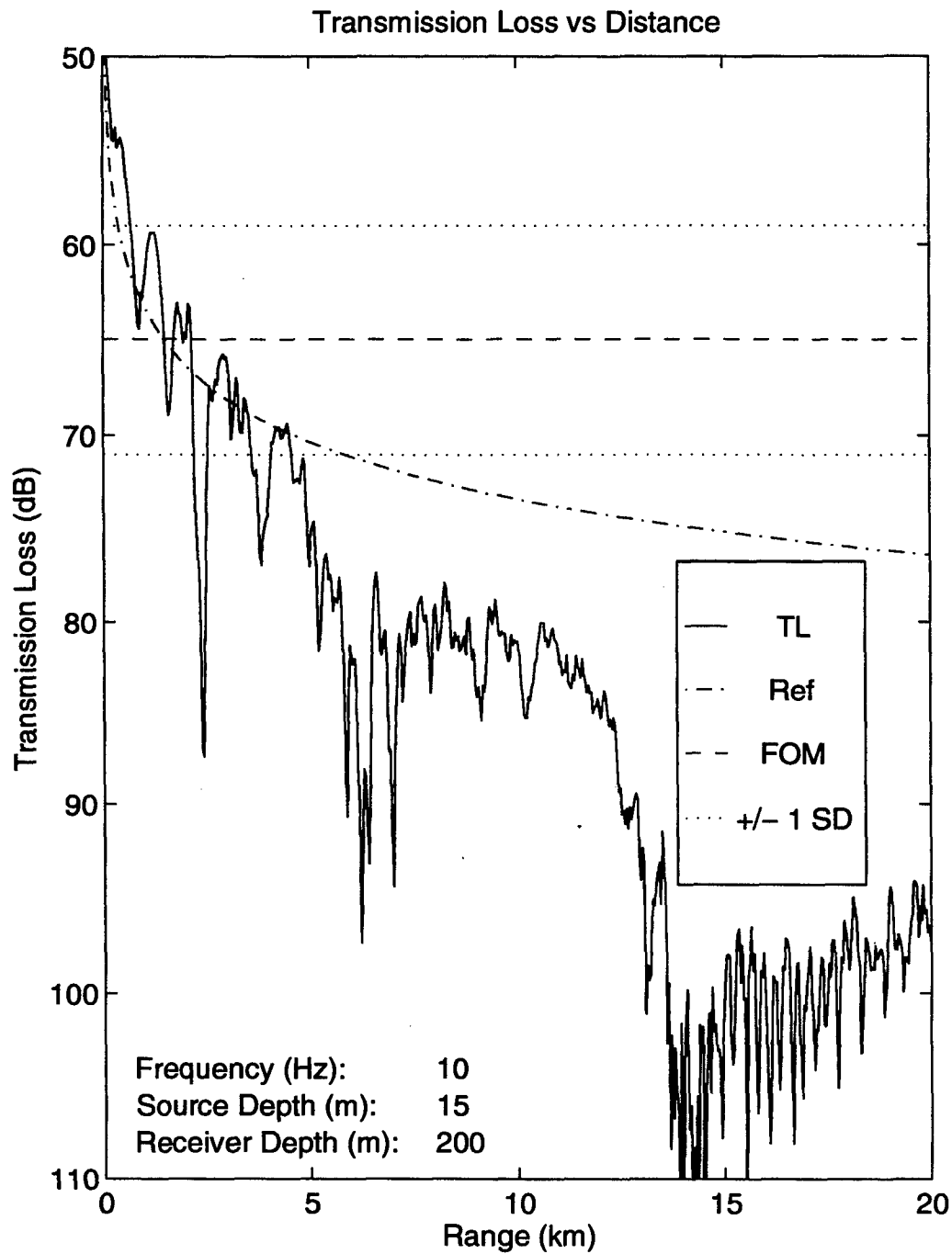


Figure 33. Transmission loss versus distance at 10 Hz for down-slope propagation in deep water in the dry season. Source at 15 m and receiver at 200 m.

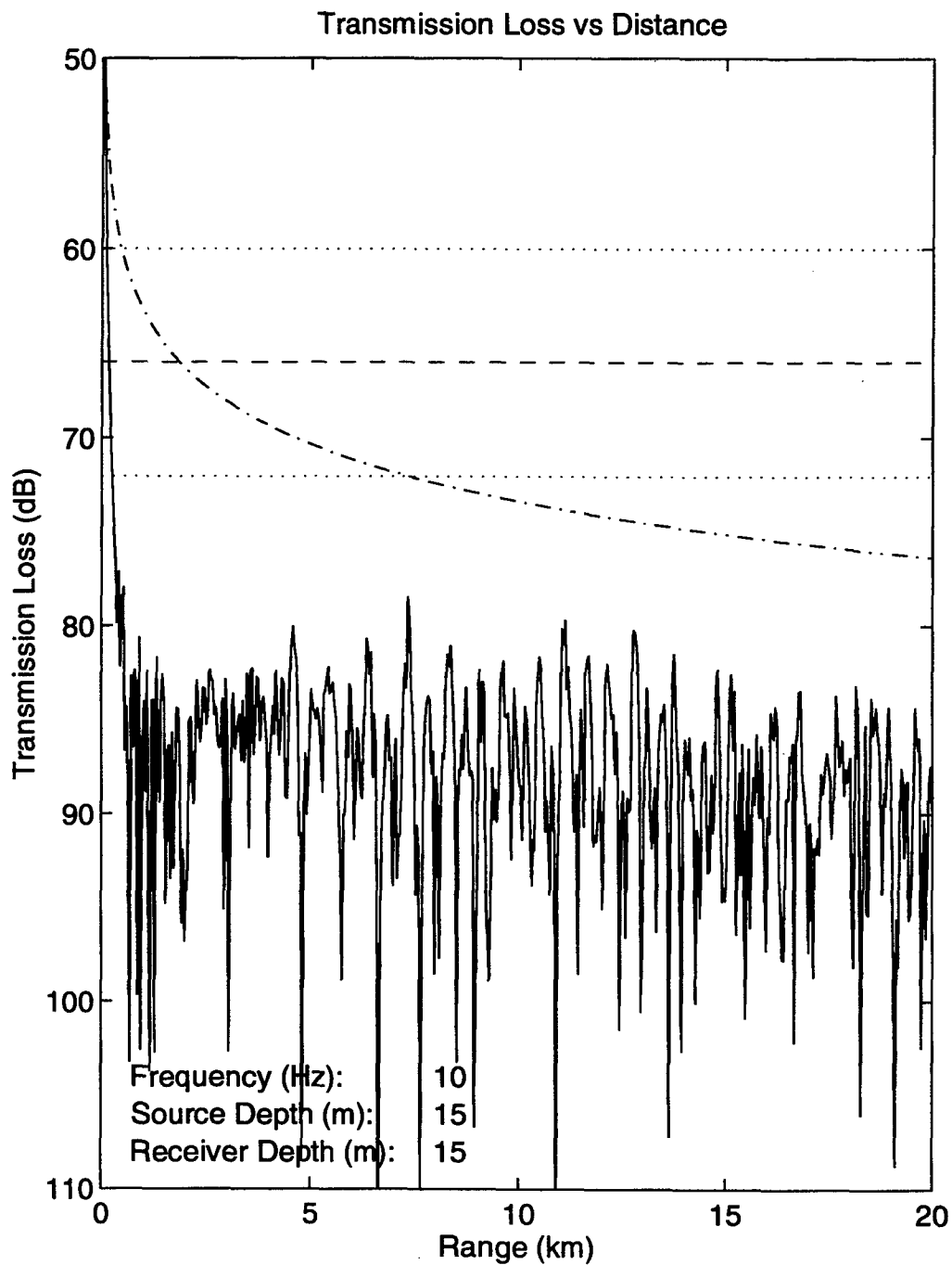


Figure 34. Transmission loss versus distance at 10 Hz for up-slope propagation in deep water in the wet season. Source and receiver at 15 m.

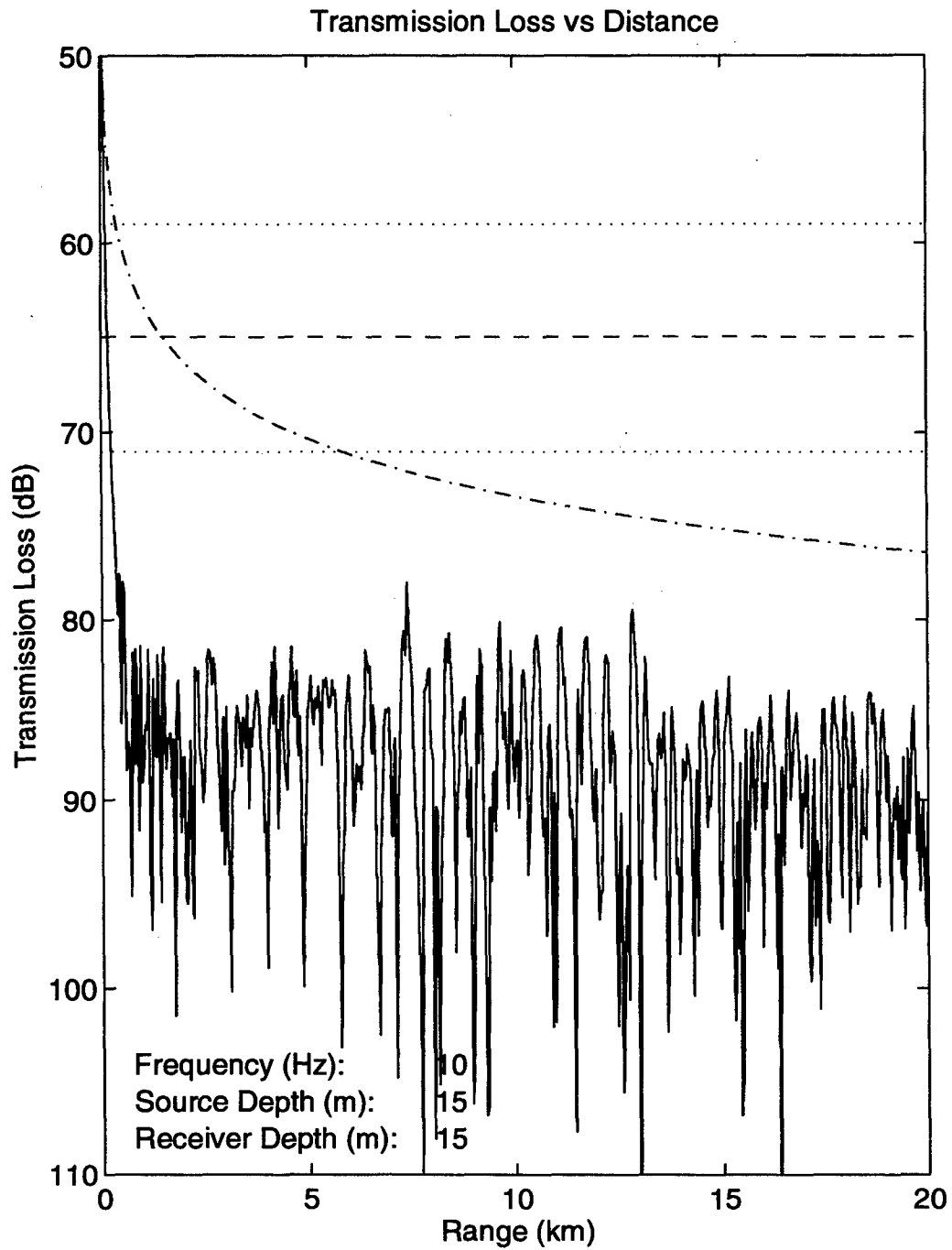


Figure 35. Transmission loss versus distance at 10 Hz for up-slope propagation in deep water in the dry season. Source and receiver at 15 m.

APPENDIX B - 50 HZ TRANSMISSION LOSS CURVES

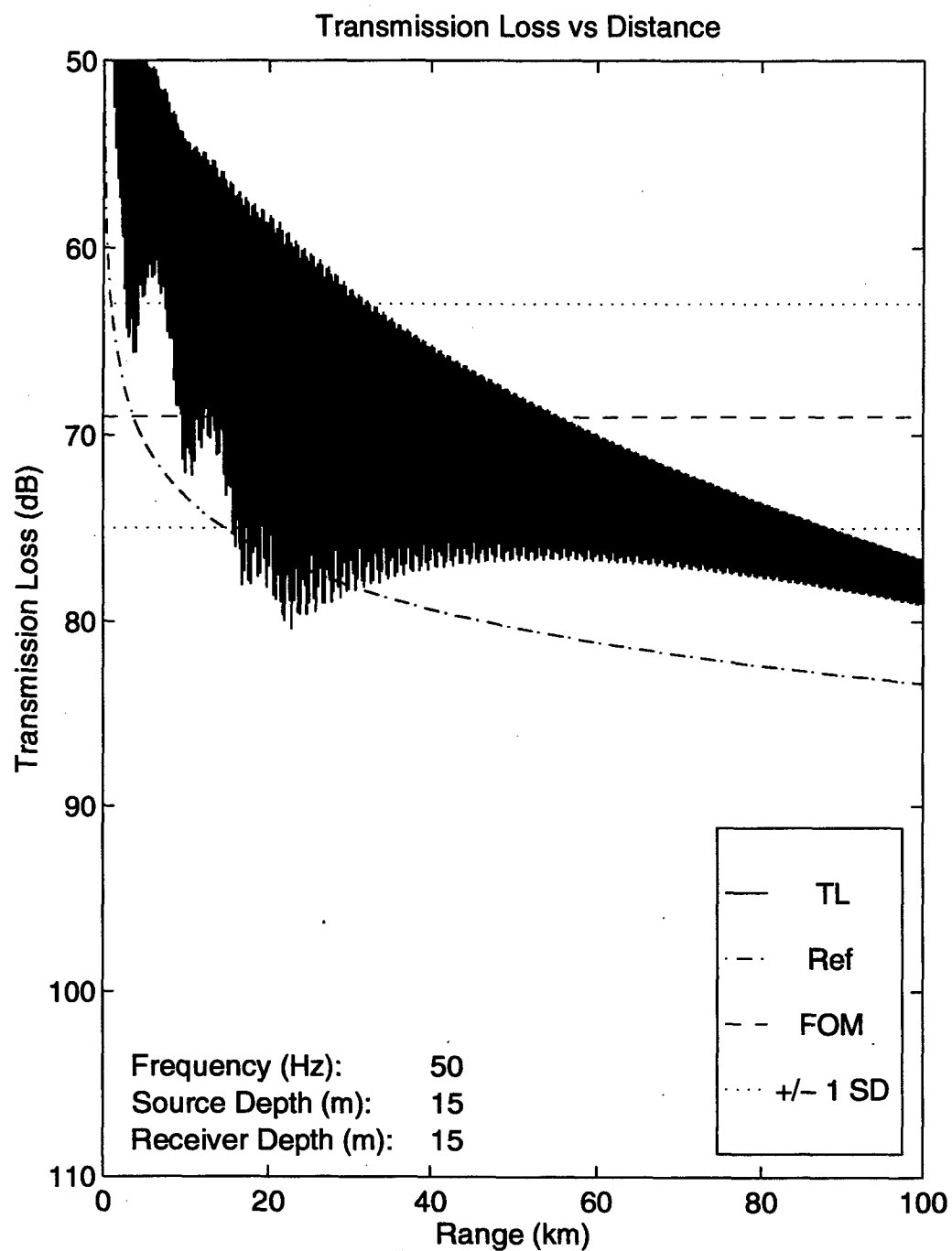


Figure 36. Transmission loss versus distance at 50 Hz for 50 m water depth in the wet season. Source and receiver at 15 m.

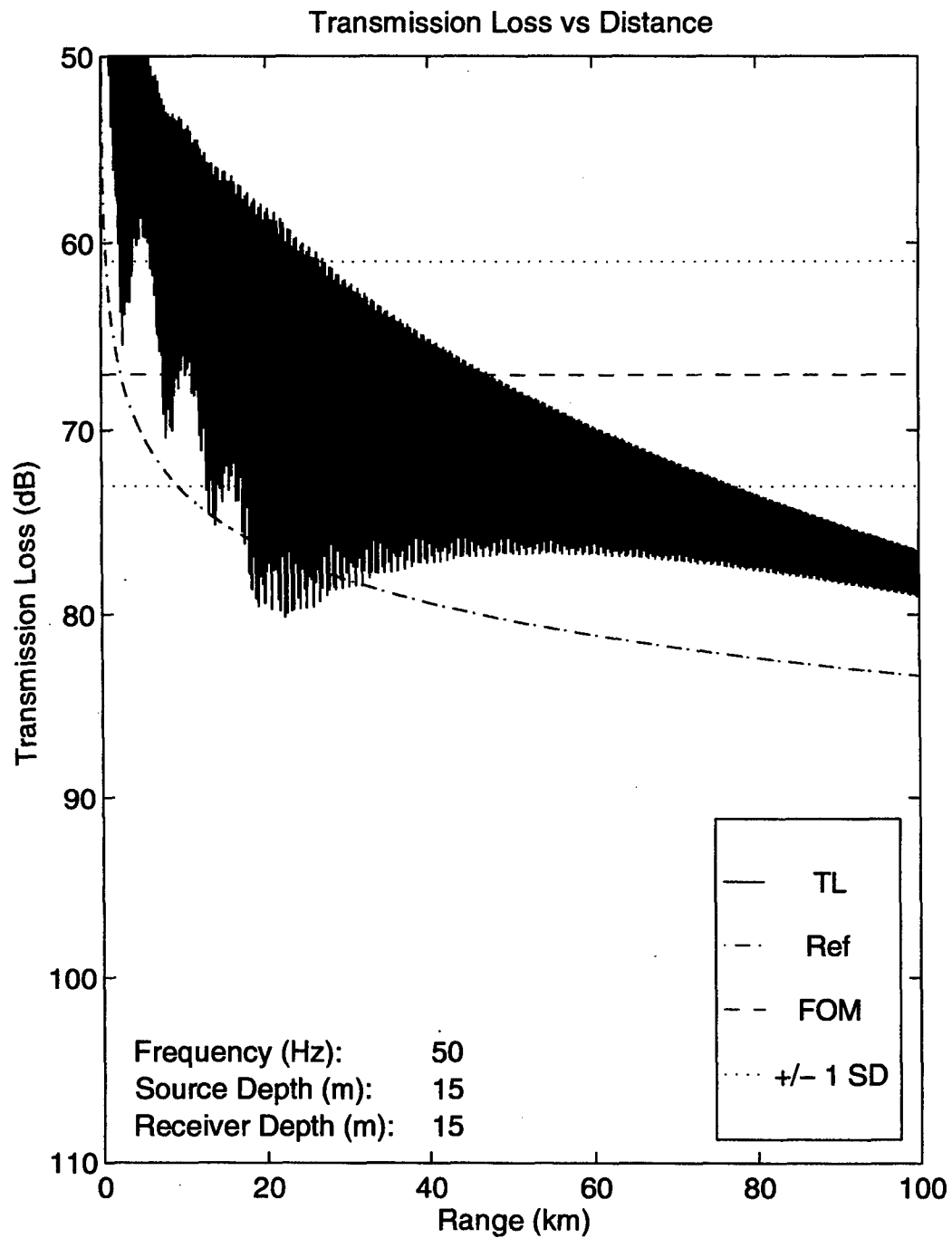


Figure 37. Transmission loss versus distance at 50 Hz for 50 m water depth in the dry season. Source and receiver at 15 m.

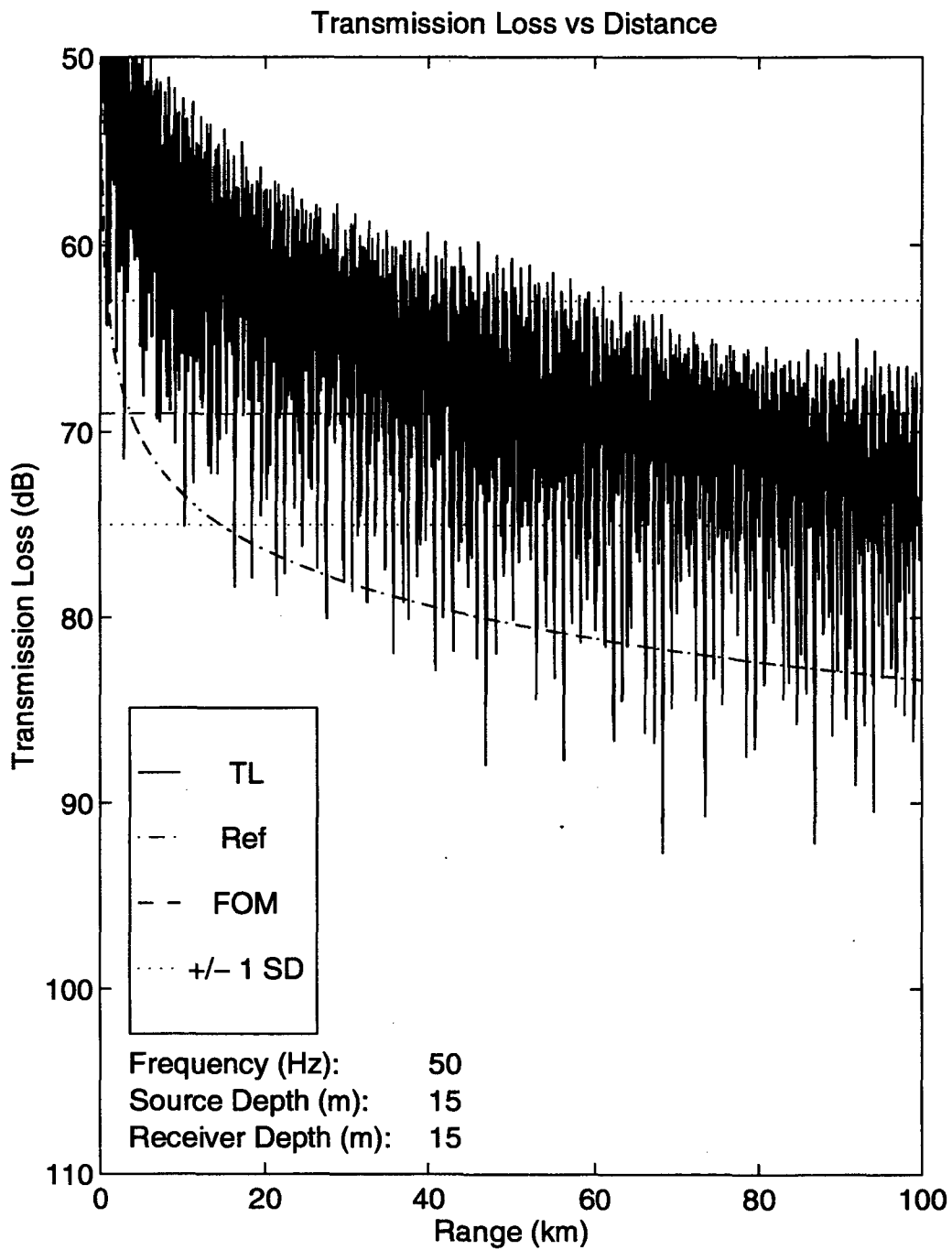


Figure 38. Transmission loss versus distance at 50 Hz for 100 m water depth in the wet season. Source and receiver at 15 m.

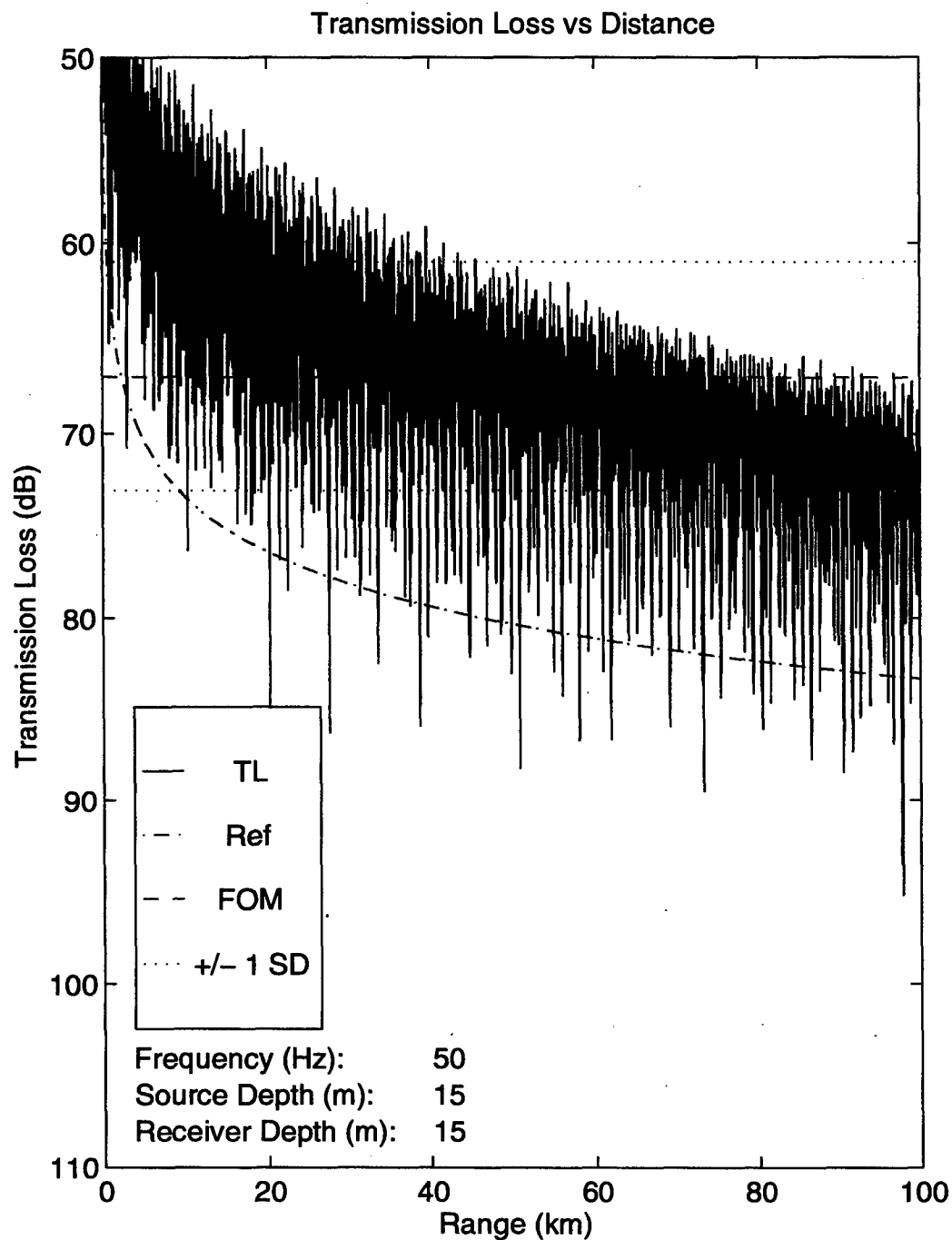


Figure 39. Transmission loss versus distance at 50 Hz for 100 m water depth in the dry season. Source and receiver at 15 m.

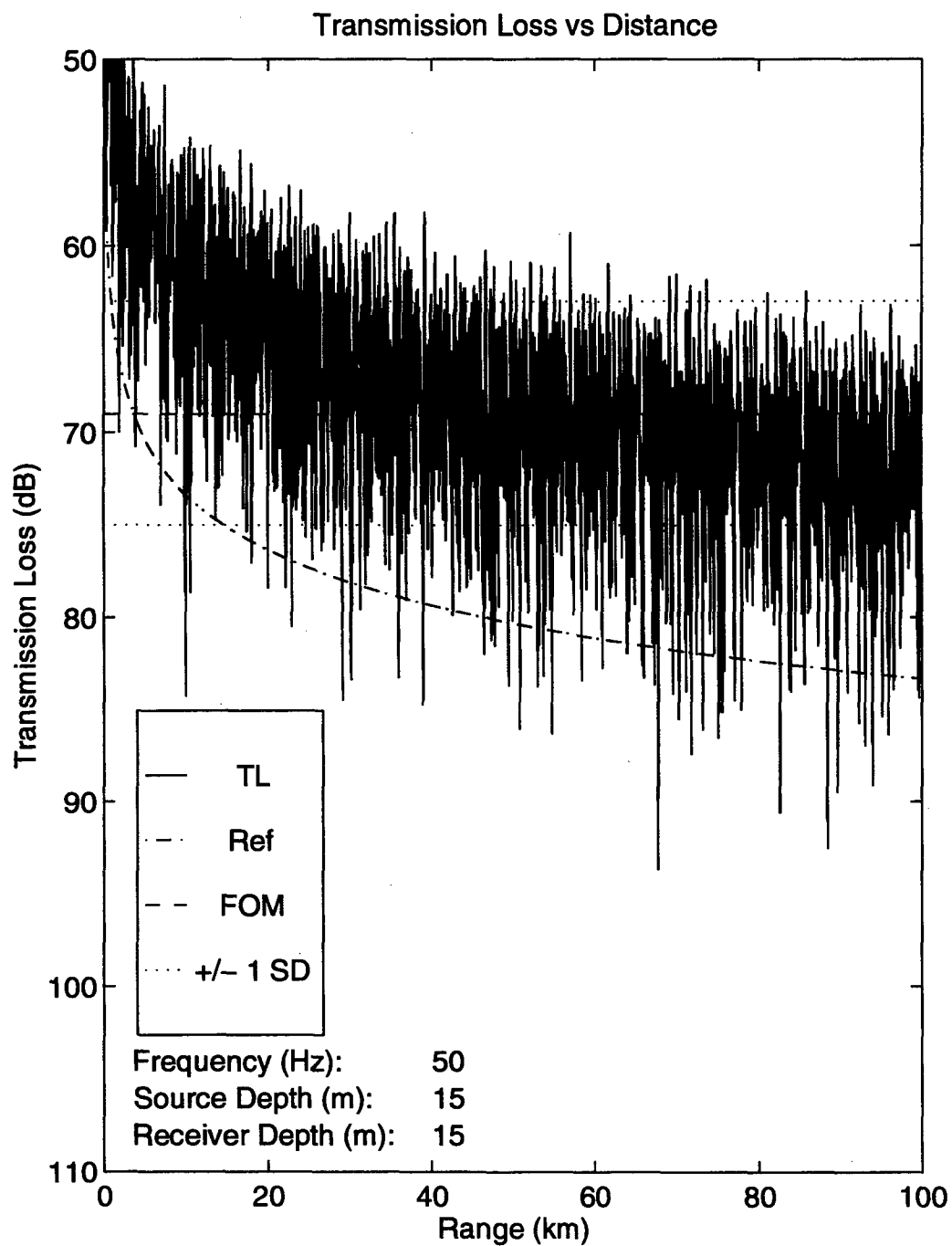


Figure 40. Transmission loss versus distance at 50 Hz for 200 m water depth in the wet season. Source and receiver at 15 m.

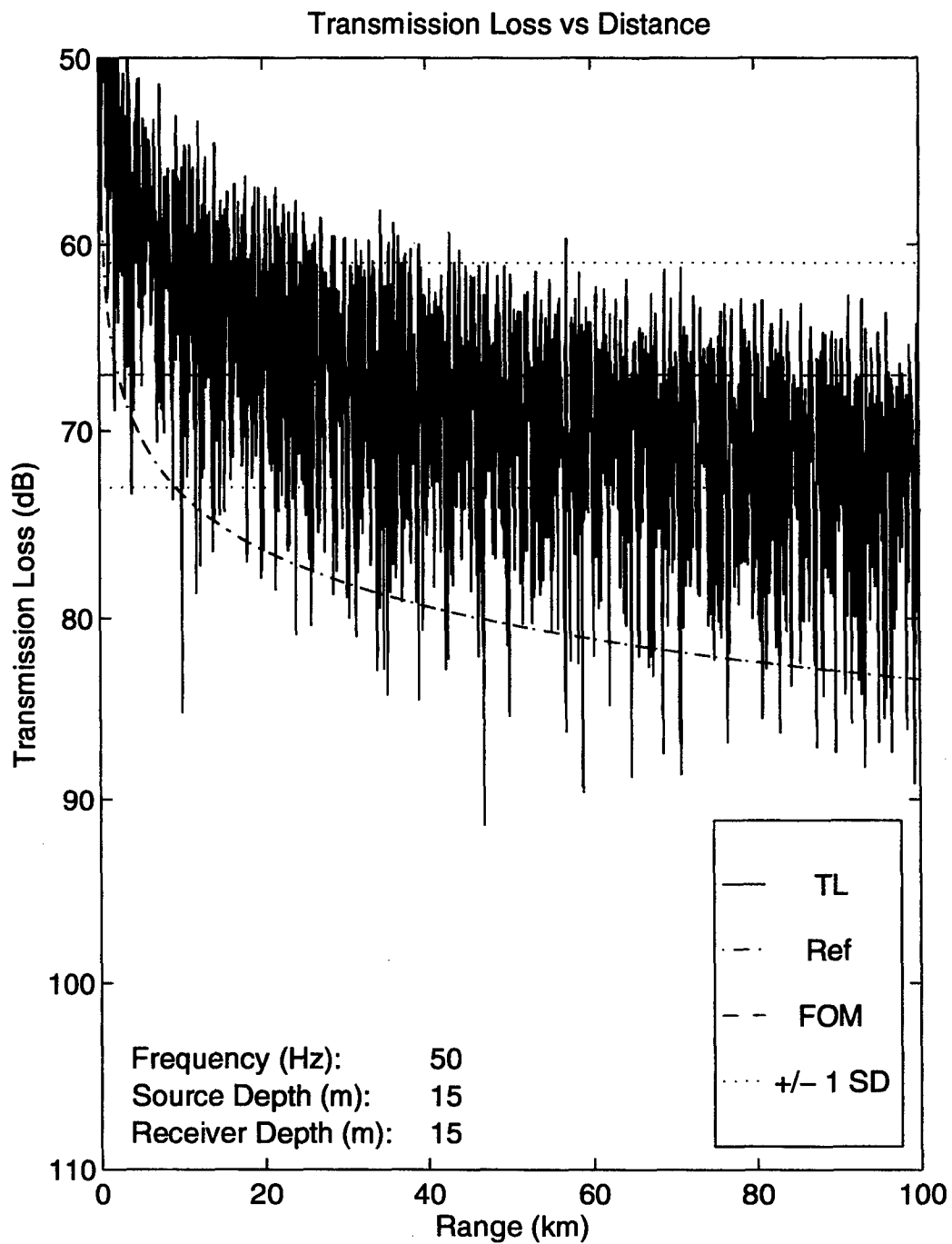


Figure 41. Transmission loss versus distance at 50 Hz for 200 m water depth in the dry season. Source and receiver at 15 m.

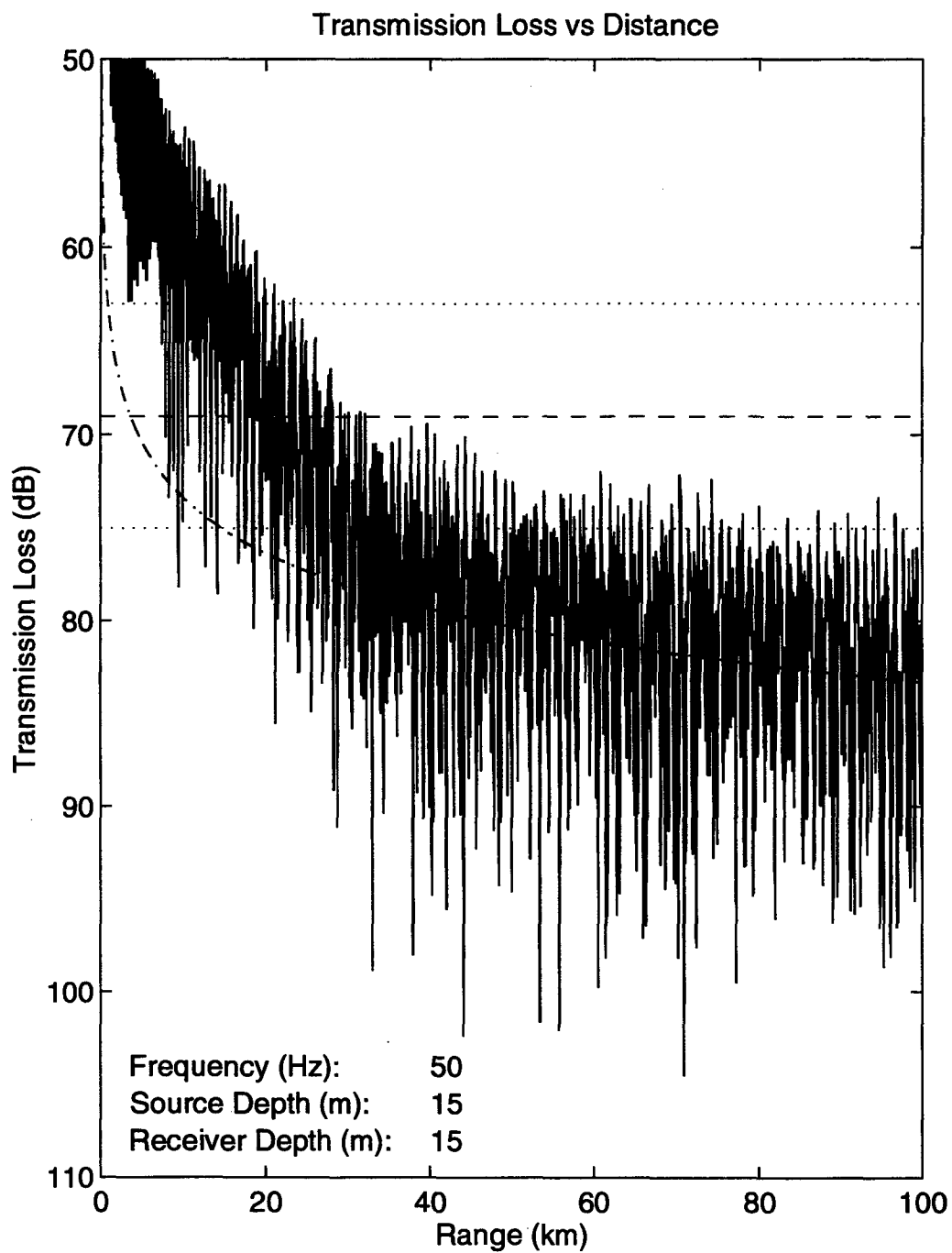


Figure 42. Transmission loss versus distance at 50 Hz for down-slope propagation in shallow water in the wet season. Source and receiver at 15 m.

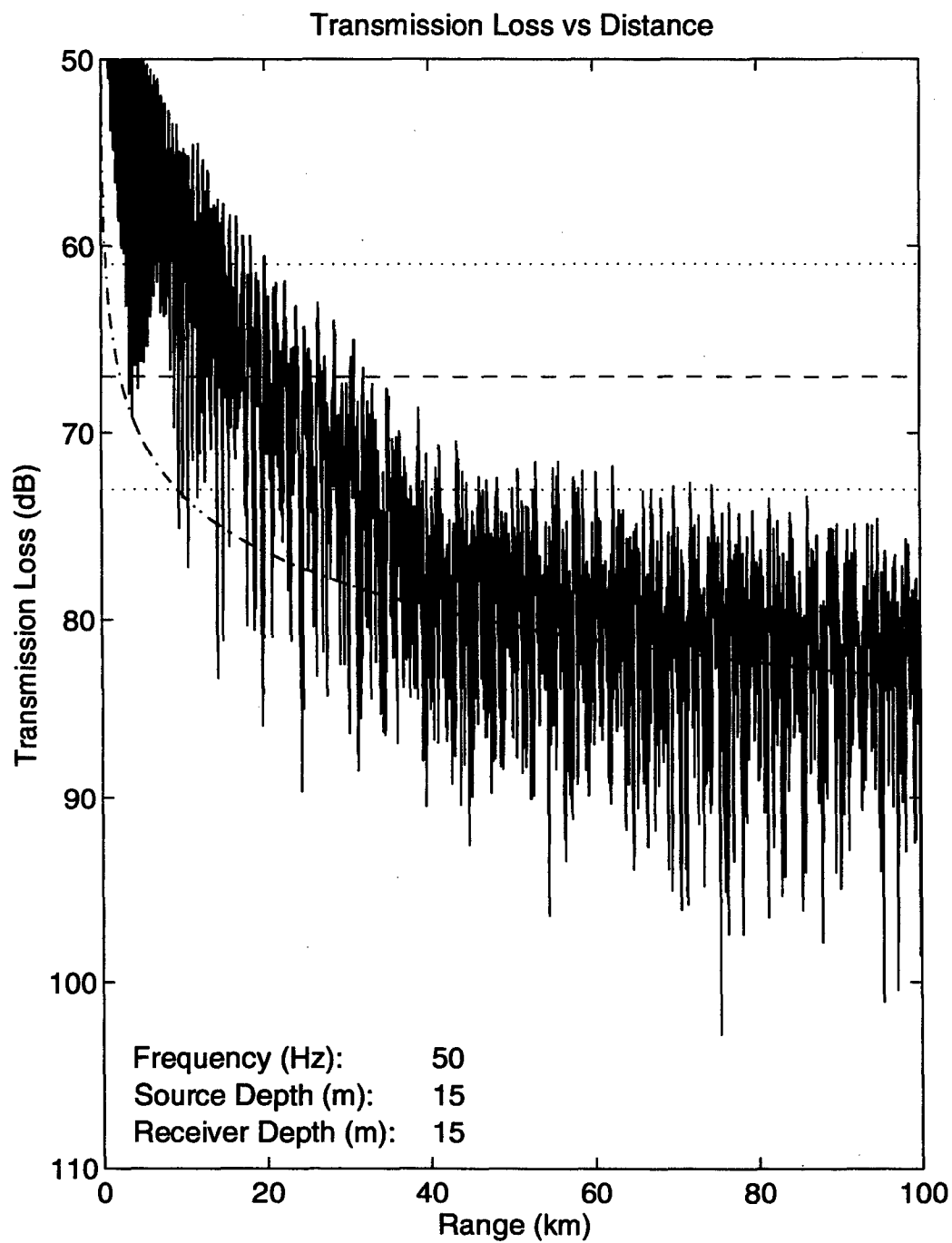


Figure 43. Transmission loss versus distance at 50 Hz for down-slope propagation in shallow water in the dry season. Source and receiver at 15 m.

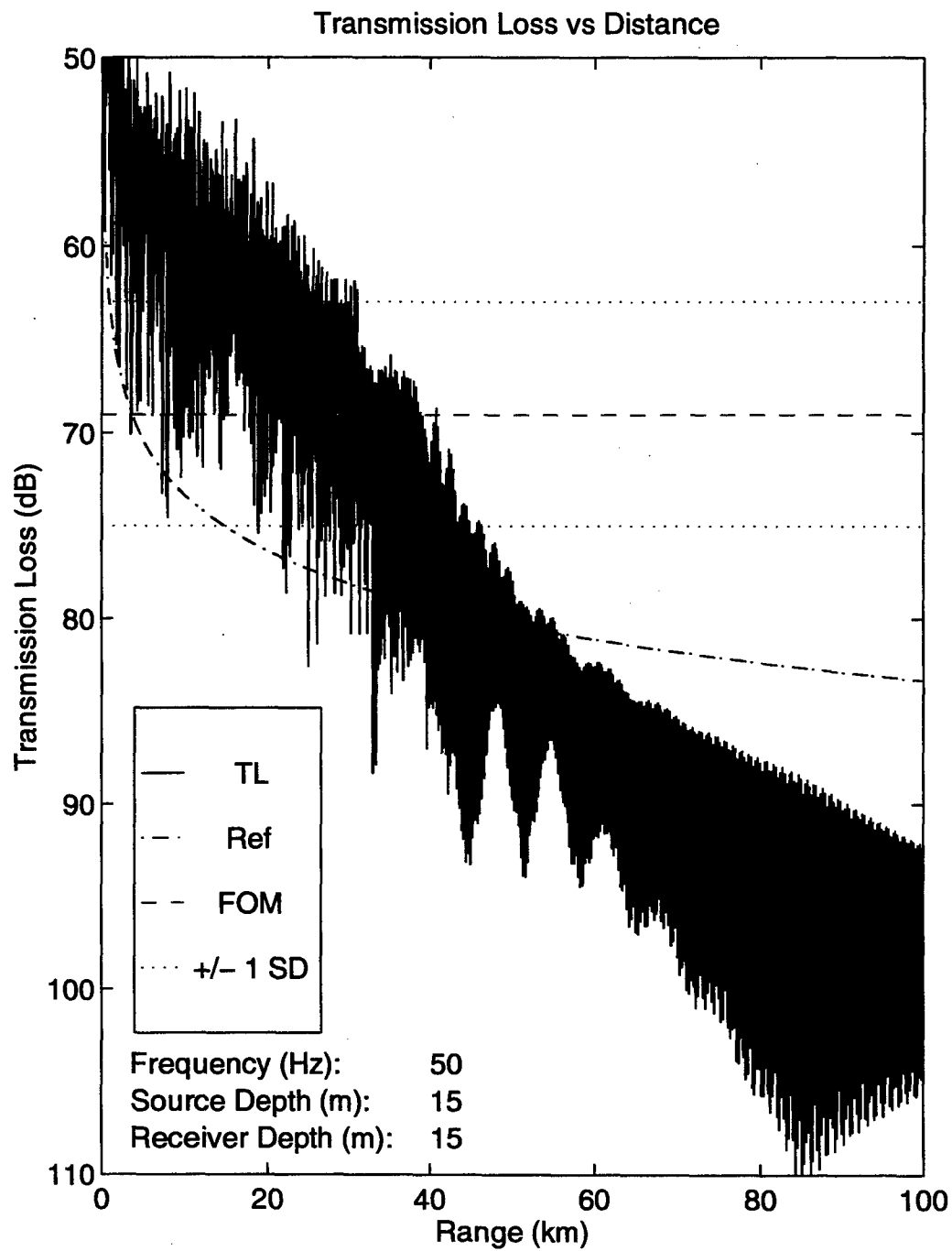


Figure 44. Transmission loss versus distance at 50 Hz for up-slope propagation in shallow water in the wet season. Source and receiver at 15 m.

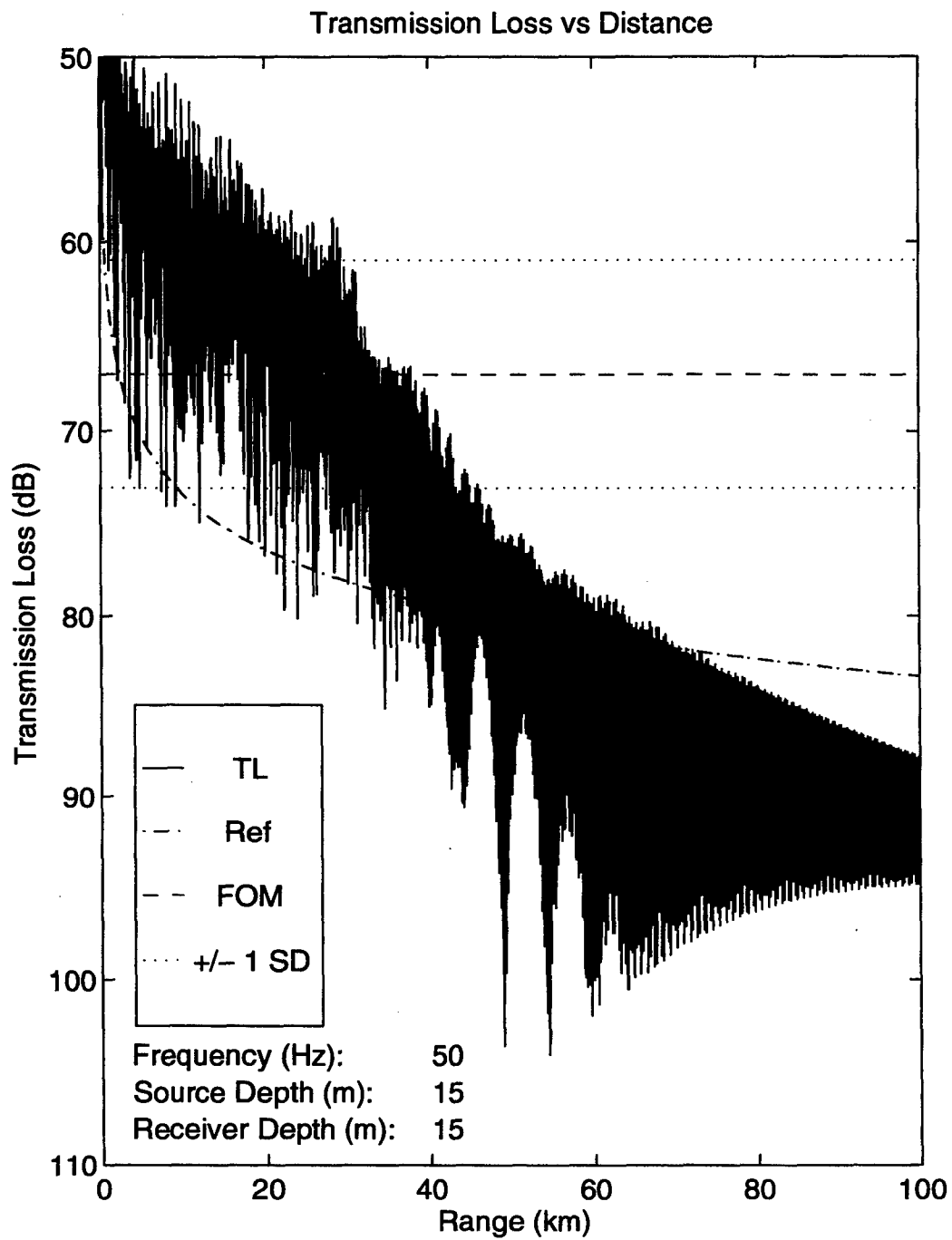


Figure 45. Transmission loss versus distance at 50 Hz for up-slope propagation in shallow water in the dry season. Source and receiver at 15 m.

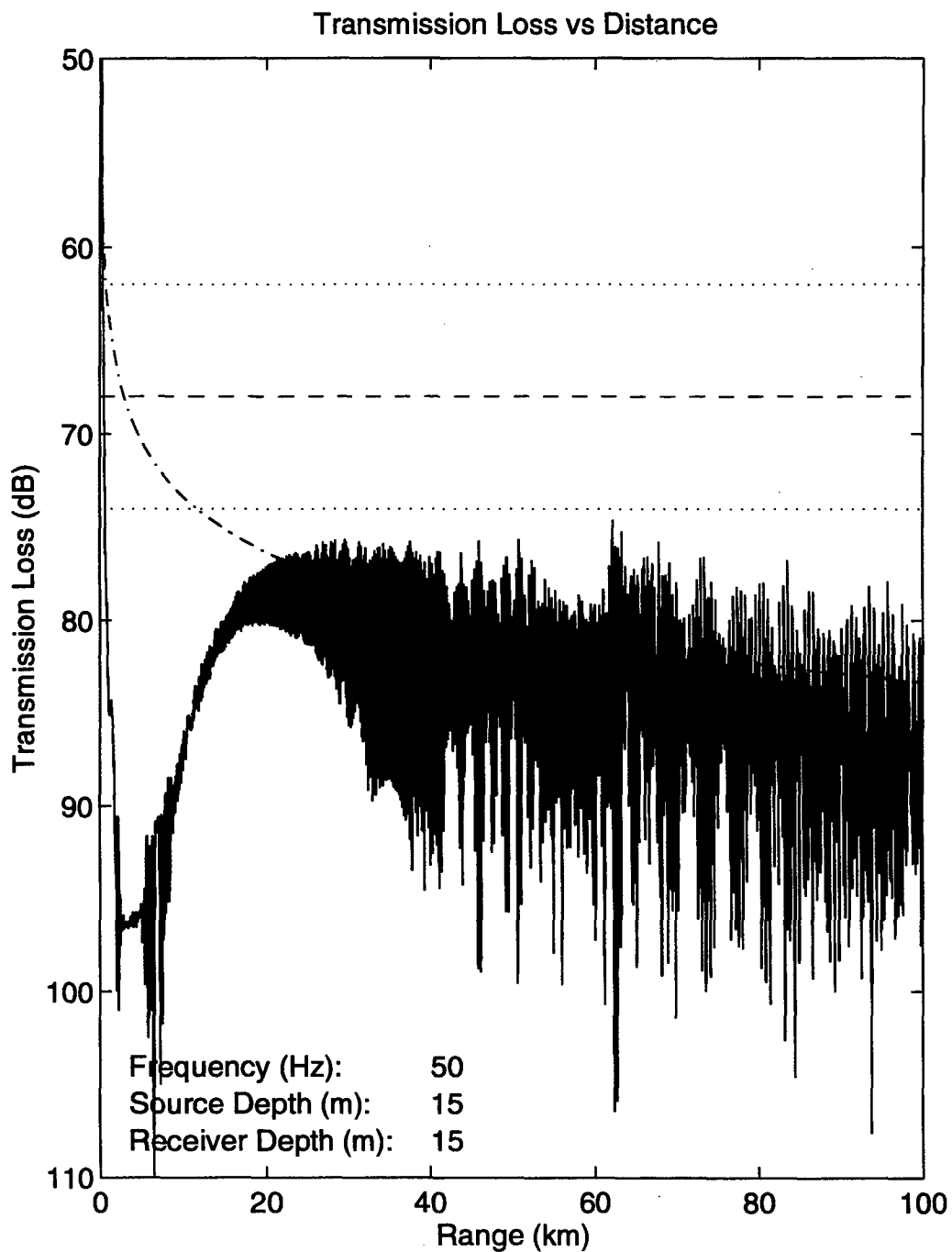


Figure 46. Transmission loss versus distance at 50 Hz for deep water in the wet season. Source and receiver at 15 m.

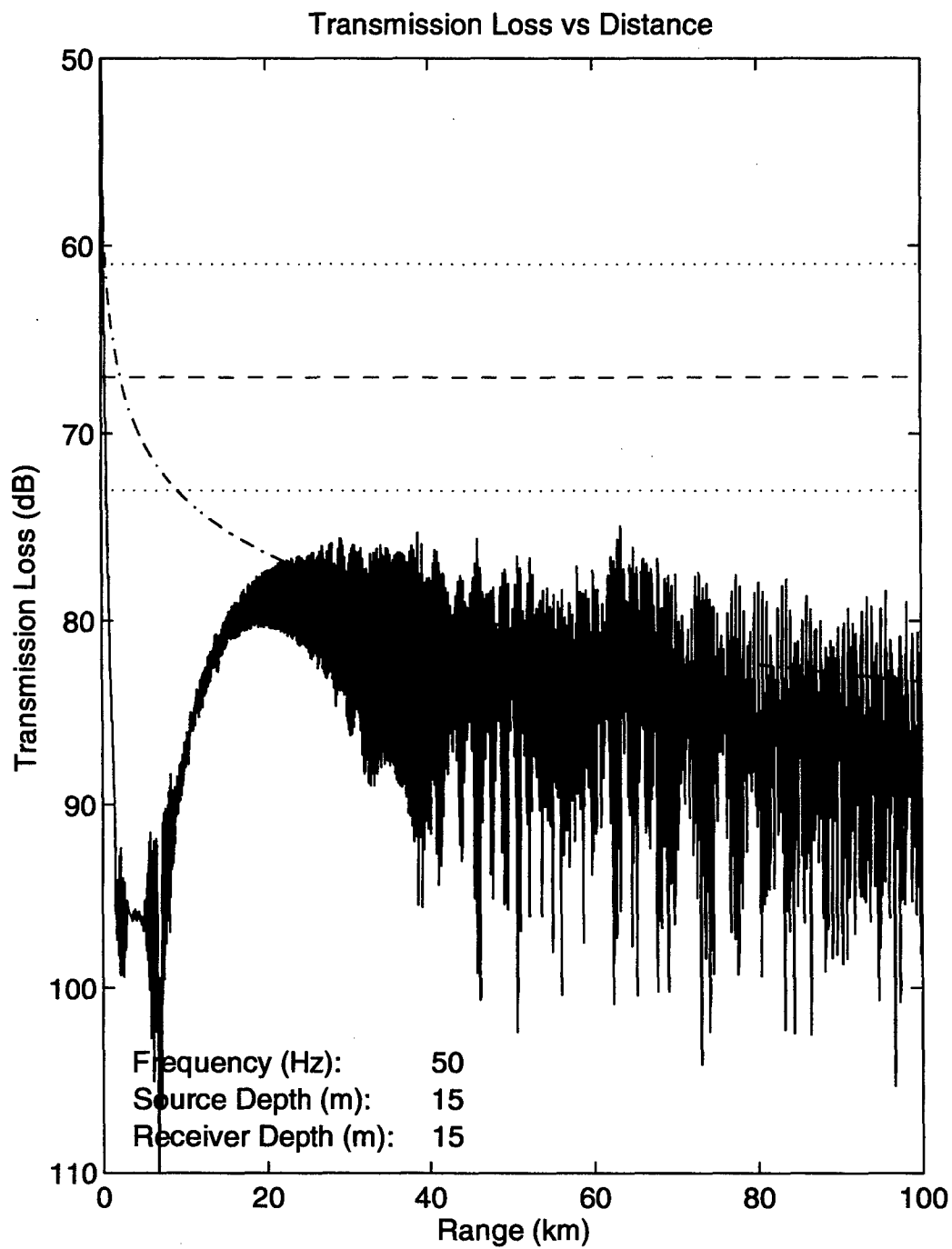


Figure 47. Transmission loss versus distance at 50 Hz for deep water in the dry season. Source and receiver at 15 m.

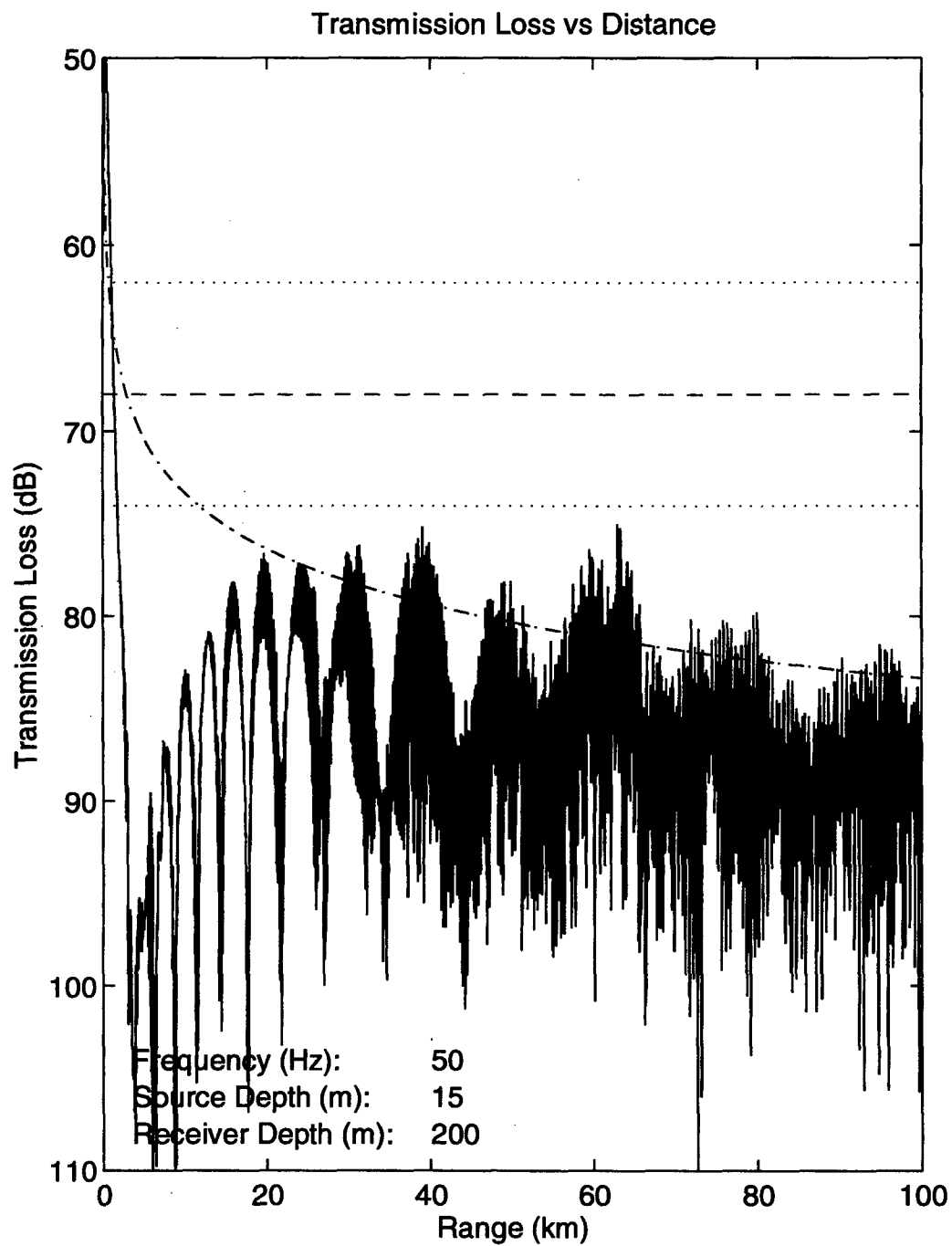


Figure 48. Transmission loss versus distance at 50 Hz for deep water in the wet season. Source at 15 m and receiver at 200 m.

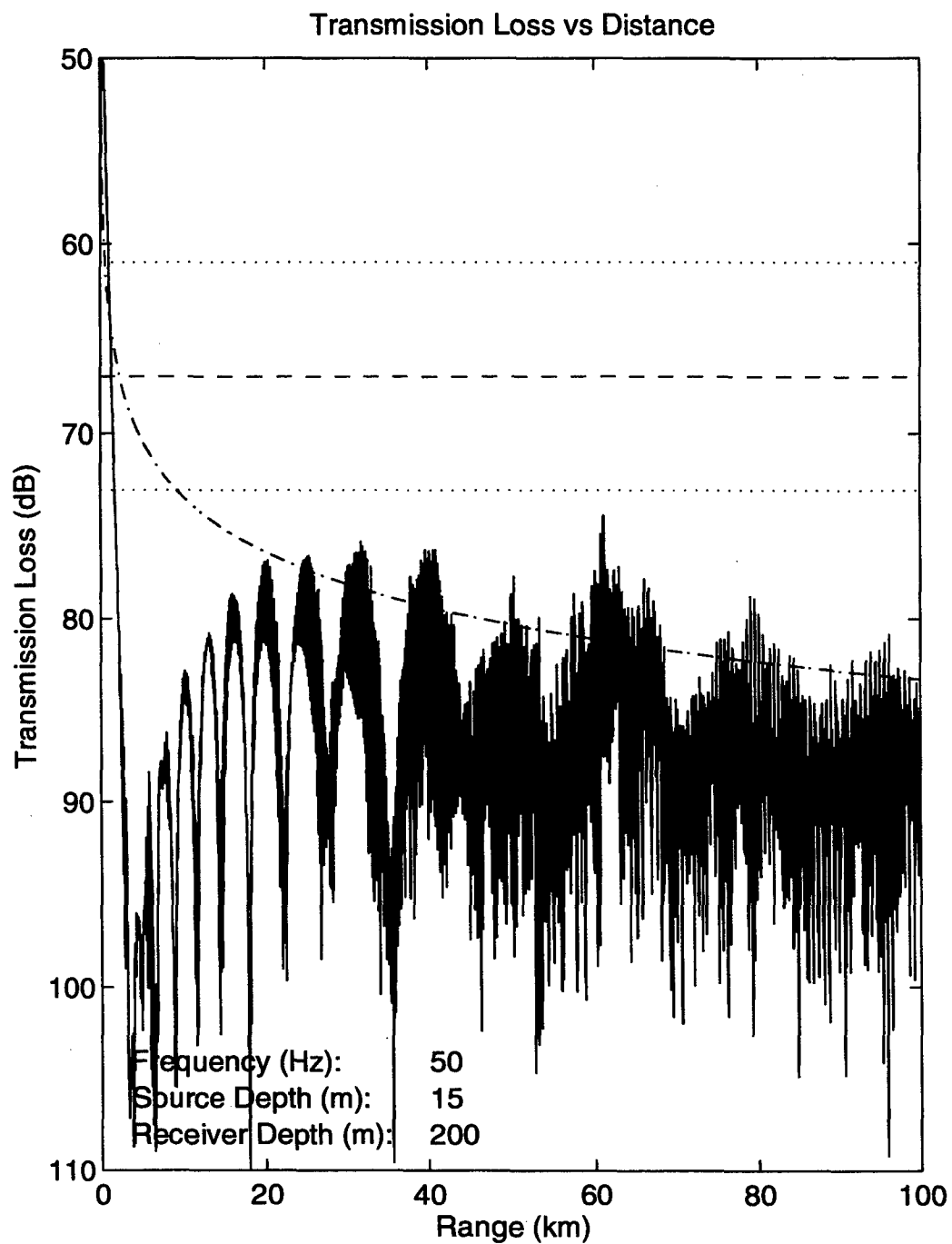


Figure 49. Transmission loss versus distance at 50 Hz for deep water in the dry season. Source at 15 m and receiver at 200 m.

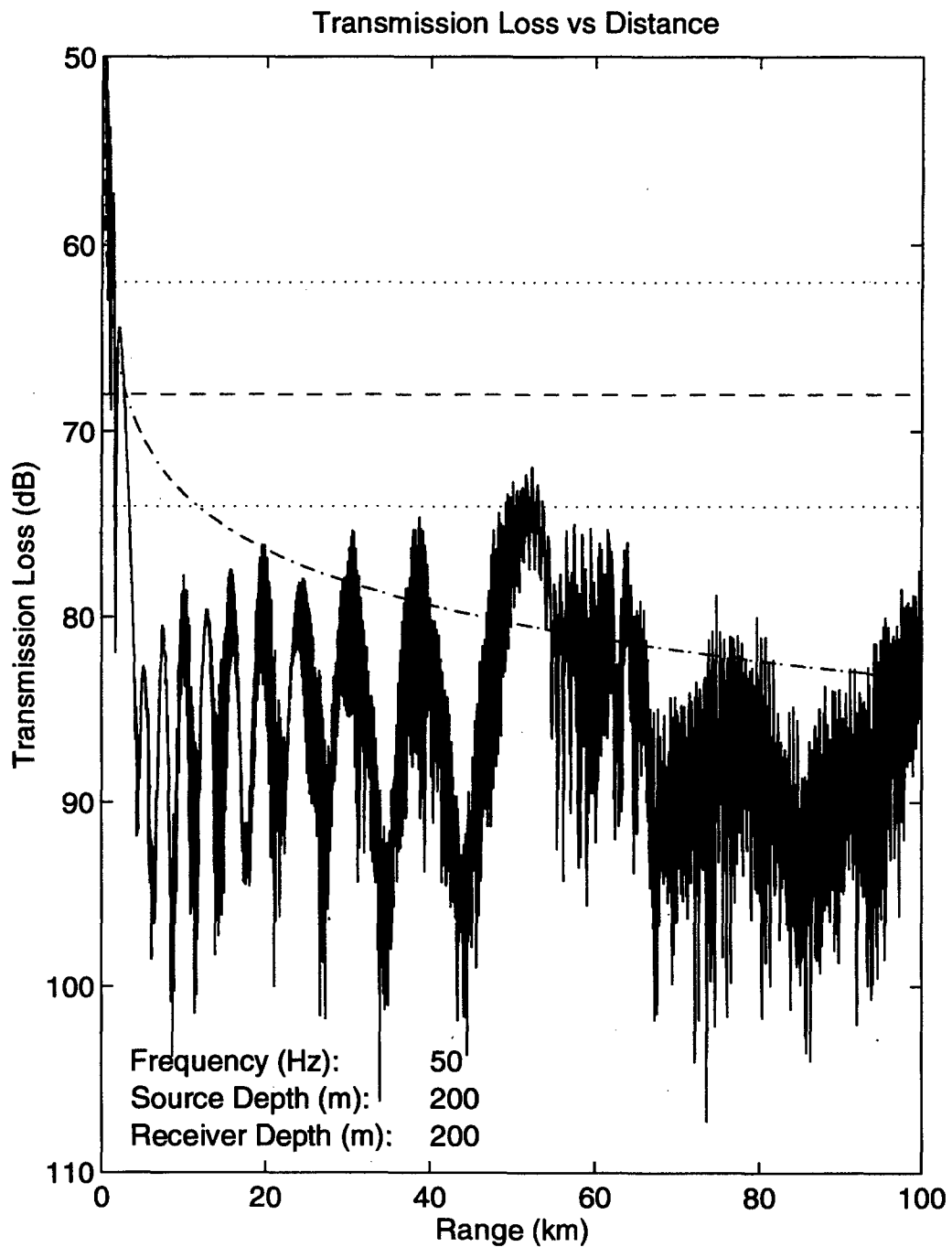


Figure 50. Transmission loss versus distance at 50 Hz for deep water in the wet season. Source and receiver at 200 m.

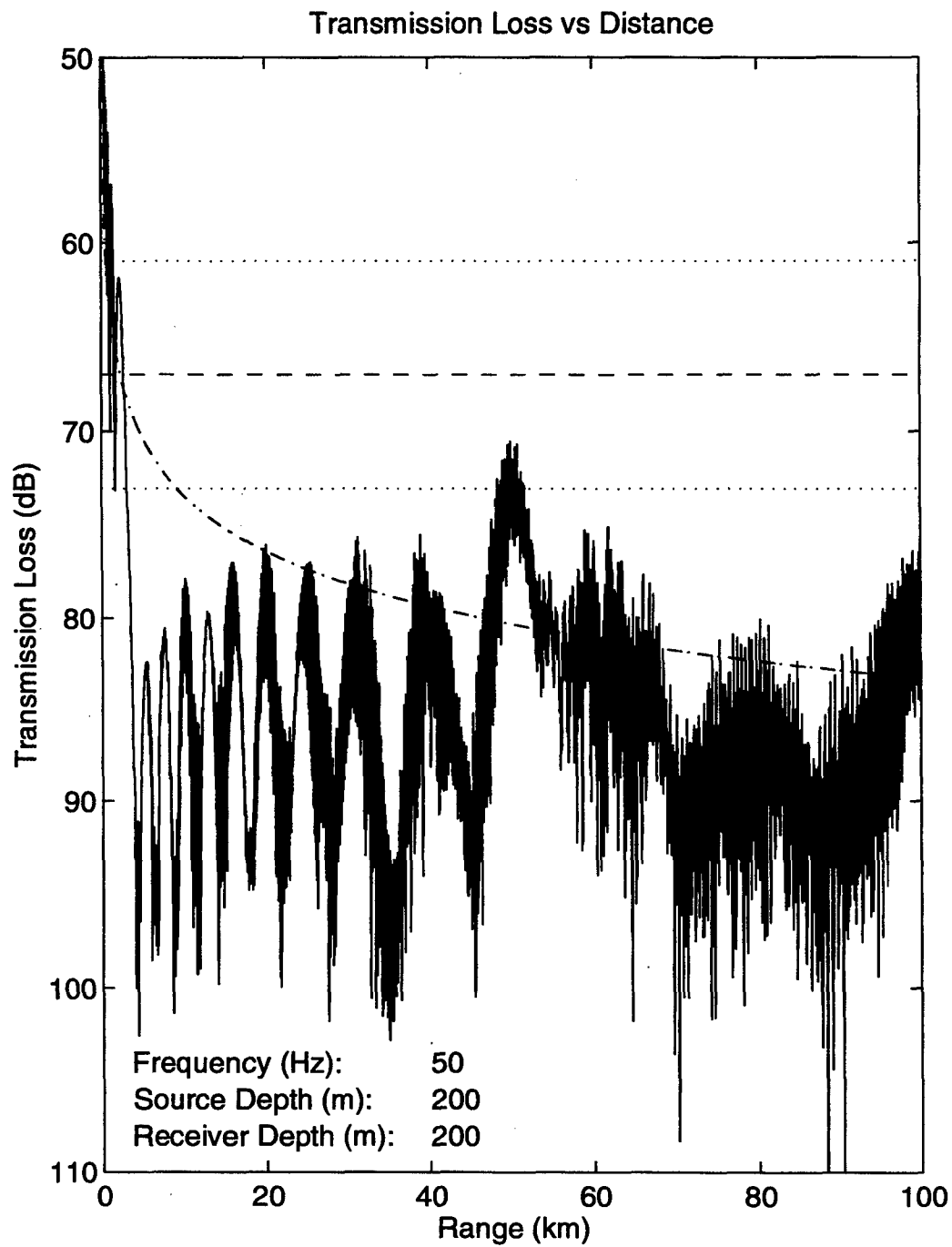


Figure 51. Transmission loss versus distance at 50 Hz for deep water in the dry season. Source and receiver at 200 m.

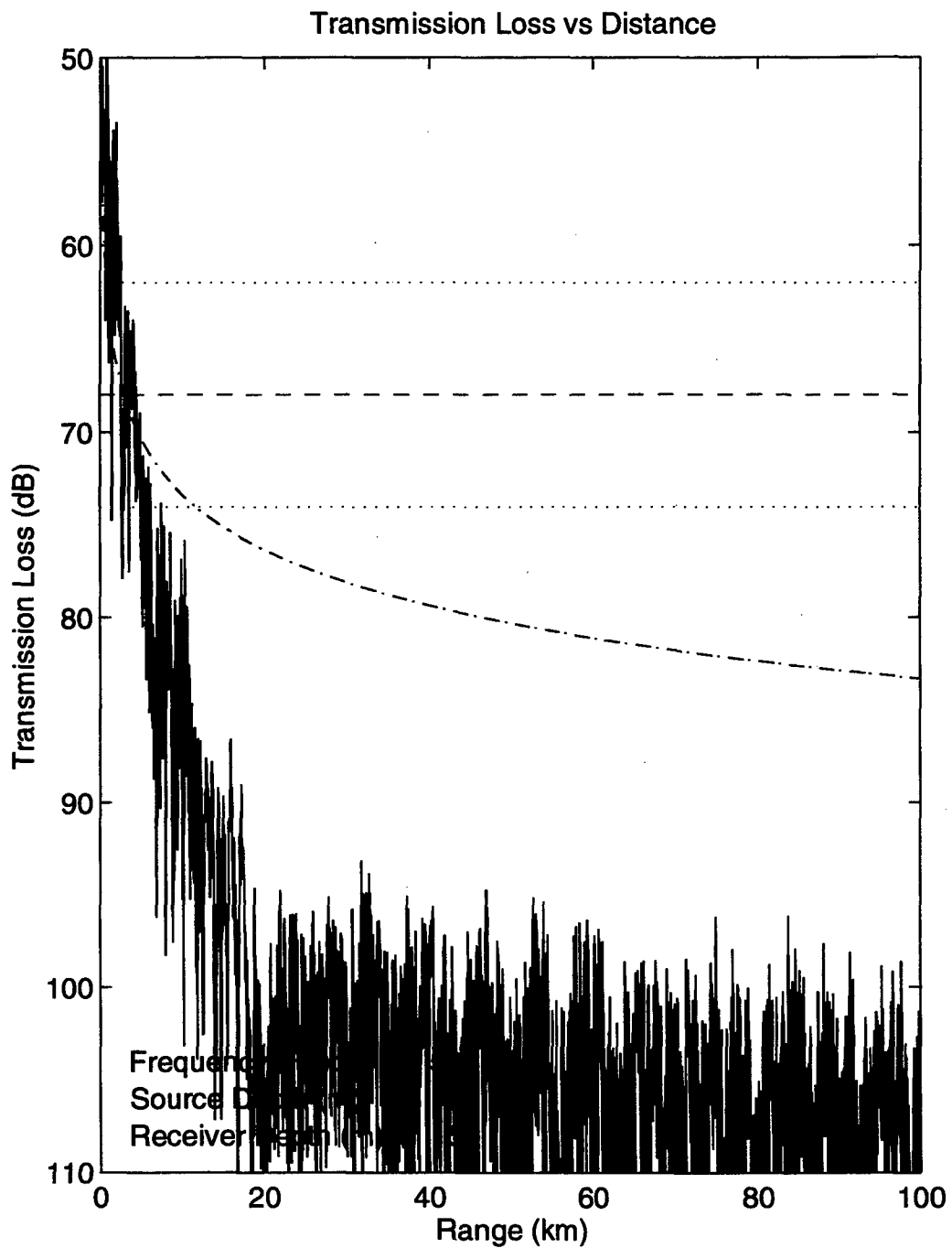


Figure 52. Transmission loss versus distance at 50 Hz for down-slope propagation in deep water in the wet season. Source and receiver at 15 m.

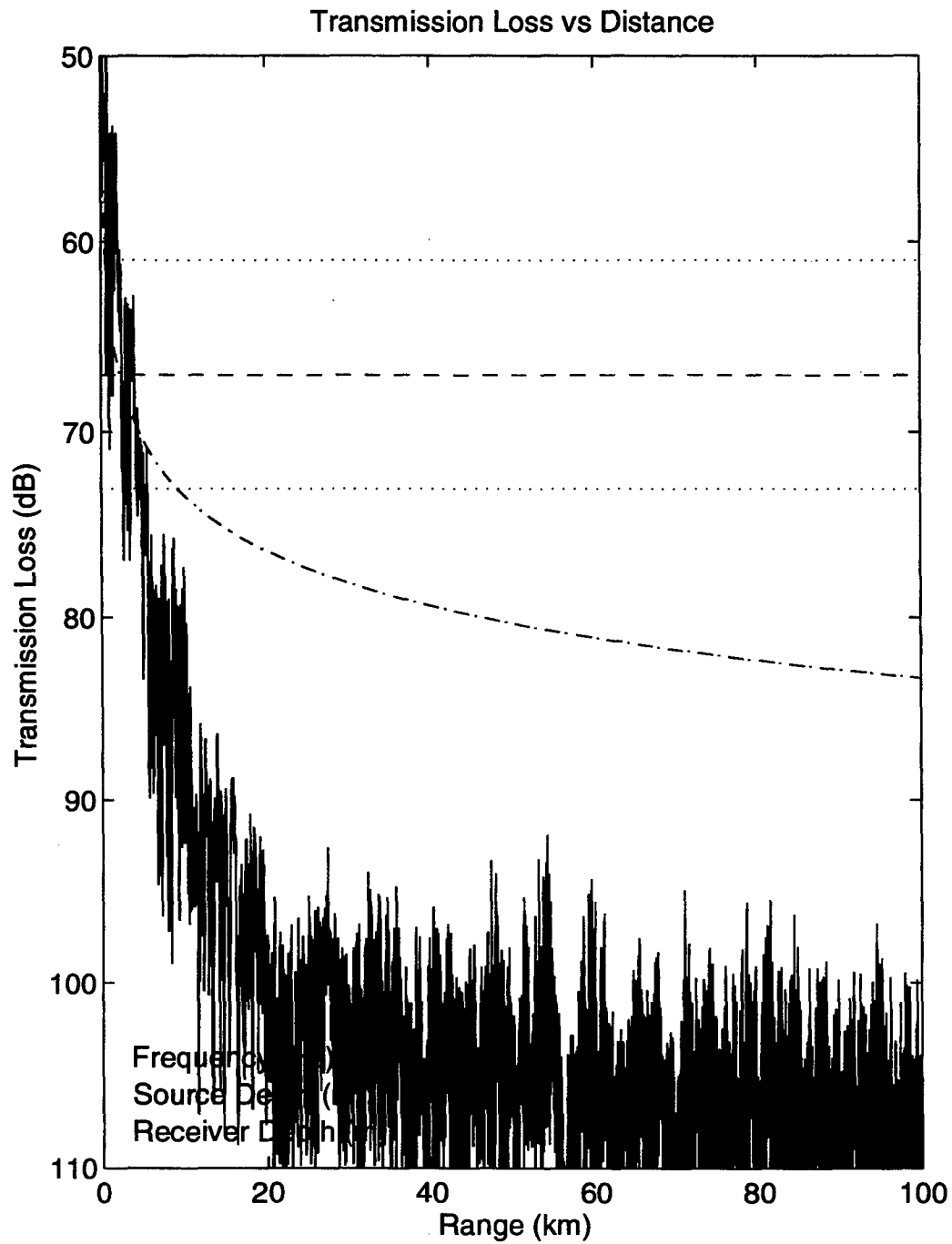


Figure 53. Transmission loss versus distance at 50 Hz for down-slope propagation in deep water in the dry season. Source and receiver at 15 m.

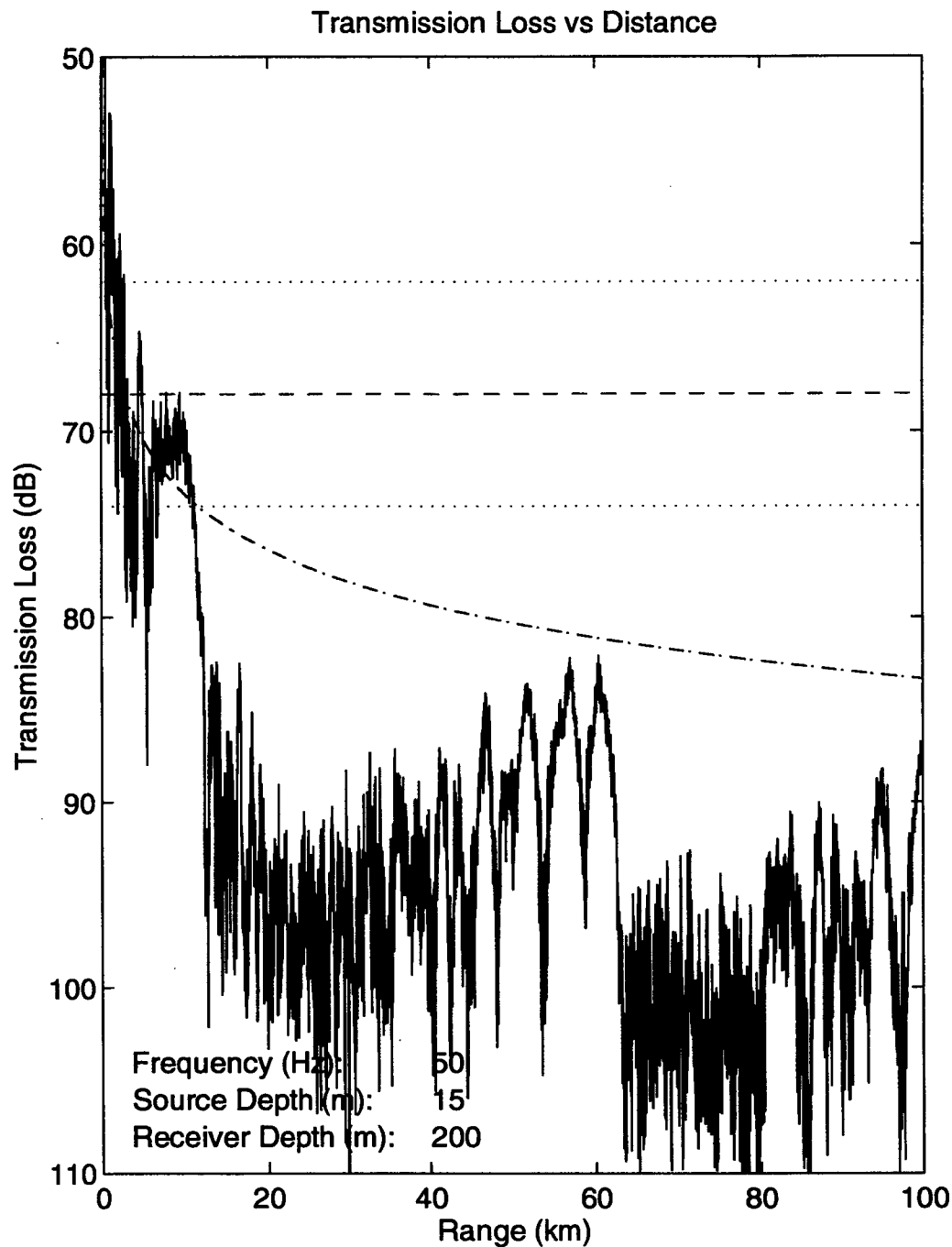


Figure 54. Transmission loss versus distance at 50 Hz for down-slope propagation in deep water in the wet season. Source at 15 m and receiver at 200 m.

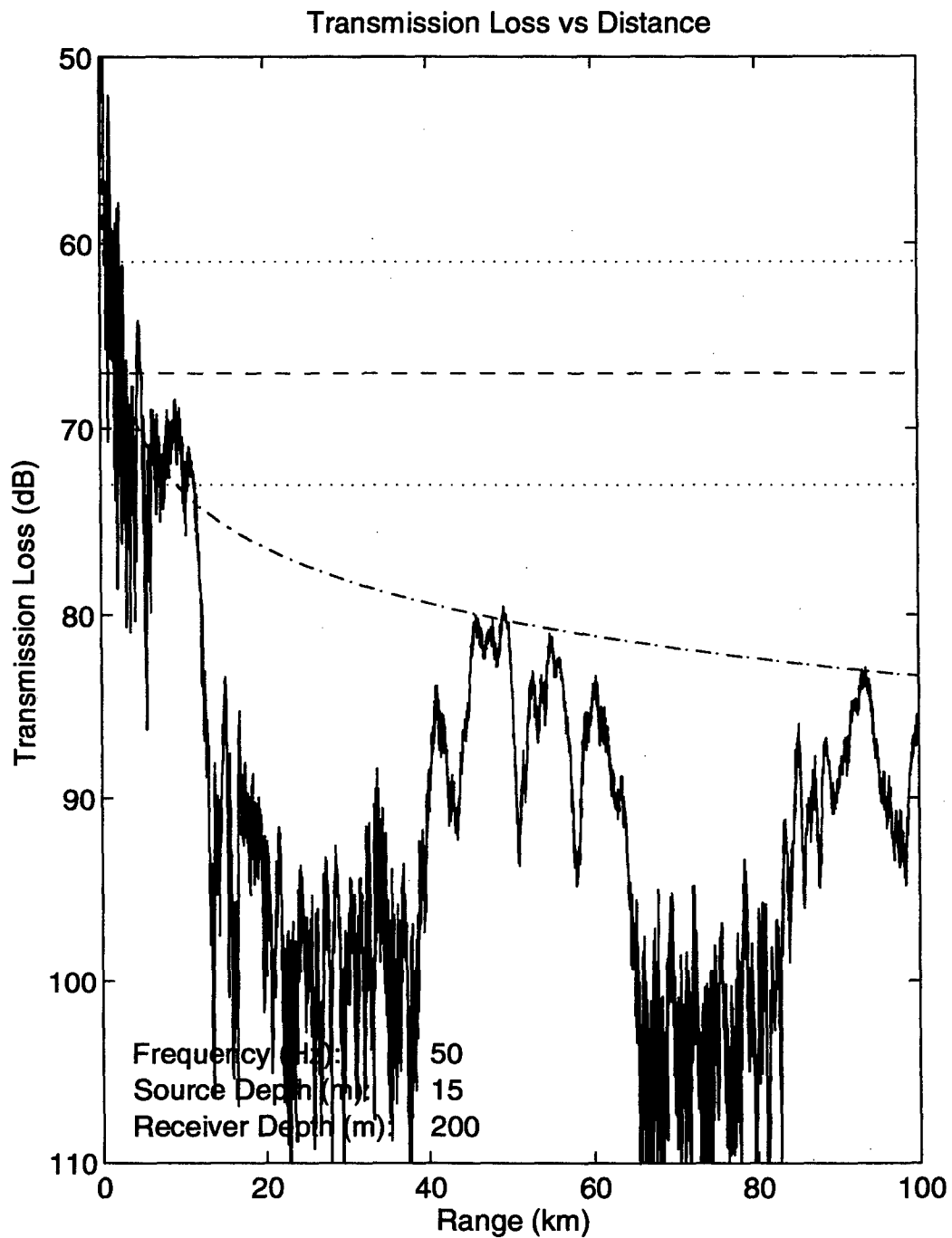


Figure 55. Transmission loss versus distance at 50 Hz for down-slope propagation in deep water in the dry season. Source at 15 m and receiver at 200 m.

APPENDIX C - 300 HZ TRANSMISSION LOSS CURVES

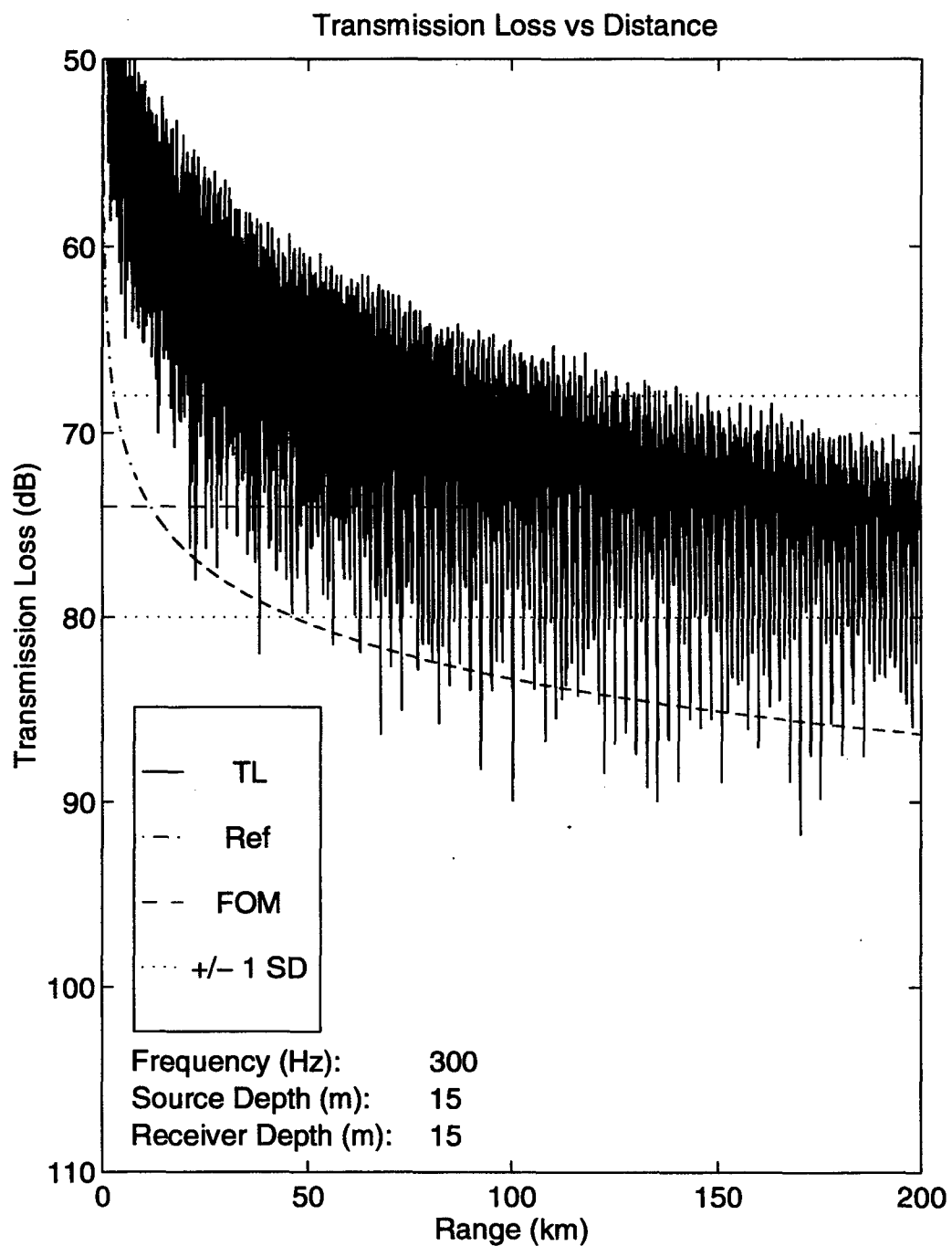


Figure 56. Transmission loss versus distance at 300 Hz for 50 m water depth in the wet season. Source and receiver at 15 m.

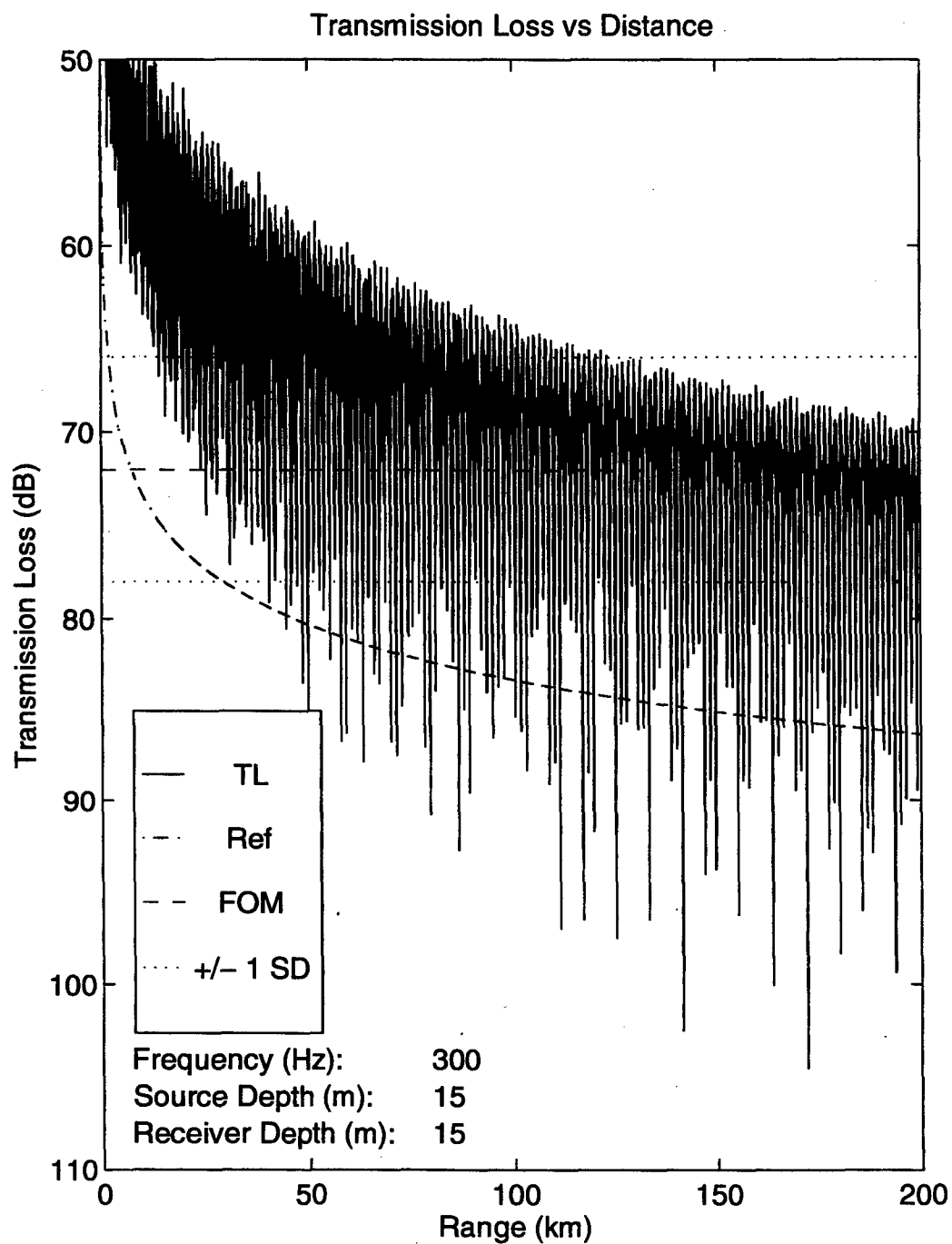


Figure 57. Transmission loss versus distance at 300 Hz for 50 m water depth in the dry season. Source and receiver at 15 m.

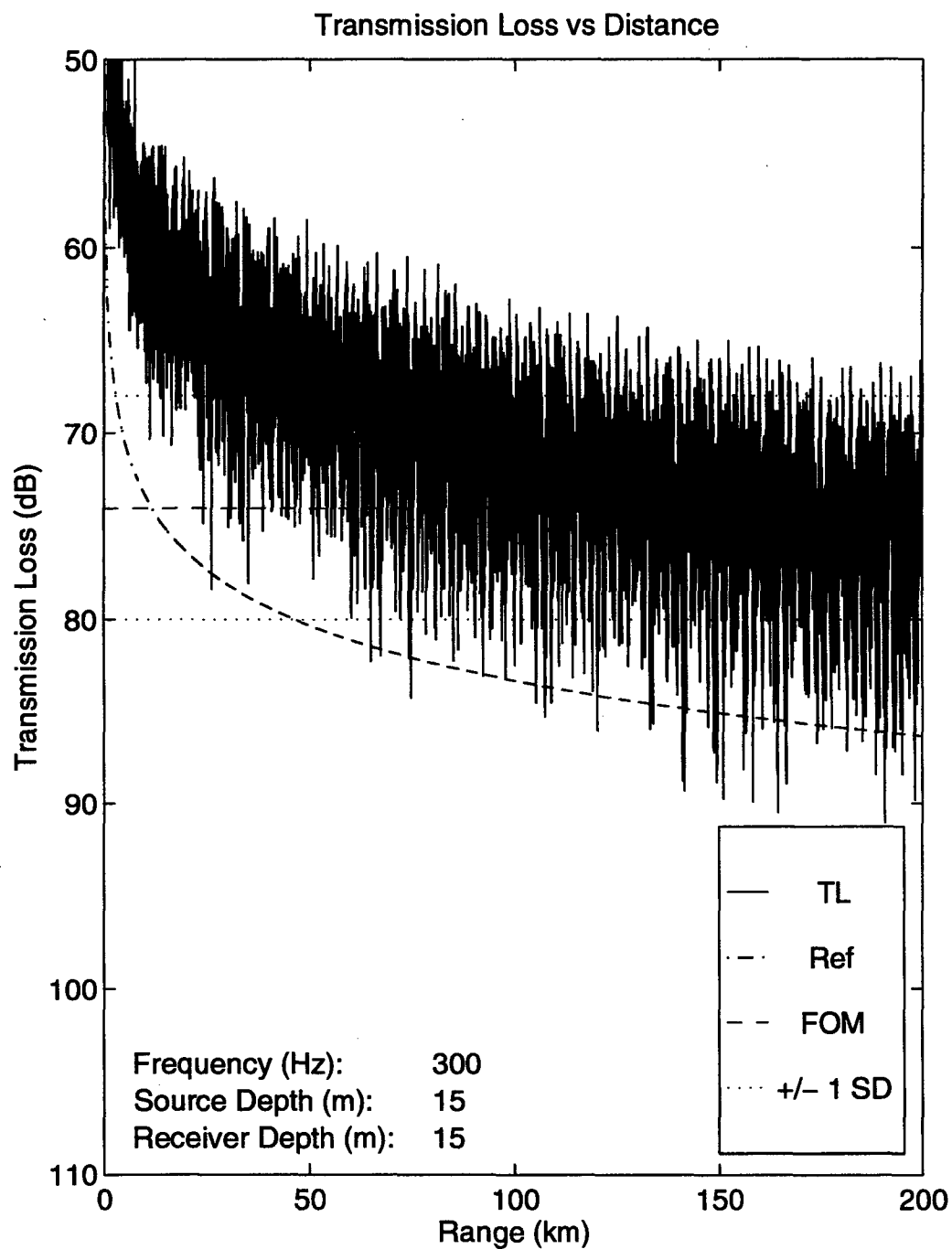


Figure 58. Transmission loss versus distance at 300 Hz for 100 m water depth in the wet season. Source and receiver at 15 m.

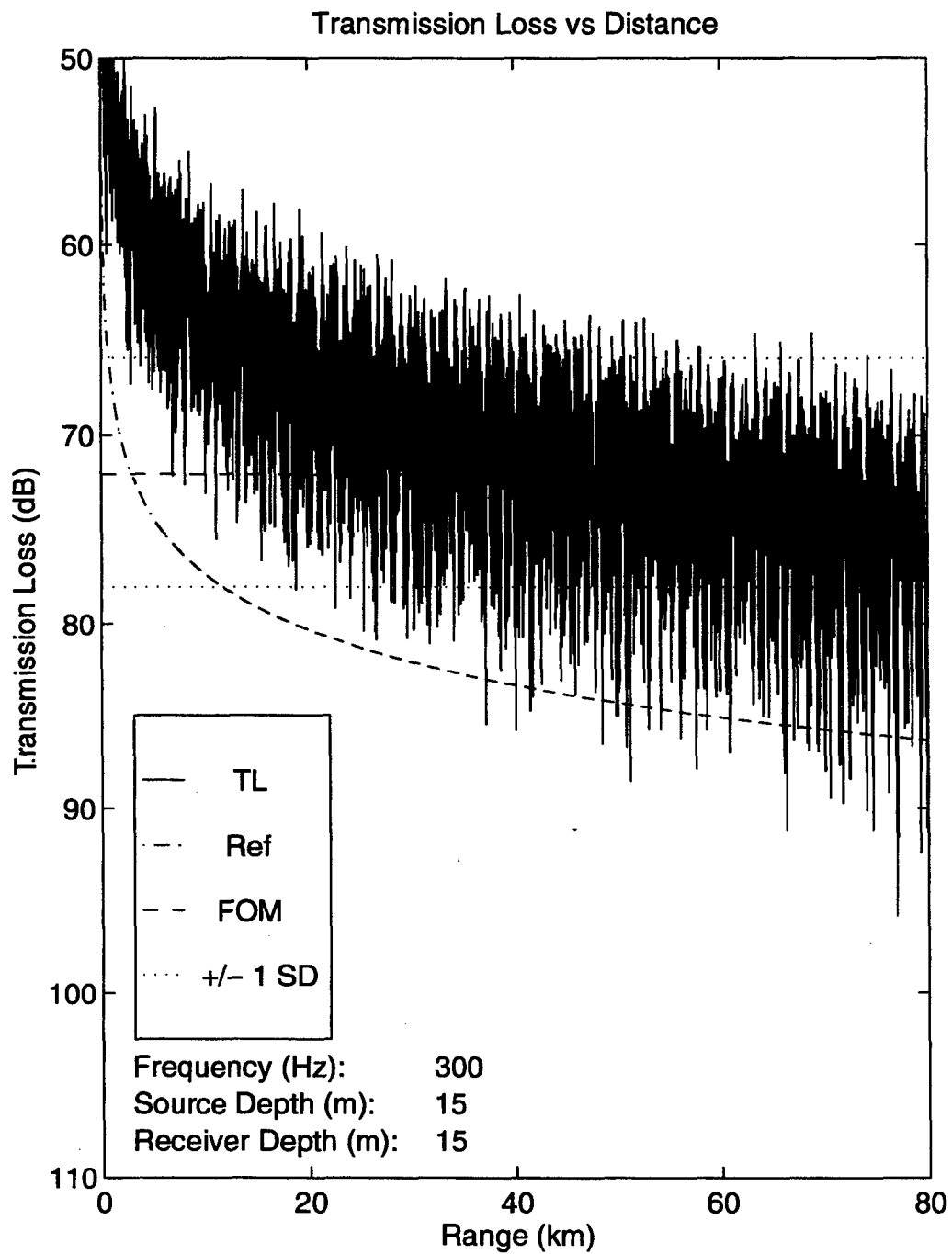


Figure 59. Transmission loss versus distance at 300 Hz for 100 m water depth in the dry season. Source and receiver at 15 m.

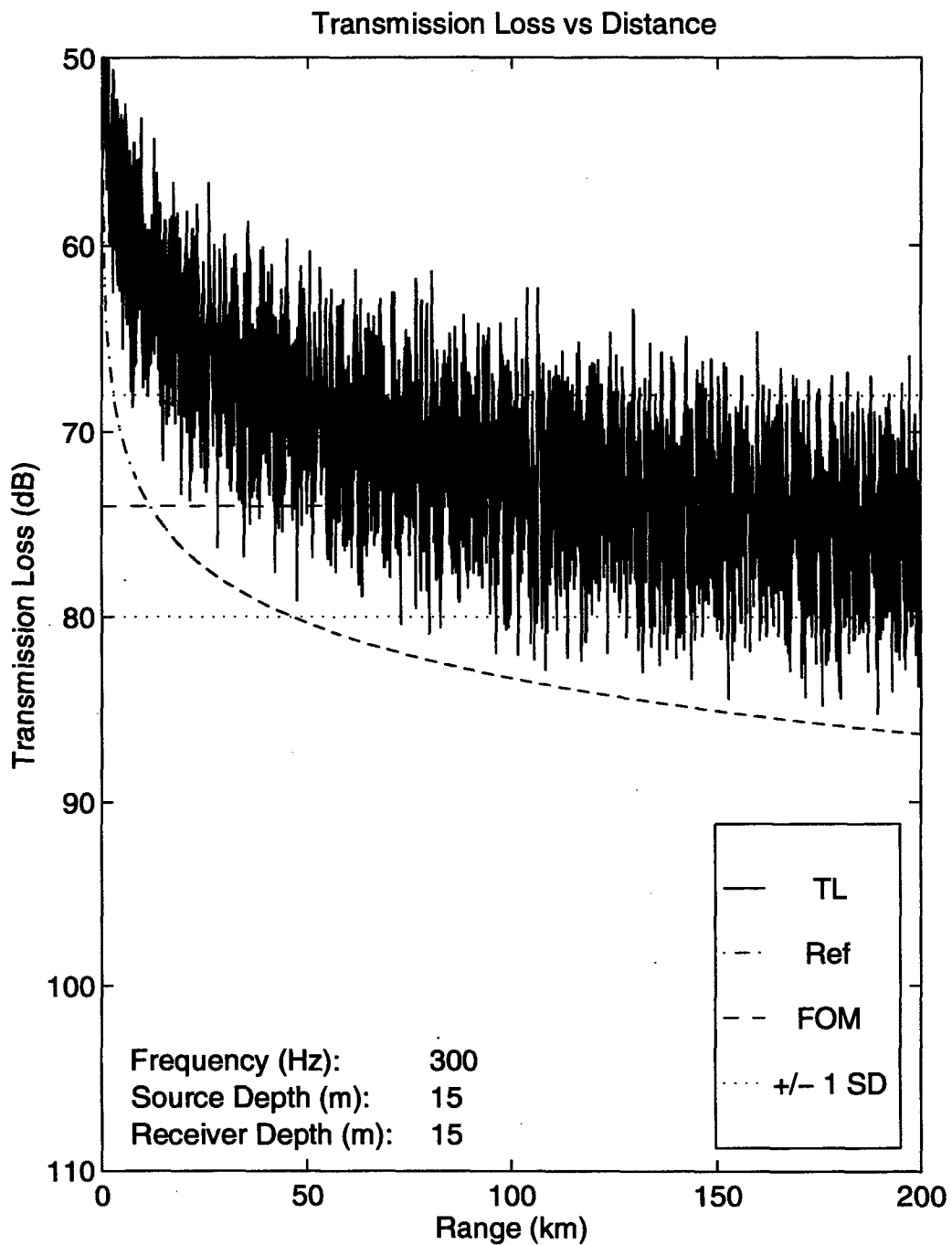


Figure 60. Transmission loss versus distance at 300 Hz for 200 m water depth in the wet season. Source and receiver at 15 m.

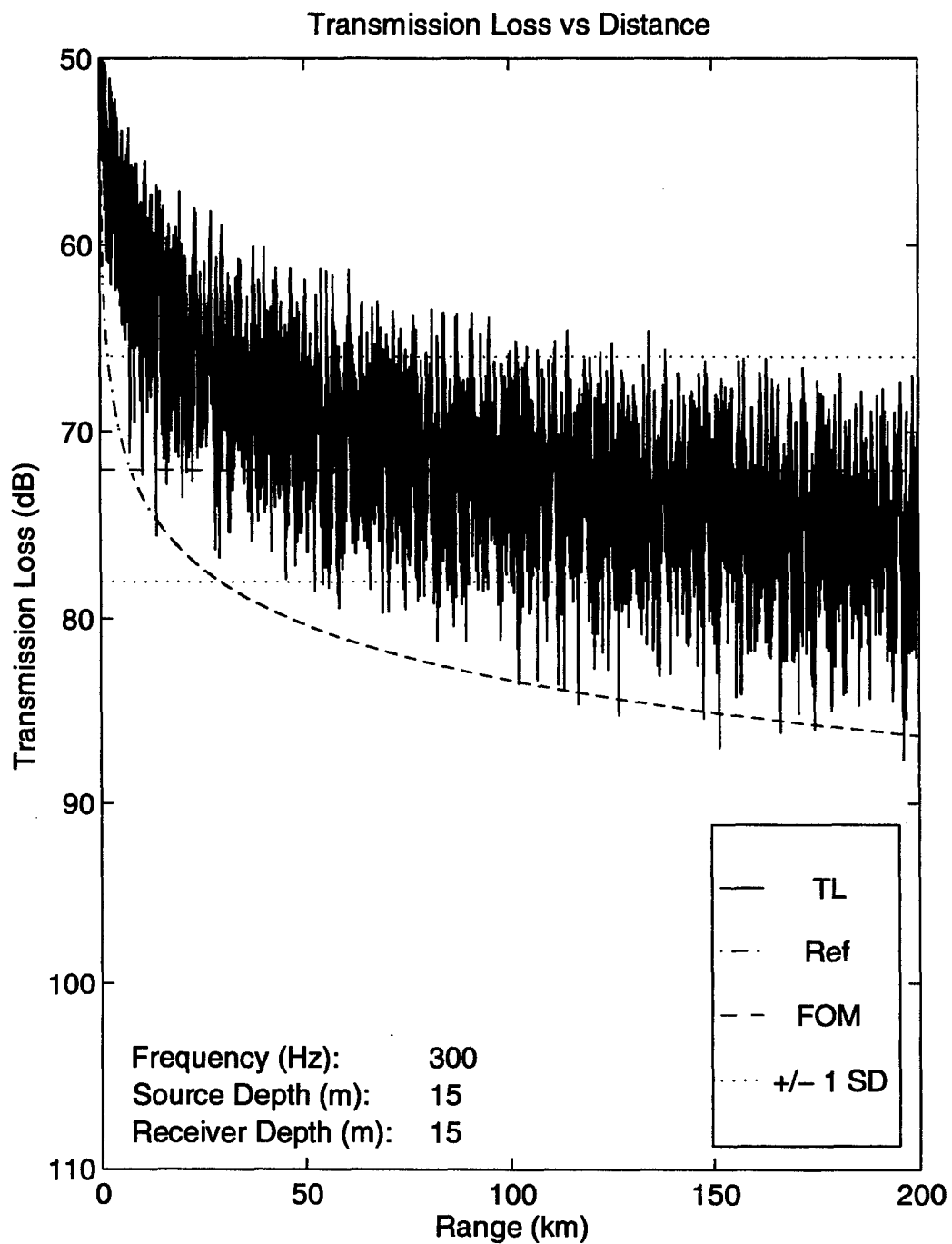


Figure 61. Transmission loss versus distance at 300 Hz for 200 m water depth in the dry season. Source and receiver at 15 m.

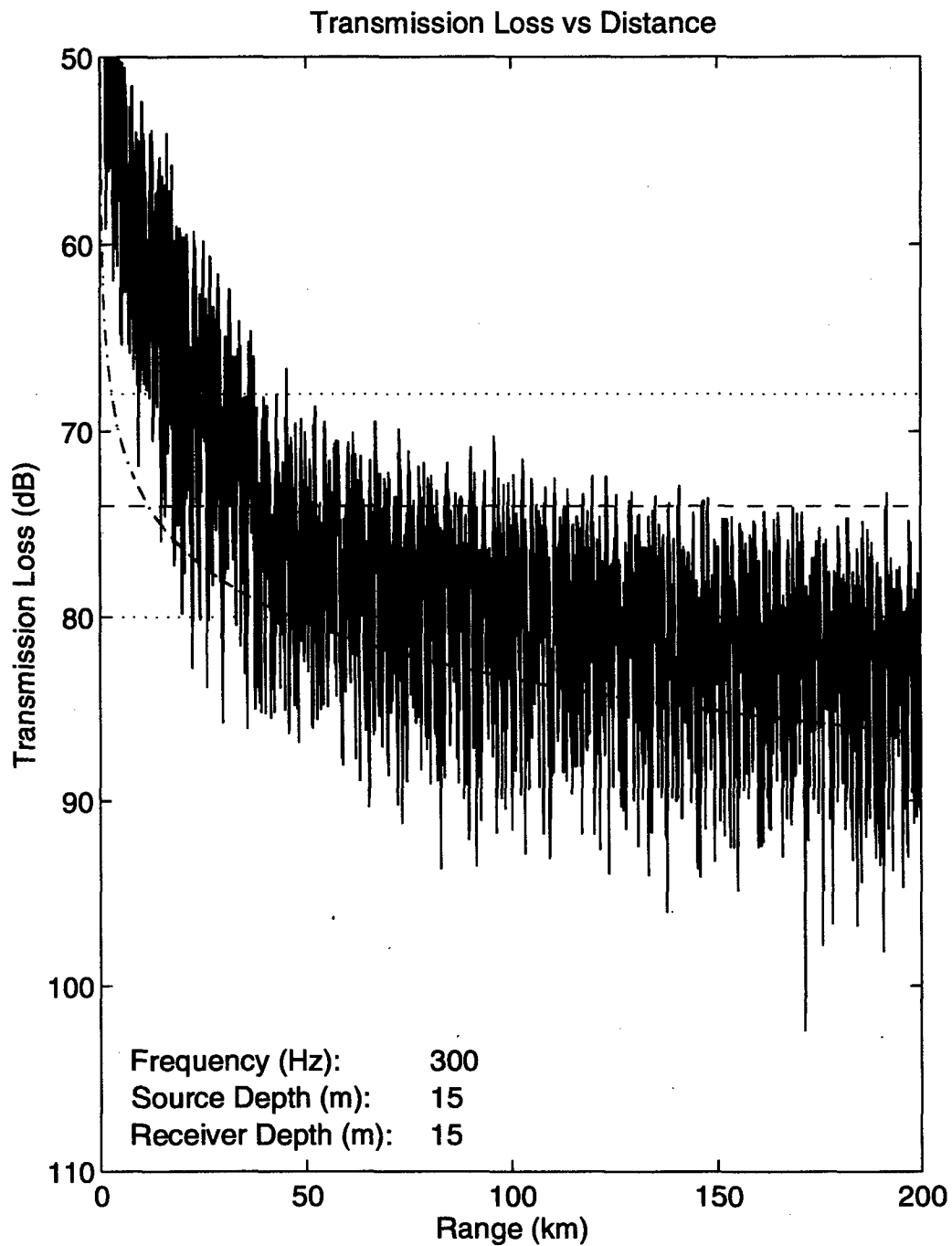


Figure 62. Transmission loss versus distance at 300 Hz for down-slope propagation in shallow water in the wet season. Source and receiver at 15 m.

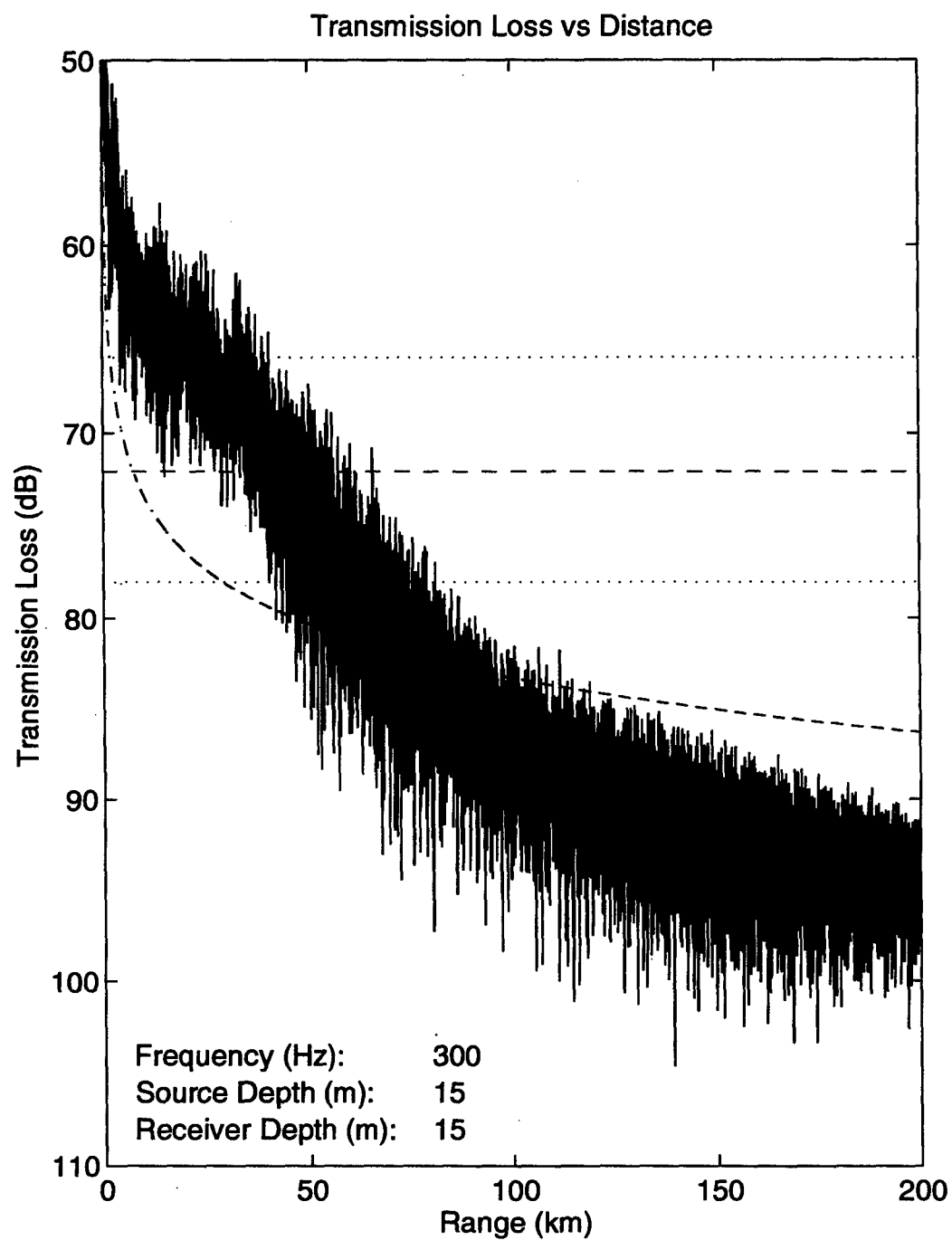


Figure 63. Transmission loss versus distance at 300 Hz for up-slope propagation in shallow water in the wet season. Source and receiver at 15 m.

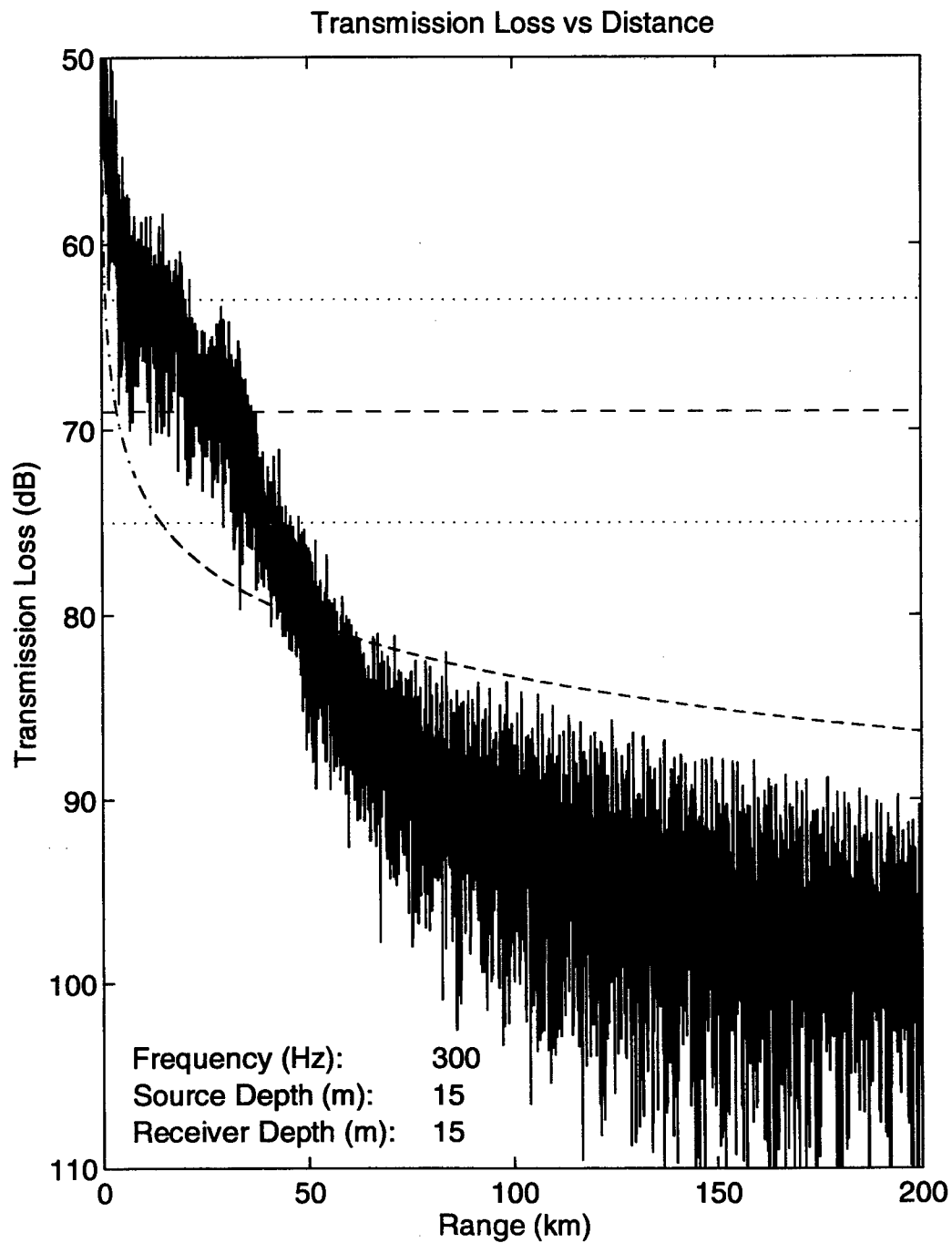


Figure 64. Transmission loss versus distance at 300 Hz for up-slope propagation in shallow water in the dry season. Source and receiver at 15 m.

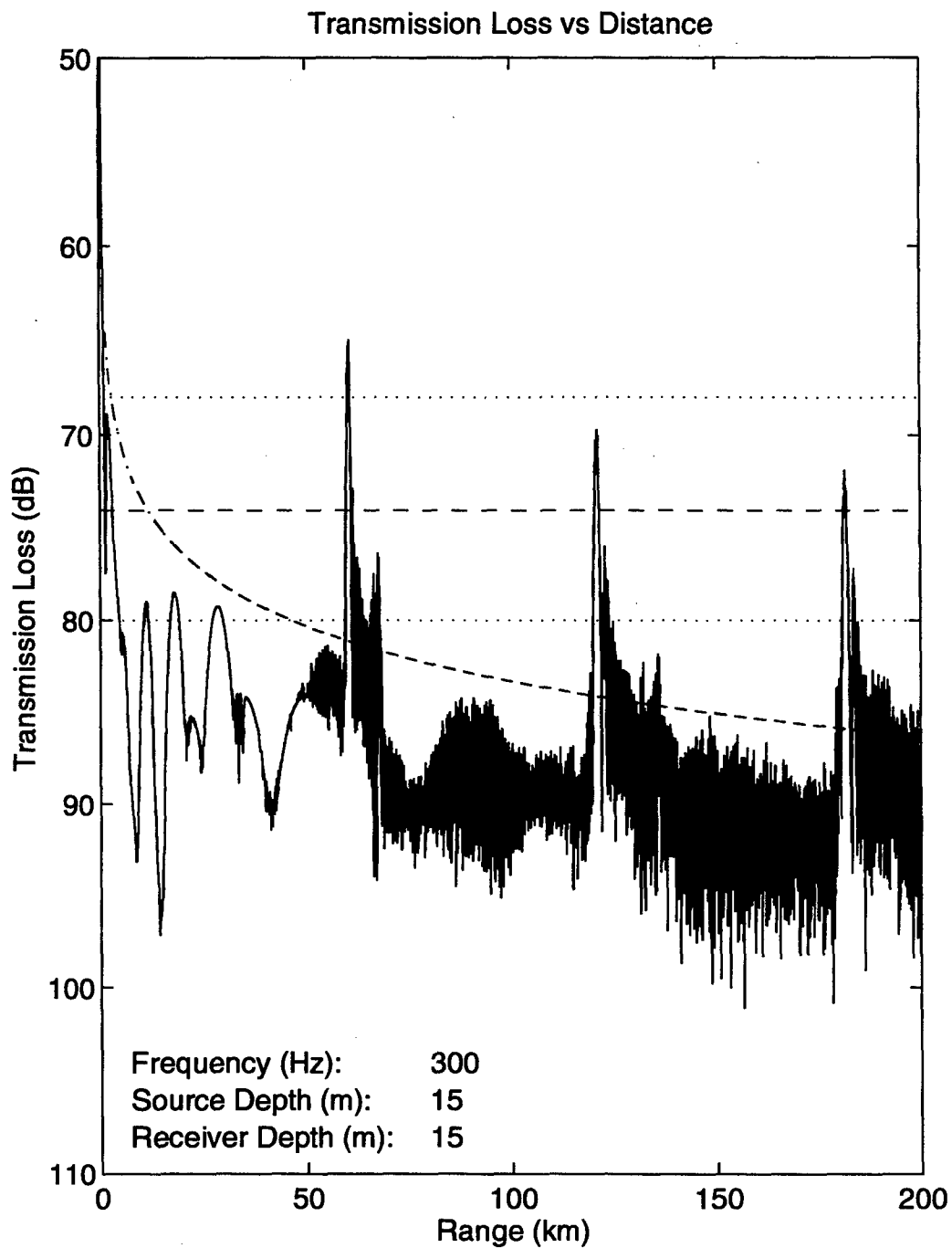


Figure 65. Transmission loss versus distance at 300 Hz for deep water in the wet season. Source and receiver at 15 m.

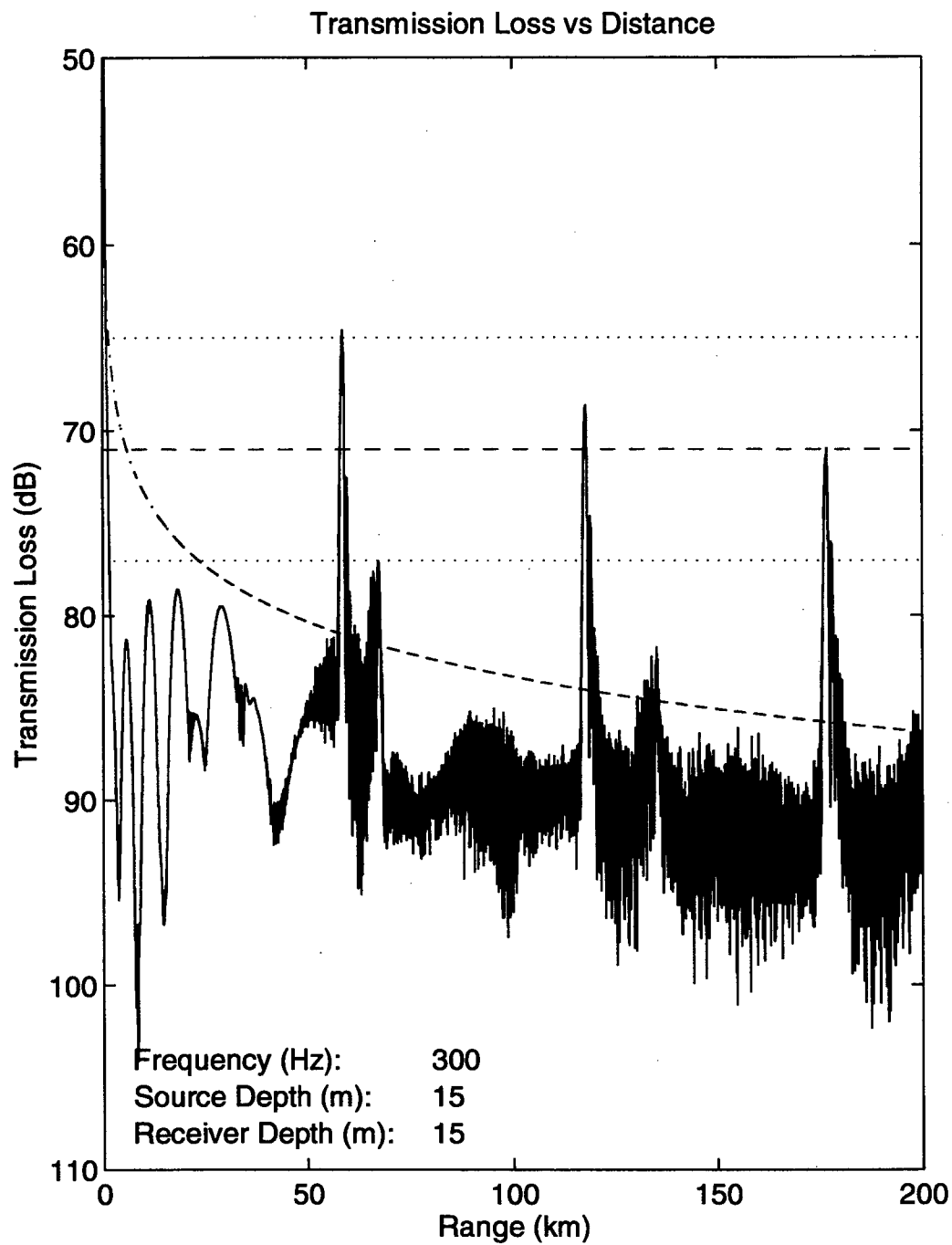


Figure 66. Transmission loss versus distance at 300 Hz for deep water in the dry season. Source and receiver at 15 m.

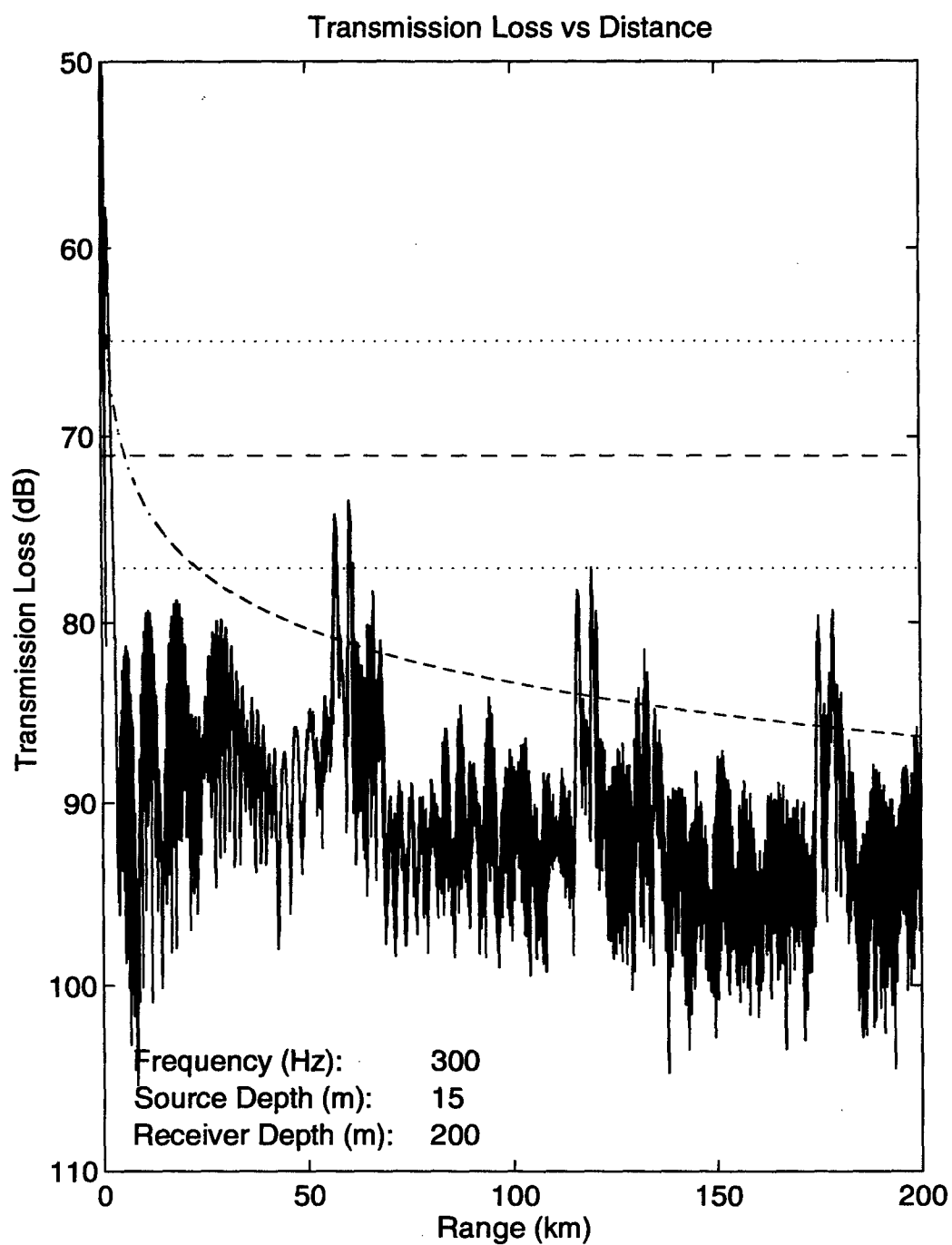


Figure 67. Transmission loss versus distance at 300 Hz for deep water in the wet season. Source at 15 m and receiver at 200 m.

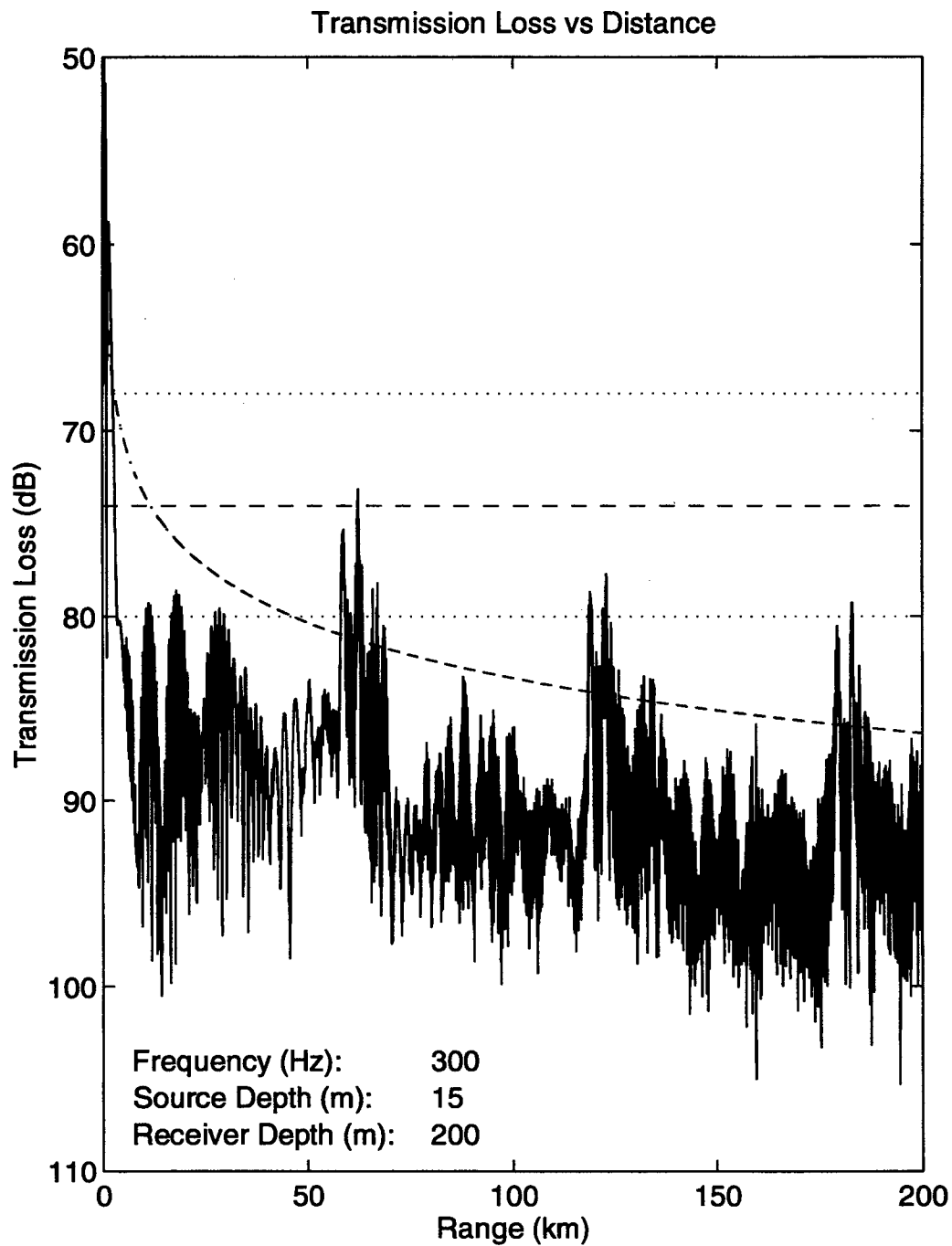


Figure 68. Transmission loss versus distance at 300 Hz for deep water in the dry season. Source at 15 m and receiver at 200 m.

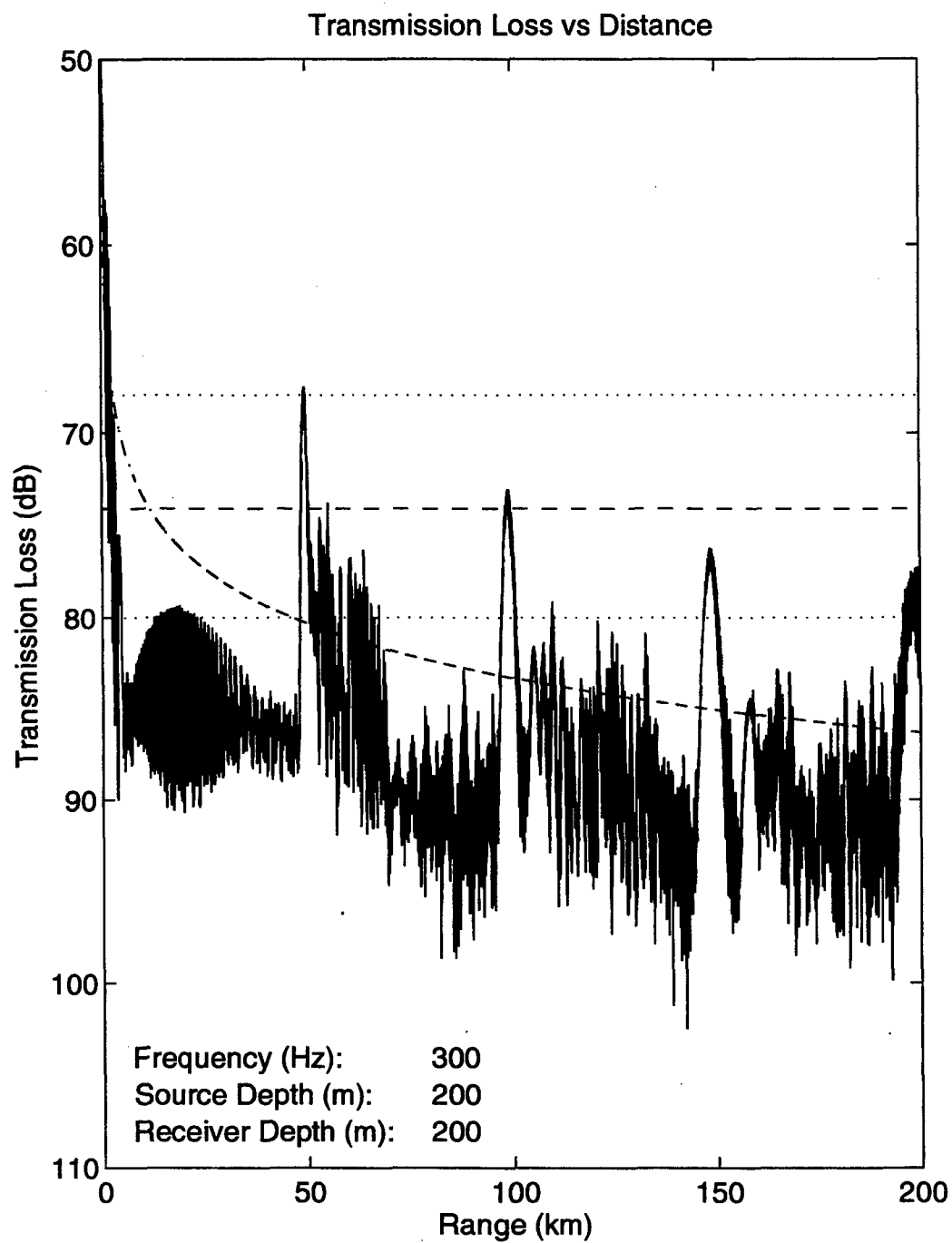


Figure 69. Transmission loss versus distance at 300 Hz for deep water in the wet season. Source and receiver at 200 m.

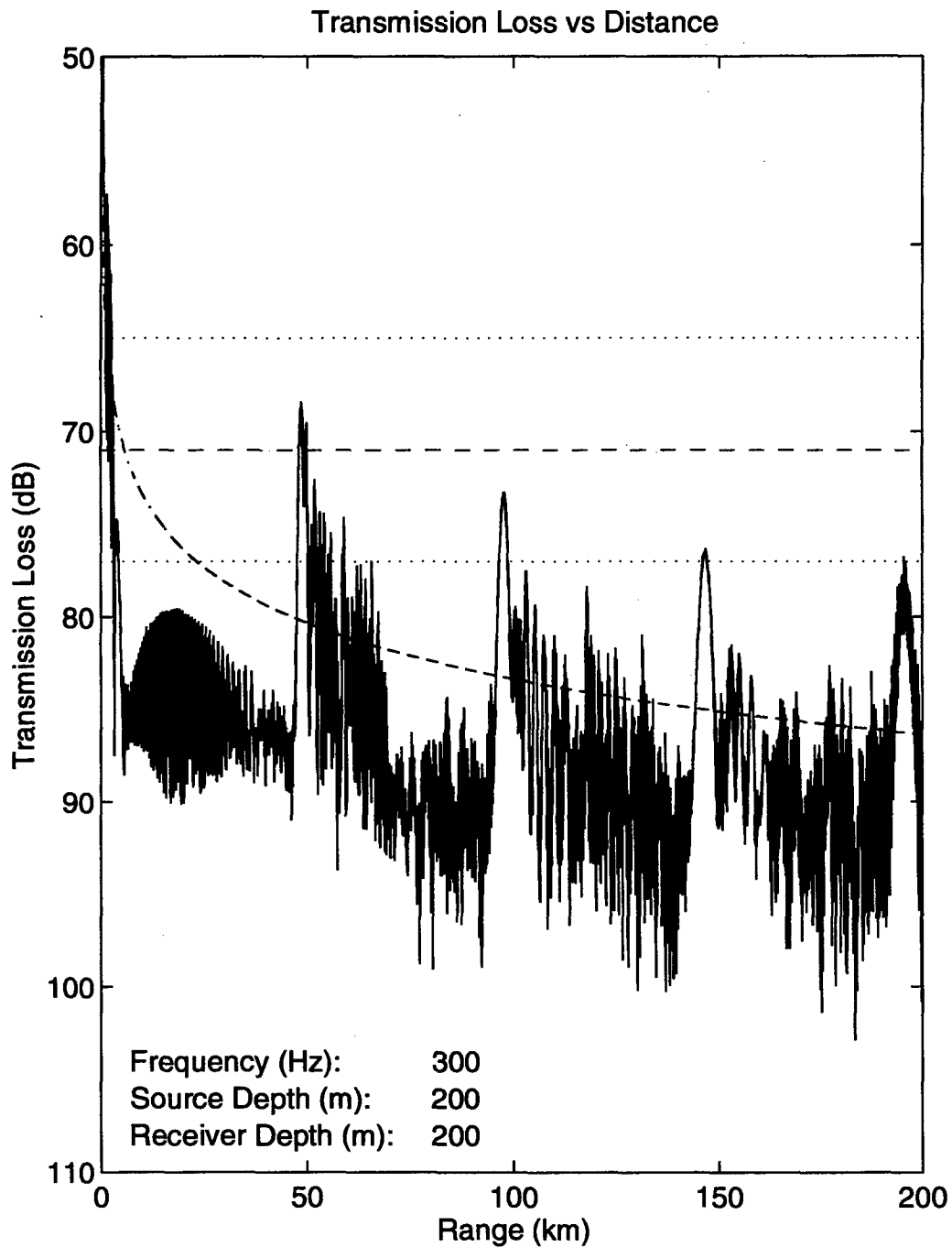


Figure 70. Transmission loss versus distance at 300 Hz for deep water in the dry season. Source and receiver at 200 m.

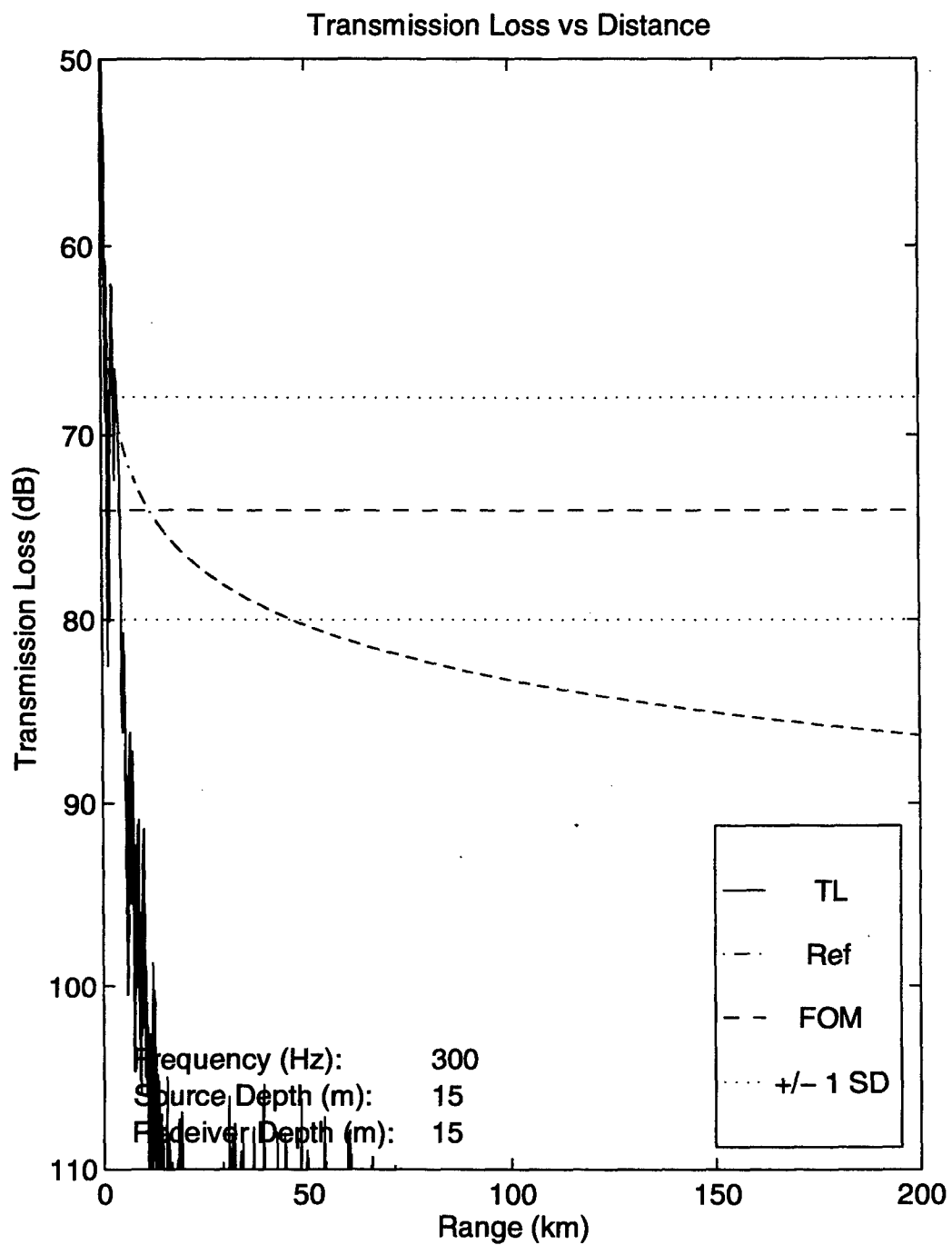


Figure 71. Transmission loss versus distance at 300 Hz for down-slope propagation in deep water in the wet season. Source and receiver at 15 m.

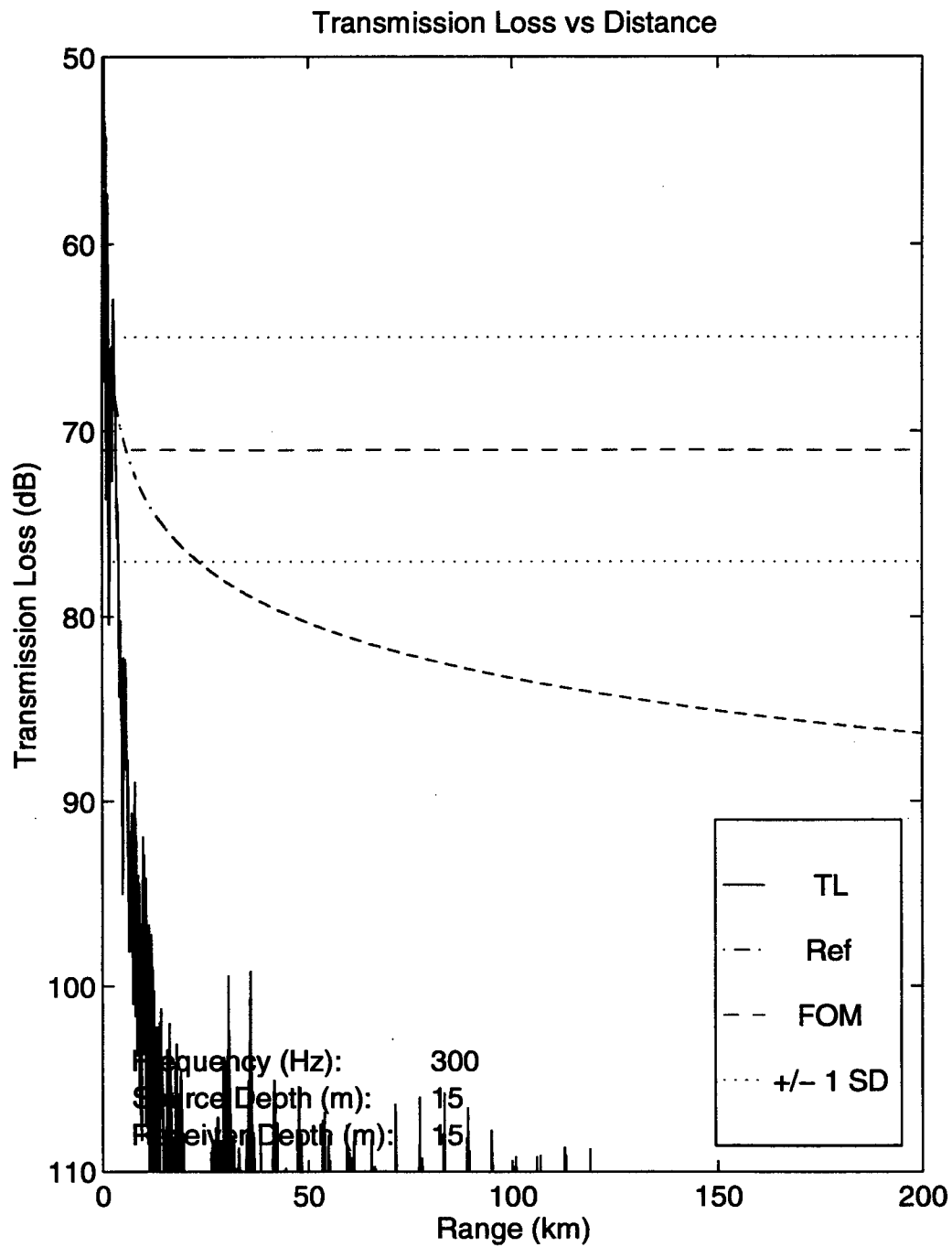


Figure 72. Transmission loss versus distance at 300 Hz for down-slope propagation in deep water in the dry season. Source and receiver at 15 m.

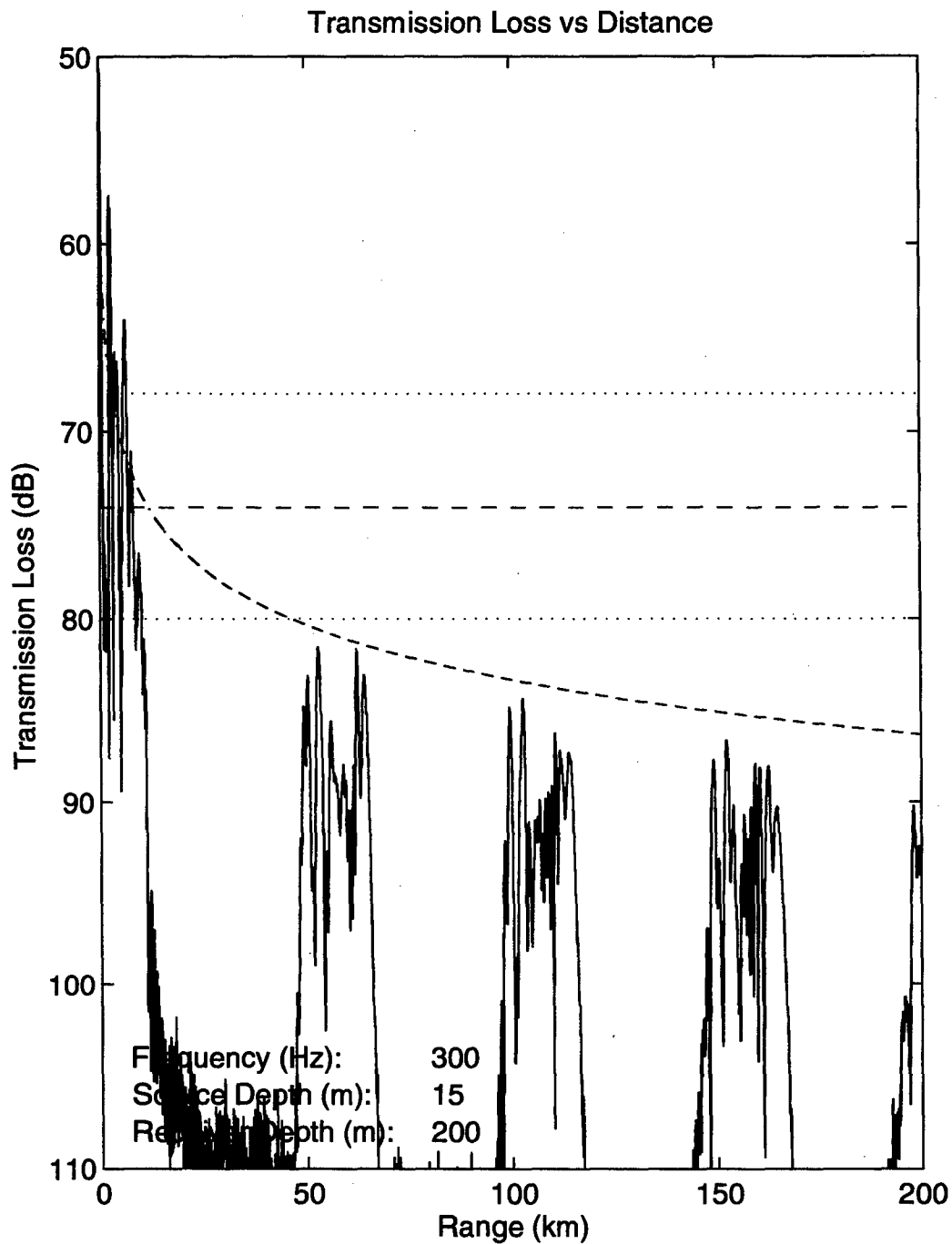


Figure 73. Transmission loss versus distance at 300 Hz for down-slope propagation in deep water in the wet season. Source at 15 m and receiver at 200 m.

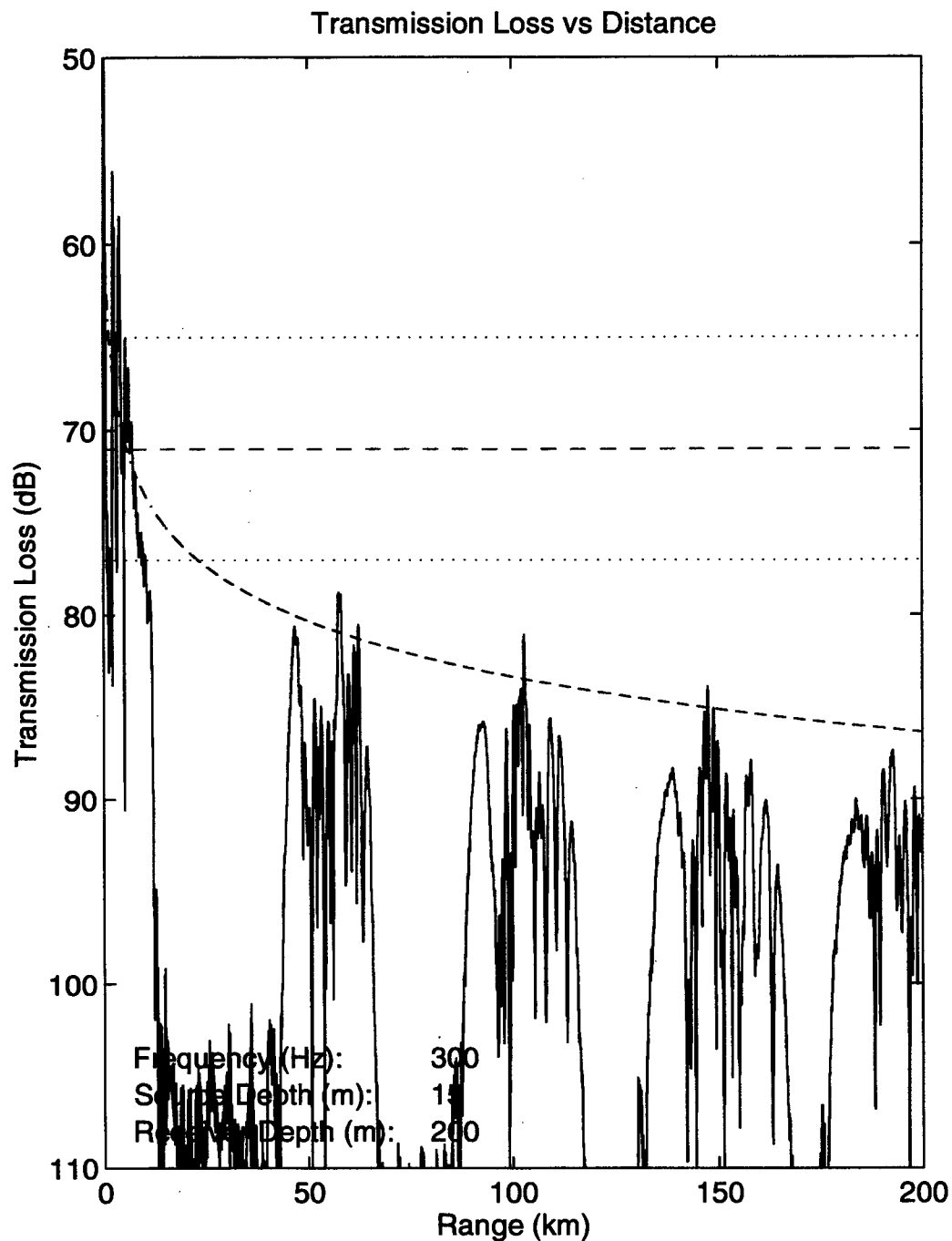


Figure 74. Transmission loss versus distance at 300 Hz for down-slope propagation in deep water in the dry season. Source at 15 m and receiver at 200 m.

INITIAL DISTRIBUTION LIST

	No. of copies
1. Defense Technical Information Center 8725 John J. Kingman Rd., STE 0944 Ft. Belvoir, VA 22060-6218	2
2. Dudley Knox Library Naval Postgraduate School 411 Dyer Rd. Monterey, CA 93943-5101	2
3. Chairman (Code OC/BF) Department of Oceanography Naval Postgraduate School Monterey, CA 93943-5000	2
4. Dr. James H. Wilson Neptune Sciences, Inc. 3834 Vista Azul San Clemente, CA 92674	2
5. Maritime Commander Australia Maritime Headquarters 1 Wylde St Potts Point, NSW 2011	2
6. Director of Oceanography and Meteorology Maritime Headquarters 1 Wylde St Potts Point, NSW 2011	2
7. Officer in Charge of the Applied Meteorology and ... Oceanography Centre Maritime Headquarters 1 Wylde St Potts Point, NSW 2011	1

8. Dr. D.H. Cato 1
Maritime Operations Division
Defence Science and Technology Organisation
PO Box 44
Pyrmont, NSW 2009
9. Leut J.A. Crouch 1
Applied Meteorology and Oceanography Centre
Maritime Headquarters
1 Wylde St
Potts Point, NSW 2011